

# Matter in Strong Magnetic Fields

Dong Lai

*Center for Radiophysics and Space Research, Department of Astronomy, Space Sciences Building  
Cornell University, Ithaca, NY 14853 \**

The properties of matter are significantly modified by strong magnetic fields,  $B \gg m_e^2 c^3 / \hbar^3 = 2.35 \times 10^9$  Gauss (1 G =  $10^{-4}$  Tesla), as are typically found on the surfaces of neutron stars. In such strong magnetic fields, the Coulomb force on an electron acts as a small perturbation compared to the magnetic force. The strong field condition can also be mimicked in laboratory semiconductors. Because of the strong magnetic confinement of electrons perpendicular to the field, atoms attain a much greater binding energy compared to the zero-field case, and various other bound states become possible, including molecular chains and three-dimensional condensed matter. This article reviews the electronic structure of atoms, molecules and bulk matter, as well as the thermodynamic properties of dense plasma, in strong magnetic fields,  $10^9 \text{ G} \ll B \lesssim 10^{16} \text{ G}$ . The focus is on the basic physical pictures and approximate scaling relations, although various theoretical approaches and numerical results are also discussed. For the neutron star surface composed of light elements such as hydrogen or helium, the outermost layer constitutes a nondegenerate, partially ionized Coulomb plasma if  $B \ll 10^{14} \text{ G}$ , and may be in the form of a condensed liquid if the magnetic field is stronger (and temperature  $\lesssim 10^6 \text{ K}$ ). For the iron surface, the outermost layer of the neutron star can be in a gaseous or a condensed phase depending on the cohesive property of the iron condensate.

## Contents

<b>I</b>	<b>Introduction</b>	<b>2</b>
A	Astrophysics Motivation . . . . .	3
B	Laboratory Physics Motivation . . . . .	4
C	Plan of This Paper . . . . .	4
D	Bibliographic Notes . . . . .	4
<b>II</b>	<b>Basics on Landau Levels</b>	<b>4</b>
<b>III</b>	<b>Atoms</b>	<b>6</b>
A	Hydrogen Atom . . . . .	6
B	High- $Z$ Hydrogenic Ions . . . . .	8
C	Heavy Atoms . . . . .	8
1	Approximate Scaling Relations . . . . .	9
2	Numerical Calculations and Results . . . . .	10
D	Intermediate Magnetic Field Regime . . . . .	11
E	Effect of Center-of-Mass Motion . . . . .	11
<b>IV</b>	<b>Molecules</b>	<b>14</b>
A	H <sub>2</sub> : Basic Mechanism of Bonding . . . . .	14
B	Numerical Calculations and Results . . . . .	14
C	Molecular Excitations . . . . .	15
D	H <sub>N</sub> Molecules: Saturation . . . . .	16
E	Intermediate Magnetic Field Regime . . . . .	17
F	Molecules of Heavy Elements . . . . .	17
<b>V</b>	<b>Linear Chains and Condensed Matter</b>	<b>18</b>
A	Basic Scaling Relations for Linear Chains . . . . .	18
B	Calculations of Linear Chains . . . . .	18
C	Cohesive Energy of Linear Chains . . . . .	19
D	3D Condensed Matter: Uniform Electron Gas Model and its Extension . . . . .	20

---

\*Electronic address: dong@astro.cornell.edu

E	Cohesive Energy of 3D Condensed Matter . . . . .	21
F	Shape and Surface Energy of Condensed Droplets . . . . .	22
<b>VI</b>	<b>Free Electron Gas in Strong Magnetic Fields</b>	<b>23</b>
<b>VII</b>	<b>Surface Layer of a Magnetized Neutron Star</b>	<b>25</b>
A	Warm Hydrogen Atmosphere . . . . .	26
B	Surface Hydrogen at Ultrahigh Fields: The Condensed Phase . . . . .	28
C	Iron Surface Layer . . . . .	30
D	Radiative Transfer and Opacities . . . . .	31
E	Magnetized Neutron Star Crust . . . . .	32
<b>VIII</b>	<b>Concluding Remarks</b>	<b>33</b>
<b>APPENDIXES</b>		<b>34</b>
<b>A</b>	<b>Jellium Model of Electron Gas in Strong Magnetic Fields</b>	<b>34</b>
<b>B</b>	<b>Thomas-Fermi Models in Strong Magnetic Fields</b>	<b>35</b>

## I. INTRODUCTION

An electron in a uniform magnetic field  $B$  gyrates in a circular orbit with radius  $\rho = m_e v / (eB)$  at the cyclotron frequency  $\omega_{ce} = eB / (m_e c)$ , where  $v$  is the velocity perpendicular to the magnetic field. In quantum mechanics, this transverse motion is quantized into Landau levels. The cyclotron energy (the Landau level spacing) of the electron is

$$\hbar\omega_{ce} = \hbar \frac{eB}{m_e c} = 11.577 B_{12} \text{ keV}, \quad (1.1)$$

and the cyclotron radius (the characteristic size of the wave packet) becomes

$$\hat{\rho} = \left( \frac{\hbar c}{eB} \right)^{1/2} = 2.5656 \times 10^{-10} B_{12}^{-1/2} \text{ cm}, \quad (1.2)$$

where  $B_{12} = B / (10^{12} \text{ G})$  is the magnetic field strength in units of  $10^{12}$  Gauss, a typical field found on the surfaces of neutron stars (see Sec. I.A). When studying matter in magnetic fields, the natural (atomic) unit for the field strength,  $B_0$ , is set by  $\hbar\omega_{ce} = e^2 / a_0$ , or equivalently by  $\hat{\rho} = a_0$ , where  $a_0$  is the Bohr radius. Thus it is convenient to define a dimensionless magnetic field strength  $b$  via

$$b \equiv \frac{B}{B_0}; \quad B_0 = \frac{m_e^2 e^3 c}{\hbar^3} = 2.3505 \times 10^9 \text{ G}. \quad (1.3)$$

For  $b \gg 1$ , the electron cyclotron energy  $\hbar\omega_{ce}$  is much larger than the typical Coulomb energy, so that the properties of atoms, molecules and condensed matter are qualitatively changed by the magnetic field.<sup>1</sup> In such a strong field regime, the usual perturbative treatment of the magnetic effects (e.g., Zeeman splitting of atomic energy levels) does not apply (see Garstang 1977 for a review of atomic physics at  $b \lesssim 1$ ). Instead, the Coulomb forces act as a perturbation to the magnetic forces, and the electrons in an atom settle into the ground Landau level. Because of the extreme confinement ( $\hat{\rho} \ll a_0$ ) of the electrons in the transverse direction (perpendicular to the field), the Coulomb force becomes much more effective in binding the electrons along the magnetic field direction. The atom attains a cylindrical structure. Moreover, it is possible for these elongated atoms to form molecular chains by covalent bonding along the field direction. Interactions between the linear chains can then lead to the formation of three-dimensional condensates. The properties of atoms, molecules and bulk matter in strong magnetic fields of  $b \gg 1$  is the subject of this review.

---

<sup>1</sup>Note that this statement applies to individual atoms, molecules and zero-pressure condensed matter. In a medium, when the density or temperature is sufficiently high, the magnetic effects can be smeared out even for  $b \gg 1$ ; see Sec. VI. The strong field condition is also modified by the ion charge; see Sec. III.C.

## A. Astrophysics Motivation

Strong magnetic fields with  $b \gg 1$  exist on the surfaces on neutron stars (NSs). Most radio pulsars and accreting NSs in X-ray binaries have surface fields in the range of  $10^{12} - 10^{13}$  G; even recycled millisecond pulsars and old NS's in low-mass X-ray binaries have fields  $B = 10^8 - 10^9$  G (e.g., Lyne and Graham-Smith 1998; Lewin *et al.* 1995). The physical upper limit to the NS magnetic field strength follows from the virial theorem of magnetohydrostatic equilibrium (Chandrasekhar & Fermi 1953; see Shapiro and Teukolsky 1983). The magnetic energy of the NS (mass  $M_{\text{NS}}$ , radius  $R_{\text{NS}}$ ),  $(4\pi R_{\text{NS}}^3/3)(B^2/8\pi)$ , can never exceed its gravitational binding energy,  $\sim GM_{\text{NS}}^2/R_{\text{NS}}$ ; this gives

$$B \lesssim 10^{18} \left( \frac{M_{\text{NS}}}{1.4M_{\odot}} \right) \left( \frac{R_{\text{NS}}}{10 \text{ km}} \right)^{-2} \text{ G.} \quad (1.4)$$

It has been suggested that magnetic fields of order  $10^{15}$  G or stronger can be generated by dynamo processes in proto-neutron stars (Thompson and Duncan 1993), and recent observations (e.g., Vasisht and Gotthelf, 1997; Kouveliotou *et al.*, 1998, 1999; Hurley *et al.* 1999; Kaspi *et al.* 1999; Mereghetti 2000) have lent support to the idea that soft gamma-ray repeaters and slowly spinning (with periods of a few seconds) “anomalous” x-ray pulsars in supernova remnants are NSs endowed with superstrong magnetic fields  $B \gtrsim 10^{14}$  G, the so-called “magnetars” (Duncan and Thompson 1992; Paczyński 1992; Thompson and Duncan, 1995, 1996). Finally, magnetism has been detected in a few dozen white dwarfs (out of a total of about 2000) in the range from  $10^5$  G to  $10^9$  G (e.g., Koester and Chanmugan 1990; Jordan 1998; Wickramasinghe and Ferrario 2000).

The main astrophysical motivation to study matter in strong magnetic fields arises from the importance of understanding NS surface layers, which play a key role in many NS processes and observed phenomena. Theoretical models of pulsar and magnetar magnetospheres depend on the cohesive properties of the surface matter in strong magnetic fields (e.g., Ruderman and Sutherland 1975; Michel 1991; Usov and Melrose 1996; Zhang and Harding 2000). More importantly, the surface layer directly mediates the thermal radiation from the NS. It has long been recognized that NSs are sources of soft X-rays during the  $\sim 10^5 - 10^6$  years of cooling phase after their birth in supernova explosions (Chiu and Salpeter 1964; Tsuruta 1964; Bahcall and Wolf 1965). The cooling history of the NS depends on poorly-constrained interior physics, such as nuclear equation of state, superfluidity and internal magnetic fields (see, e.g., Pethick 1992, Page 1998, Tsuruta 1998, Prakash *et al.* 2000; Yakovlev *et al.* 2001 for review). The advent of imaging X-ray telescopes in recent years has now made it possible to observe isolated NSs directly by their surface radiation. In particular, recent X-ray observatories such as ROSAT have detected pulsed X-ray thermal emission from a number of radio pulsars (see Becker and Trümper 1997, Becker 2000, Becker & Pavlov 2001 for review). Some of the observed X-rays are likely to be produced by nonthermal magnetospheric emission, but at least three pulsars (PSR B1055-52, B0656+14, Geminga) show emission dominated by a thermal component emitted from the whole NS surface, with temperatures in the range  $(2 - 10) \times 10^5$  K. A few of the X-ray emitting radio pulsars show thermal-like radiation of higher temperatures, in the range  $(1 - 5) \times 10^6$  K, from an area much smaller than that of the stellar surface, indicating a hot polar cap on the NS surface. Several nearby pulsars have also been detected in the extreme ultraviolet (Edelstein, Foster and Bowyer 1995; Korpela and Bowyer 1998) and in the optical band (e.g., Pavlov *et al.* 1997; Caraveo *et al.* 2000) with spectra consistent with thermal radiation from NS surfaces. On the other hand, old isolated NSs ( $10^8 - 10^9$  of which are thought to exist in the Galaxy), heated through accretion from interstellar material, are also expected to be common sources of soft X-ray/EUV emission (e.g, Treves and Colpi 1991; Blaes and Madau 1993; Treves *et al.* 2000). Several radio-quiet isolated accreting NSs have been detected in the X-ray and optical band (e.g., Walter, Wolk and Neuhäuser 1996; Caraveo, Bignami and Trümper 1996; Walter and Matthews 1997). Finally, the quiescent X-ray emissions from soft gamma-ray repeaters and anomalous X-ray pulsars may be powered by the internal heating associated with decaying magnetic fields (Thompson and Duncan 1996). The X-rays originate near the stellar surface, and therefore allow one to probe radiative transport in the superstrong field regime. Observations indicate that some of the sources (particularly anomalous X-ray pulsars) have a thermal component in their X-ray spectra (e.g., Mereghetti 2000). Overall, the detections of surface emission from NSs can provide invaluable information on the structure and evolution of NSs, and enable one to put constraints on the nuclear equation of state, various heating/accretion processes, magnetic field structure and surface chemical composition. The recently launched X-ray telescopes, including Chandra X-ray Observatory and XMM-Newton Observatory, have much improved sensitivity and spectral resolution in the soft X-ray band, making it promising for spectroscopic studies of isolated or slowly-accreting NSs. Since the surface layer/atmosphere directly determines the characteristics of the thermal emission, proper interpretations of the observations require a detailed understanding of the physical properties of the NS envelope in the presence of intense magnetic fields ( $B \gtrsim 10^{12}$  G).

## B. Laboratory Physics Motivation

The highest static magnetic field currently produced in a terrestrial laboratory is 45 Tesla ( $4.5 \times 10^5$  G), far below  $B_0$ ; stronger transient field of order  $10^3$  Tesla can be produced using explosive flux compression techniques, but this is still below  $B_0$  (e.g., Crow *et al.* 1998). However, high magnetic-field conditions can be mimicked in some semiconductors where a small effective electron mass  $m_*$  and a large dielectric constant  $\varepsilon$  reduce the Coulomb force relative to the magnetic force. For hydrogen-like excitons in semiconductors, the atomic unit of length is  $a_{0*} = \varepsilon \hbar^2 / (m_* e^2)$ , and the corresponding natural unit for magnetic field is  $B_{0*} = m_*^2 e^3 c / (\varepsilon^2 \hbar^3)$ . For example, in GaAs, the dielectric constant is  $\varepsilon = 12.56$ , and the electron bound to a positively charged donor has an effective mass  $m_* = 0.00665 m_e$ , thus  $B_{0*} = 6.57$  Tesla. The critical field  $B_{0*}$  can be as small as 0.2 Tesla for InSb. Such a low value of  $B_{0*}$  implies that the structure of excitons, biexcitonic molecules and quantum dots (which resemble multi-electron atoms; see Kastner 1992) in semiconductors must experience significant changes already in laboratory magnetic fields (e.g., Timofeev and Chernenko 1995; Lieb *et al.* 1995; Klaassen *et al.* 1998). Some of the earliest studies of atoms in superstrong magnetic fields (Elliot and Loudon 1960; Hasegawa and Howard 1961) were motivated by applications in semiconductor physics.

## C. Plan of This Paper

In this paper we review the properties of different forms of matter (atoms, molecules and bulk condensed matter) in strong magnetic fields. We also discuss astrophysical situations where magnetized matter plays an important role. We shall focus on magnetic field strengths in the range of  $B \gg 10^9$  G so that  $b \gg 1$  is well-satisfied, although in several places (Sec. III.D and Sec. IV.E) we will also touch upon issues for  $b \gtrsim 1$ . Throughout the paper, our emphasis is on physical understanding and analytic approximate relations (whenever they exist), rather than on computational techniques for the electronic structure calculations, although we will discuss the later aspects and provide pointers to the literature.

This paper is organized as follows. After a brief summary of the basics of electron Landau levels in Section II, we discuss the physics of various bound states in strong magnetic fields in Section III (Atoms), Section IV (Molecules) and Section V (Condensed Matter). Section VI summarizes the thermodynamic properties of free electron gas (at finite density and temperature). In Section VII we review the physical properties of the envelope of a strongly magnetized neutron star.

Throughout the paper we shall use real physical units and atomic units (a.u.) interchangeably, whichever is more convenient. Recall that in atomic units, mass and length are expressed in units of the electron mass  $m_e$  and the Bohr radius  $a_0 = 0.529 \times 10^{-8}$  cm, energy in units of  $2 \text{ Ryd} = e^2/a_0 = 2 \times 13.6$  eV; field strength in units of  $B_0$  [Eq. (1.3)], temperature in units of  $3.16 \times 10^5$  K, and pressure in units of  $e^2/a_0^4 = 2.94 \times 10^{14}$  dynes  $\text{cm}^{-2}$ .

## D. Bibliographic Notes

Theoretical research on matter in superstrong magnetic fields started in the early sixties. A large number of papers have been written on the subject over the years and they are scattered in astrophysics atomic/molecular physics and condensed matter physics literatures. Although we have tried to identify original key papers whenever possible, our references put more emphasis on recent works from which earlier papers can be found. We apologize to the authors of the relevant papers which are not mentioned here.

In recent years there has been no general review article that covers the broad subject of matter in strong magnetic fields, although good review articles exist on aspects of the problem. Extensive review of atoms (especially for H and He) in strong magnetic fields, including tabulations of numerical results, can be found in the monograph “Atoms in Strong Magnetic Fields” by Ruder *et al.* (1994). A recent reference is the conference proceedings on “Atoms and Molecules in Strong Magnetic Fields” edited by Schmelcher and Schweizer (1998). An insightful, short review of earlier works is Ruderman (1974). Other reviews on general physics in strong magnetic fields include Canuto and Ventura (1977) and the monograph by Meszaros (1992).

## II. BASICS ON LANDAU LEVELS

The quantum mechanics of a charged particle in a magnetic field is presented in many texts (e.g., Landau and Lifshitz 1977; Canuto and Ventura 1977; Sokolov and Ternov 1968; Mészáros 1992). Here we summarize the basics needed for our later discussion.

For a free particle of charge  $e_i$  and mass  $m_i$  in a constant magnetic field (assumed to be along the  $z$ -axis), the kinetic energy of transverse motion is quantized into Landau levels

$$E_{\perp} = \frac{1}{2}m_i\mathbf{v}_{\perp}^2 = \frac{1}{2m_i}\mathbf{\Pi}_{\perp}^2 \rightarrow \left(n_L + \frac{1}{2}\right)\hbar\omega_c, \quad n_L = 0, 1, 2, \dots \quad (2.1)$$

where  $\omega_c = |e_i|B/(m_i c)$  is the cyclotron (angular) frequency,  $\mathbf{\Pi} = \mathbf{P} - (e_i/c)\mathbf{A} = m_i\mathbf{v}$  is the mechanical momentum,  $\mathbf{P} = -i\hbar\nabla$  is the canonical momentum, and  $\mathbf{A}$  is the vector potential of the magnetic field.

A Landau level is degenerate, reflecting the fact that the energy is independent of the location of the guiding center of the gyration. To count the degeneracy, it is useful to define the *pseudomomentum* (or the generalized momentum)

$$\mathbf{K} = \mathbf{\Pi} + (e_i/c)\mathbf{B} \times \mathbf{r}. \quad (2.2)$$

That  $\mathbf{K}$  is a constant of motion (i.e., it commutes with the Hamiltonian) can be easily seen from the classical equation of motion for the particle,  $d\mathbf{\Pi}/dt = (e_i/c)(d\mathbf{r}/dt) \times \mathbf{B}$ . Mathematically, the conservation of  $\mathbf{K}$  is the result of the invariance of the Hamiltonian under a spatial translation plus a gauge transformation (Avron *et al.* 1978). The parallel component  $K_z$  is simply the linear momentum, while the constancy of the perpendicular component  $\mathbf{K}_{\perp}$  is the result of the fact that the guiding center of the gyro-motion does not change with time. The position vector  $\mathbf{R}_c$  of this guiding center is related to  $\mathbf{K}_{\perp}$  by

$$\mathbf{R}_c = \frac{c\mathbf{K}_{\perp} \times \mathbf{B}}{e_i B^2} = \frac{c}{e_i B}\mathbf{\Pi}_{\perp} \times \hat{\mathbf{B}} + \mathbf{r}_{\perp}, \quad (2.3)$$

( $\hat{\mathbf{B}}$  is the unit vector along  $\mathbf{B}$ ). Clearly, the radius of gyration,  $\rho = m_i c v_{\perp}/(|e_i|B)$ , is quantized according to

$$|\mathbf{r}_{\perp} - \mathbf{R}_c| = \frac{c}{|e_i|B}|\mathbf{\Pi}_{\perp}| \rightarrow (2n_L + 1)^{1/2}\hat{\rho}, \quad (2.4)$$

where

$$\hat{\rho} = \left(\frac{\hbar c}{|e_i|B}\right)^{1/2} = b^{-1/2} \quad (2.5)$$

is the cyclotron radius (or the magnetic length). We can use  $\mathbf{K}$  to classify the eigenstates. However, since the two components of  $\mathbf{K}_{\perp}$  do not commute,  $[K_x, K_y] = -i\hbar(e_i/c)B$ , only one of the components can be diagonalized for stationary states. This means that the guiding center of the particle can not be specified. If we use  $K_x$  to classify the states, then the wavefunction has the well-known form  $e^{K_x x/\hbar}\phi(y)$  (Landau and Lifshitz 1977), where the function  $\phi(y)$  is centered at  $y_c = -cK_x/(e_i B)$  [see Eq. (2.3)]. The Landau degeneracy in an area  $\mathcal{A}_g = L_g^2$  is thus given by

$$\frac{L_g}{h} \int dK_x = \frac{L_g}{h}|K_{x,g}| = \mathcal{A}_g \frac{|e_i|B}{hc} = \frac{\mathcal{A}_g}{2\pi\hat{\rho}^2}, \quad (2.6)$$

where we have used  $K_{x,g} = -e_i B L_g/c$ . On the other hand, if we choose to diagonalize  $K_{\perp}^2 = K_x^2 + K_y^2$ , we obtain the Landau wavefunction  $W_{nm}(\mathbf{r}_{\perp})$  in cylindrical coordinates (Landau and Lifshitz 1977), where  $m$  is the ‘‘orbital’’ quantum number (denoted by  $s$  or  $-s$  in some references). For the ground Landau level, this is (for  $e_i = -e$ )

$$W_{0m}(\mathbf{r}_{\perp}) \equiv W_m(\rho, \phi) = \frac{1}{(2\pi m!)^{1/2}\hat{\rho}} \left(\frac{\rho}{\sqrt{2}\hat{\rho}}\right)^m \exp\left(\frac{\rho^2}{4\hat{\rho}^2}\right) \exp(-im\phi), \quad (2.7)$$

where the normalization  $\int d^2\mathbf{r}_{\perp} |W_m|^2 = 1$  is adopted. The (transverse) distance of the guiding center of the particle from the origin of the coordinates is given by

$$|\mathbf{R}_c| \rightarrow \rho_m = (2m + 1)^{1/2}\hat{\rho}, \quad m = 0, 1, 2, \dots \quad (2.8)$$

The corresponding value of  $K_{\perp}$  is  $K_{\perp}^2 = (\hbar|e_i|B/c)(2m + 1)$ . Note that  $K_{\perp}^2$  assumes discrete values since  $m$  is required to be an integer in order for the wavefunction to be single-valued. The degeneracy  $m_g$  of the Landau level in an area  $\mathcal{A}_g = \pi R_g^2$  is then determined by  $\rho_{m_g} \simeq (2m_g)^{1/2}\hat{\rho} = R_g$ , which again yields  $m_g = \mathcal{A}_g|e_i|B/(hc)$  as in Eq. (2.6). We shall refer to different  $m$ -states as different Landau orbitals. Note that despite the similarity between equations (2.8) and (2.4), their physical meanings are quite different: the circle  $\rho = \rho_m$  does not correspond to any gyro-motion of the particle, and the energy is independent of  $m$ .

We also note that  $K_{\perp}^2$  is related to the  $z$ -projection of angular momentum  $J_z$ , as is evident from the  $e^{-im\phi}$  factor in the cylindrical wavefunction [Eq. (2.7)]. In general, we have

$$\begin{aligned} J_z &= xP_y - yP_x = \frac{1}{2e_i B}(\mathbf{K}_{\perp}^2 - \mathbf{\Pi}_{\perp}^2) \\ &= (m - n_L) \frac{|e_i|}{e_i}, \end{aligned} \quad (2.9)$$

where we have used  $\mathbf{\Pi}_{\perp}^2 = (\hbar|e_i|/c)B(2n_L + 1)$ .

Including the spin energy of the electron ( $e_i \rightarrow -e$ ,  $\omega_c \rightarrow \omega_{ce}$ ),  $E_{\sigma_z} = e\hbar/(2m_e c)\boldsymbol{\sigma} \cdot \mathbf{B} = \hbar\omega_{ce}\sigma_z/2$ , the total electron energy can be written as

$$E = n_L \hbar\omega_{ce} + \frac{p_z^2}{2m_e}, \quad (2.10)$$

where the index  $n_L$  now includes the spin. For the ground Landau level ( $n_L = 0$ ), the spin degeneracy is one ( $\sigma_z = -1$ ); for excited levels, the spin degeneracy is two.

For extremely strong magnetic fields such that  $\hbar\omega_{ce} \gtrsim m_e c^2$ , or

$$B \gtrsim B_{\text{rel}} = \frac{m_e^2 c^3}{e\hbar} = \frac{B_0}{\alpha^2} = 4.414 \times 10^{13} \text{ G}, \quad (2.11)$$

( $\alpha = e^2/\hbar c$  is the fine structure constant), the transverse motion of the electron becomes relativistic. Equation (2.10) for the energy of a free electron should be replaced by (e.g., Johnson and Lippmann 1949)

$$E = [c^2 p_z^2 + m_e^2 c^4 (1 + 2n_L \beta)]^{1/2}, \quad (2.12)$$

where

$$\beta \equiv \frac{B}{B_{\text{rel}}} = \alpha^2 b. \quad (2.13)$$

Higher order corrections in  $e^2$  to Eq. (2.12) have the form  $(\alpha/4\pi)m_e c^2 F(\beta)$ , with  $F(\beta) = -\beta$  for  $\beta \ll 1$  and  $F(\beta) = [\ln(2\beta) - (\gamma + 3/2)]^2 + \dots$  for  $\beta \gg 1$ , where  $\gamma = 0.5772$  is Euler's constant (Schwinger 1988); these corrections will be neglected.

When studying bound states (atoms, molecules and condensed matter near zero pressure) in strong magnetic fields (Sec. III-Sec. V), we shall use nonrelativistic quantum mechanics, even for  $B \gtrsim B_{\text{rel}}$ . The nonrelativistic treatment of bound states is valid for two reasons: (i) For electrons in the ground Landau level, the free electron energy reduces to  $E \simeq m_e c^2 + p_z^2/(2m_e)$ ; the electron remains nonrelativistic in the  $z$ -direction (along the field axis) as long as the binding energy  $E_B$  is much less than  $m_e c^2$ ; (ii) The shape of the Landau wavefunction in the relativistic theory is the same as in the nonrelativistic theory, as seen from the fact that  $\hat{\rho}$  is independent of the particle mass. Therefore, as long as  $E_B/(m_e c^2) \ll 1$ , the relativistic effect on bound states is a small correction (Angelier and Deutch 1978). For bulk matter under pressure, the relativistic correction becomes increasingly important as density increases (Sec. VI).

### III. ATOMS

#### A. Hydrogen Atom

In a strong magnetic field with  $b \gg 1$ , the electron is confined to the ground Landau level ("adiabatic approximation"), and the Coulomb potential can be treated as a perturbation. Assuming infinite proton mass (see Sec. III.E), the energy spectrum of the H atom is specified by two quantum numbers,  $(m, \nu)$ , where  $m$  measures the mean transverse separation [Eq. (2.8)] between the electron and the proton, while  $\nu$  specifies the number of nodes in the  $z$ -wavefunction. We may write the electron wavefunction as  $\Phi_{m\nu}(\mathbf{r}) = W_m(\mathbf{r}_{\perp})f_{m\nu}(z)$ . Substituting this function into the Schrödinger equation and averaging over the transverse direction we obtain a one-dimensional Schrödinger equation for  $f_{m\nu}(z)$ :

$$-\frac{\hbar^2}{2m_e \hat{\rho}^2} f_{m\nu}'' - \frac{e^2}{\hat{\rho}} V_m(z) f_{m\nu} = E_{m\nu} f_{m\nu}, \quad (m, \nu = 0, 1, 2, \dots) \quad (3.1)$$

The averaged potential is given by

$$V_m(z) = \int d^2\vec{r}_\perp |W_m(\vec{r}_\perp)|^2 \frac{1}{r}. \quad (3.2)$$

Here and henceforth we shall employ  $\hat{\rho}$  as our length unit in all the wavefunctions and averaged potentials, making them dimensionless functions (thus,  $f''_{m\nu} = d^2 f_{m\nu}(z)/dz^2$ , with  $z$  in units of  $\hat{\rho}$ ).

There are two distinct types of states in the energy spectrum  $E_{m\nu}$ . The “tightly bound” states have no node in their  $z$ -wavefunctions ( $\nu = 0$ ). The transverse size of the atom in the  $(m, 0)$  state is  $L_\perp \sim \rho_m = [(2m+1)/b]^{1/2}$ . For  $\rho_m \ll 1$ , the atom is elongated with  $L_z \gg L_\perp$ . We can estimate the longitudinal size  $L_z$  by minimizing the energy,  $E \sim L_z^{-2} - L_z^{-1} \ln(L_z/L_\perp)$ , giving

$$L_z \sim \frac{1}{2 \ln(1/\rho_m)} = l_m^{-1}, \quad (3.3)$$

where

$$l_m \equiv \ln \frac{b}{2m+1}. \quad (3.4)$$

The energy of the tightly bound state is then

$$E_m \simeq -0.16A l_m^2 \quad (\text{for } 2m+1 \ll b) \quad (3.5)$$

(recall that the energy is in units of 1 a.u. =  $e^2/a_0$ ). For  $\rho_m \gtrsim 1$ , or  $2m+1 \gtrsim b$  [but still  $b \gg (2m+1)^{-1}$  so that the adiabatic approximation ( $|E_m| \ll b$ ) is valid], we have  $L_z \sim \rho_m^{1/2}$ , and the energy levels are approximated by

$$E_m \simeq -0.6 \left( \frac{b}{2m+1} \right)^{1/2} \quad [\text{for } 2m+1 \gtrsim b \gg (2m+1)^{-1}]. \quad (3.6)$$

In Eqs. (3.5) and (3.6), the numerical coefficients are obtained from numerical solutions of the Schrödinger equation (3.1); the coefficient  $A$  in (3.5) is close to unity for the range of  $b$  of interest ( $1 \ll b \lesssim 10^6$ ) and varies slowly with  $b$  and  $m$  (e.g.,  $A \simeq 1.01 - 1.3$  for  $m = 0 - 5$  when  $B_{12} = 1$ , and  $A \simeq 1.02 - 1.04$  for  $m = 0 - 5$  when  $B_{12} = 10$ ). Note that  $E_m$  asymptotically approaches  $-0.5 l_m^2$  when  $b \rightarrow \infty$ ; see Hasagawa & Howard 1961 and Haines & Roberts 1969). For the ground state,  $(m, \nu) = (0, 0)$ , the sizes of the atomic wavefunction perpendicular and parallel to the field are of order  $L_\perp \sim \hat{\rho} = b^{-1/2}$  and  $L_z \sim l_0^{-1}$ , where  $l_0 \equiv \ln b$ . The binding energy  $|E(\text{H})|$  (or the ionization energy  $Q_1$ ) of the atom is given by

$$Q_1 = |E(\text{H})| \simeq 0.16A l_0^2, \quad (3.7)$$

where  $A$  can be approximated by  $A = 1 + 1.36 \times 10^{-2} [\ln(1000/b)]^{2.5}$  for  $b < 10^3$  and  $A = 1 + 1.07 \times 10^{-2} [\ln(b/1000)]^{1.6}$  for  $b \geq 10^3$  (this is accurate to within 1% for  $100 \lesssim b \lesssim 10^6$ ). Figure 1 depicts  $Q_1$  as a function of  $B$ . Numerical values of  $Q_1$  for selected  $B$ 's are given in Table I. Numerical values of  $E_m$  for different  $B$ 's can be found, for example, in Ruder *et al.* (1994). A fitting formula for  $E_m$  (accurate to within 0.1 – 1% at  $0.1 \lesssim b \lesssim 10^4$ ) is given by Potekhin (1998):

$$E_m = -\frac{1}{2} \ln \left\{ \exp [(1+m)^{-2}] + p_1 [\ln(1+p_2 b^{0.5})]^2 \right\} - \frac{1}{2} p_3 [\ln(1+p_4 b^{p_5})]^2, \quad (3.8)$$

where  $p_1 - p_5$  are independent of  $b$  (for the  $m = 0$  state, the parameters  $p_1 - p_5$  are 15.55, 0.378, 2.727, 0.3034 and 0.438, respectively). Note that, unlike the field-free case, the excitation energy  $\Delta E_m = |E(\text{H})| - |E_m|$  is small compared to  $|E(\text{H})|$ .

Another type of states of H atom have nodes in the  $z$ -wavefunctions ( $\nu > 0$ ). These states are “weakly bound”. For example, the  $\nu = 1$  state has about the same binding energy as the ground state of a zero-field H atom,  $E \simeq -13.6$  eV, since the equation governing this odd-parity state is almost the same as the radial equation satisfied by the  $s$ -state of the zero-field H atom. The energy levels of the weakly bound states are approximately given by (Haines and Roberts 1969)

$$E_{m\nu} = -\frac{1}{2(\nu_1 + \delta)^2}, \quad (\nu_1 = 1, 2, 3, \dots) \quad (3.9)$$

TABLE I. Energy releases (in eV) in various atomic and molecular processes in a strong magnetic field; the values of  $Q$ 's give the relative binding energies of different forms of hydrogen in the ground state. Here  $B_{12} = B/(10^{12} \text{ G})$ . The zero-point energies of the protons have been ignored in calculating the  $Q$ 's for molecules. For  $\text{H}_2$ , the two columns give  $Q_2^{(\infty)}$  (with infinite proton mass) and  $Q_2$  [including zero-point energy correction; see Eq. (4.10)]; for  $\text{H}_\infty$ , the two columns give  $Q_\infty^{(\infty)}$  (with infinite proton mass) and  $Q_\infty$  [including zero-point energy correction; see Eq. (5.21)]. Note that for  $B_{12} \lesssim 0.25$ , the lowest energy state of  $\text{H}_2$  corresponds to the weakly bound state, while for  $B_{12} \gtrsim 0.25$ , the tightly bound state is the ground state (see Sec. IV.C). The results are obtained using the numerical methods described in Lai *et al.* (1992) and Lai and Salpeter (1996). The numbers are generally accurate to within 10%.

$B_{12}$	e+p=H	H+e=H <sup>-</sup>	H+p=H <sub>2</sub> <sup>+</sup>	H+H=H <sub>2</sub>		H <sub>∞</sub> +H=H <sub>∞+1</sub>	
	$Q_1$	$Q(\text{H}^-)$	$Q(\text{H}_2^+)$	$Q_2^{(\infty)}$	$Q_2$	$Q_\infty^{(\infty)}$	$Q_\infty$
0.1	76.4	6.9	23.6	14	(13)	3.8	(1.2)
0.5	130	11	51.8	31	(21)	16.3	(10)
1	161	13	70.5	46	(32)	29	(20)
5	257	20	136	109	(80)	91	(71)
10	310	24	176	150	(110)	141	(113)
50	460	37	308	294	(236)	366	(306)
100	541	42	380	378	(311)	520	(435)
500	763	57	599	615	(523)	1157	(964)
1000	871	64	722	740	(634)	1630	(1350)

where

$$\delta = \begin{cases} 2\rho_m/a_0, & \text{for } \nu = 2\nu_1 - 1; \\ [\ln(a_0/\rho_m)]^{-1}, & \text{for } \nu = 2\nu_1. \end{cases} \quad (3.10)$$

[More accurate fitting formula for  $\delta$  is given in Potekhin (1998)]. The sizes of the wavefunctions are  $\rho_m$  perpendicular to the field and  $L_z \sim \nu^2 a_0$  along the field.

The above results assume a fixed Coulomb potential produced by the proton (i.e., infinite proton mass). The use of a reduced electron mass  $m_e m_p / (m_e + m_p)$  introduces a very small correction to the energy [of order  $(m_e/m_p)|E_{m\nu}|$ ]. However, in strong magnetic fields, the effect of the center-of-mass motion on the energy spectrum is complicated. An analysis of the two-body problem in magnetic fields shows that even for the H atom “at rest”, there is a proton cyclotron correction,  $m\hbar\omega_{cp} = m(m_e/m_p)b$  a.u., to the energy [see Eq. (3.40)]. We will return to this issue in Sec. III.E.

## B. High- $Z$ Hydrogenic Ions

The result in Sec. III.A can be easily generalized to hydrogenic ions (with one electron and nuclear charge  $Z$ ). The adiabatic approximation (where the electron lies in the ground Landau level) holds when  $\hat{\rho} \ll a_0/Z$ , or

$$b \gg Z^2. \quad (3.11)$$

For a tightly bound state,  $(m, \nu) = (m, 0)$ , the transverse size is  $L_\perp \sim \rho_m$ , while the longitudinal size is

$$L_z \sim \left( Z \ln \frac{1}{Z\rho_m} \right)^{-1}. \quad (3.12)$$

The energy is given by

$$E_m \simeq -0.16 AZ^2 \left[ \ln \frac{1}{Z^2} \left( \frac{b}{2m+1} \right) \right]^2 \quad (3.13)$$

for  $b \gg (2m+1)Z^2$ . Results for the weakly bound states ( $\nu > 0$ ) can be similarly generalized from Eqs. (3.9)-(3.10).

## C. Heavy Atoms

We can imagine constructing a multi-electron atom by placing electrons at the lowest available energy levels of a hydrogenic ion. This picture also forms the basis for more detailed calculations of heavy atoms which include electron-electron interactions in a self-consistent manner.

### 1. Approximate Scaling Relations

The lowest levels to be filled are the tightly bound states with  $\nu = 0$ . When  $a_0/Z \gg \sqrt{2Z-1}\hat{\rho}$ , i.e.,

$$b \gg 2Z^3, \quad (3.14)$$

all electrons settle into the tightly bound levels with  $m = 0, 1, 2, \dots, Z-1$ . The energy of the atom is approximately given by the sum of all the eigenvalues of Eq. (3.13). Accordingly, we obtain an asymptotic expression for  $Z \gg 1$  (Kadomtsev and Kudryavtsev 1971)

$$E \sim -Z^3 l_Z^2, \quad (3.15)$$

where

$$l_Z = \ln\left(\frac{a_0}{Z\sqrt{2Z-1}\hat{\rho}}\right) \simeq \ln\sqrt{\frac{b}{2Z^3}}. \quad (3.16)$$

The size of the atom is given by

$$L_\perp \sim (2Z-1)^{1/2}\hat{\rho}, \quad L_z \sim \frac{a_0}{Zl_Z}. \quad (3.17)$$

For intermediate-strong fields (but still strong enough to ignore the Landau excitation),

$$Z^{4/3} \ll b \ll 2Z^3, \quad (3.18)$$

many  $\nu > 0$  states of the inner Landau orbitals (states with relatively small  $m$ ) are populated by the electrons. In this regime a Thomas-Fermi type model for the atom is appropriate (at least for the ‘‘core’’ electrons in small Landau orbitals), i.e., the electrons can be treated as a one-dimensional Fermi gas in a more or less spherical atomic cavity (Kadomtsev 1970; Mueller *et al.* 1971). The electrons occupy the ground Landau level, with the  $z$ -momentum up to the Fermi momentum  $p_F \sim n_e/b$ , where  $n_e$  is the number density of electrons inside the atom (recall that the degeneracy of a Landau level is  $eB/hc \sim b$ ). The kinetic energy of electrons per unit volume is  $\varepsilon_k \sim b p_F^3 \sim n_e^3/b^2$ , and the total kinetic energy is  $E_k \sim R^3 n_e^3/b^2 \sim Z^3/b^2 R^6$ , where  $R$  is the radius of the atom. The potential energy is  $E_p \sim -Z^2/R$ . Therefore the total energy of the atom can be written as

$$E \sim \frac{Z^3}{b^2 R^6} - \frac{Z^2}{R}. \quad (3.19)$$

Minimizing  $E$  with respect to  $R$  yields

$$R \sim Z^{1/5} b^{-2/5}, \quad E \sim -Z^{9/5} b^{2/5}. \quad (3.20)$$

For these relations to be valid, the electrons must stay in the ground Landau level; this requires  $Z/R \ll \hbar\omega_{ce} = b$ , which corresponds to  $b \gg Z^{4/3}$ . More elaborate Thomas-Fermi type models have been developed for this regime, giving approximately the same scaling relations (see Appendix B).

We now consider multi-electron negative ions. First imagine forming a  $\text{H}^-$  ion by attaching an extra electron to a H atom in the ground state (with  $m = 0$ ). The extra electron can only settle into the  $m = 1$  state, which, if we ignore the screening of the proton potential due the first ( $m = 0$ ) electron, has a binding energy of  $|E_1|$  as in Eq. (3.5). The Coulomb repulsion between the two electrons reduces the binding of the  $m = 1$  electron. The repulsive energy is of order  $(\ln\sqrt{b})/L_z$ , which is of the same order as  $|E_1|$ . But the repulsive energy is smaller than  $|E_1|$  because of the cylindrical charge distribution of both electrons. Therefore  $\text{H}^-$  is bound relative to  $\text{H}+e$  and its ionization potential is proportional to  $(\ln\sqrt{b})^2$ .

Similar consideration can be applied to a  $Z$ -ion (nuclear charge  $Z$ ) with  $N$  electrons in the superstrong field regime ( $b \gg Z^3$ ) (Kadomtsev and Kudryavtsev 1971). The sizes of the ion perpendicular and parallel to the field are, respectively,

$$R \sim \sqrt{\frac{2N-1}{b}}, \quad L_z \sim \frac{1}{Zl}, \quad \text{with } l = \ln\left(\frac{L_z}{R}\right). \quad (3.21)$$

The ground state energy of the ion is

$$E \simeq -\frac{N}{8} l^2 (4Z - N + 1)^2. \quad (3.22)$$

Applying this result for hydrogen ions ( $Z = 1$ ), we see that the ionization potential of  $\text{H}^-$  to  $\text{H}+e$  is about 1/10 of the binding energy of the H atom. Also we see that for  $n > 2$ , the negative ion  $\text{H}^{-(n-1)}$  is unbound. This estimate is confirmed by numerical calculations (Lai, Salpeter and Shapiro 1992).

## 2. Numerical Calculations and Results

Reliable values for the energy of a multi-electron atom for  $b \gg 1$  can be calculated using the Hartree-Fock method (Virtamo 1976; Pröschel *et al.* 1982; Neuhauser *et al.* 1987). For an electron in the ground Landau level with spin aligned antiparallel to the magnetic field (“adiabatic approximation”), the kinetic energy and spin energy add up to  $(1/2m_e)p_z^2$ . Thus the Hamiltonian for a neutral atom with  $Z$  electrons is

$$H = \sum_i \frac{1}{2m_e} p_{zi}^2 - Ze^2 \sum_i \frac{1}{r_i} + e^2 \sum_{i<j} \frac{1}{r_{ij}}, \quad (3.23)$$

where  $i$  labels electrons. The basis one-electron wavefunctions are

$$\Phi_{m\nu}(\mathbf{r}) = W_m(\rho, \phi) f_{m\nu}(z), \quad m, \nu = 0, 1, 2, \dots \quad (3.24)$$

In the Hartree-Fock approximation, the  $Z$ -electron wave function is formed by the antisymmetrized product of  $Z$  one-electron basis functions. Averaging the Hamiltonian over the transverse Landau functions, we obtain

$$\begin{aligned} \langle H \rangle &= \frac{\hbar^2}{2m_e \hat{\rho}^2} \sum_{m\nu} \int dz |f'_{m,\nu}(z)|^2 - \frac{Ze^2}{\hat{\rho}} \sum_{m\nu} \int dz |f_{m,\nu}(z)|^2 V_m(z) \\ &\quad + E_{\text{dir}} + E_{\text{exch}}, \end{aligned} \quad (3.25)$$

where  $V_m(z)$  is given by Eq. (3.2). The direct and exchange energies for electron-electron interaction are given by

$$E_{\text{dir}} = \frac{e^2}{2\hat{\rho}} \sum_{m\nu, m'\nu'} \int dz dz' D_{mm'}(z - z') |f_{m\nu}(z)|^2 |f_{m'\nu'}(z')|^2, \quad (3.26)$$

$$E_{\text{exch}} = -\frac{e^2}{2\hat{\rho}} \sum_{m\nu, m'\nu'} \int dz dz' E_{mm'}(z - z') f_{m\nu}(z) f_{m'\nu'}(z') f_{m\nu}^*(z') f_{m'\nu'}^*(z). \quad (3.27)$$

where

$$D_{mm'}(z_1 - z_2) = \int d^2 \mathbf{r}_{1\perp} d^2 \mathbf{r}_{2\perp} |W_m(\mathbf{r}_{1\perp})|^2 |W_{m'}(\mathbf{r}_{2\perp})|^2 \frac{1}{r_{12}}, \quad (3.28)$$

$$E_{mm'}(z_1 - z_2) = \int d^2 \mathbf{r}_{1\perp} d^2 \mathbf{r}_{2\perp} W_m(\mathbf{r}_{1\perp}) W_{m'}(\mathbf{r}_{2\perp}) W_m^*(\mathbf{r}_{2\perp}) W_{m'}^*(\mathbf{r}_{1\perp}) \frac{1}{r_{12}}. \quad (3.29)$$

(Useful mathematical relations for evaluating  $V_m, D_{mm'}, E_{mm'}$  are given in, e.g., Sokolov and Ternov 1968; Virtamo and Jauho 1975; Pröschel *et al.* 1982; Lai *et al.* 1992). Varying  $\langle H \rangle$  with respect to  $f_{m\nu}$ 's, we obtain the Hartree-Fock equations

$$\left[ -\frac{\hbar^2}{2m_e \hat{\rho}^2} \frac{d^2}{dz^2} - \frac{Ze^2}{\hat{\rho}} V_m(z) + \frac{e^2}{\hat{\rho}} K_m(z) - \varepsilon_{m\nu} \right] f_{m\nu}(z) = \frac{e^2}{\hat{\rho}} J_{m\nu}(z), \quad (3.30)$$

where the direct and exchange potentials are

$$K_m(z) = \sum_{m'\nu'} \int dz' |f_{m'\nu'}(z')|^2 D_{mm'}(z - z'), \quad (3.31)$$

$$J_{m\nu}(z) = \sum_{m'\nu'} f_{m'\nu'}(z) \int dz' f_{m'\nu'}^*(z') f_{m\nu}(z') E_{mm'}(z - z'). \quad (3.32)$$

After iteratively solving Eqs. (3.30)-(3.32) for the eigenvalues  $\varepsilon_{m\nu}$  and eigenfunction  $f_{m\nu}$ , the total energy of the atom can be obtained from

$$E = \sum_{m\nu} \varepsilon_{m\nu} - E_{\text{dir}} - E_{\text{exch}}. \quad (3.33)$$

Accurate energies of He atom as a function of  $B$  in the adiabatic approximation (valid for  $b \gg Z^2$ ) were obtained by Virtamo (1976) and Pröschel *et al.* (1982). This was extended to  $Z$  up to 26 (Fe atom) by Neuhauser *et al.* (1987)

(see also Miller and Neuhauser 1991). Numerical results can be found in these papers. Neuhauser *et al.* (1987) gave an approximate fitting formula

$$E \simeq -160 Z^{9/5} B_{12}^{2/5} \text{ eV} \quad (3.34)$$

for  $0.5 \lesssim B_{12} \lesssim 5$ . (Comparing with the numerical results, the accuracy of the formula is about 1% for  $Z \simeq 18 - 26$  and becomes 5% for  $Z \sim 10$ .) For the He atom, more accurate results (which relax the adiabatic approximation) are given in Ruder *et al.* (1994) and in Jones *et al.* (1999a) (this paper also considers the effect of electron correlation).

The Hartree-Fock method is approximate because electron correlations are neglected. Due to their mutual repulsion, any pair of electrons tend to be more distant from each other than the Hartree-Fock wave function would indicate. In zero-field, this correlation effect is especially pronounced for the spin-singlet states of electrons for which the spatial wave function is symmetrical. In strong magnetic fields, the electron spins are all aligned antiparallel to the magnetic field, the spatial wavefunction is antisymmetric with respect to the interchange of two electrons. Thus the error in the Hartree-Fock approach is expected to be significantly smaller than the 1% accuracy characteristic of zero-field Hartree-Fock calculations (Weissbluth 1978; Neuhauser *et al.* 1987; Schmelcher, Ivanov and Becken 1999).

Other calculations of heavy atoms in strong magnetic fields include Thomas-Fermi type statistical models (see Fushiki *et al.* 1992 for a review and Appendix B for a brief summary) and density functional theory (Jones 1985, 1986; Kössl *et al.* 1988; Relovsky and Ruder 1996). The Thomas-Fermi type models are useful in establishing asymptotic scaling relations, but are not adequate for obtaining accurate binding energy and excitation energies. The density functional theory can potentially give results as accurate as the Hartree-Fock method, but, without calibration with other methods, it is difficult to establish its accuracy *a priori* (see Neuhauser *et al.* 1987; Vignale and Rasolt 1987, 1988). Lieb *et al.* (1992, 1994a, b) have presented detailed discussions of the asymptotic behaviors of heavy atoms (as  $Z \rightarrow \infty$ ) for five different magnetic field regimes:  $b \ll Z^{4/3}$ ,  $b \sim Z^{4/3}$ ,  $Z^{4/3} \ll b \ll Z^3$ ,  $b \sim Z^3$  and  $b \gg Z^3$  [see also eqs. (3.14)-(3.18)]. They showed that various density functional type theories become exact in these asymptotic limits: the Thomas-Fermi theory corresponds to the first three regimes, and a “density-matrix functional” theory can be applied to the fifth regime [see Johnsen & Yngvason (1996) for numerical calculations of heavy atoms based on this theory].

#### D. Intermediate Magnetic Field Regime

For  $B \sim B_0 \sim 10^9$  G, the adiabatic approximation is no longer valid, and electrons can occupy excited Landau levels. In this intermediate field regime, neither Coulomb nor magnetic effects can be treated as a perturbation. Accurate energy levels of H atom for arbitrary field strengths were first calculated by Rösner *et al.* (1984); the method involves expansion of the wavefunction in terms of either spherical harmonics or cylindrical Landau orbitals, and subsequent approximate solution of the system of the coupled integral-differential equations (See Ruder *et al.* 1994 for tabulated numerical results). Recent calculations of H atom in magnetic fields include Goldman and Chen (1991), Chen and Goldman (1992) (relativistic effects), Melezhik (1993), Fassbinder and Schweizer (1996) (with magnetic and electric fields), Kravchenko *et al.* (1996) (exact solution for nonrelativistic electron) and references therein. Ruder *et al.* (1994) presented (less accurate) results for He atoms calculated using a similar Hartree-Fock method as in Rösner *et al.* (1984). Recent studies of multi-electron atoms (including radiative transitions) for intermediate field regime have used more elaborate implementations of Hartree-Fock method with different basis functions (see Jones *et al.* 1996, 1999a, Becken *et al.* 1999, Becken and Schmelcher 2000, Ivanov and Schmelcher 1998, 1999, 2000). Accurate calculation of the hydrogen negative ion ( $\text{H}^-$ ) was presented by Al-Hujaj and Schmelcher (2000) (and references therein). Quantum Monte Carlo method has also been developed to calculate He atom (Jones *et al.* 1997). Accurate energy levels for He atom at  $B \sim 10^9$  G are needed to interpret the spectrum of magnetic white dwarf GD229 (see Jordan *et al.* 1998; Jones *et al.* 1999b).

#### E. Effect of Center-of-Mass Motion

Our discussion so far has implicitly assumed infinite nuclear mass, i.e., we have been concerned with the energy levels of electrons in the static Coulomb potential of a fixed ion. It has long been recognized that in strong magnetic fields, the effects of finite nuclear mass and center-of-mass (CM) motion on the atomic structure are nontrivial (e.g., Gor'kov and Dzyaloshinskii 1968; Avron *et al.* 1978; Herold *et al.* 1981; Baye and Vincke 1990; Vincke *et al.* 1992; Pavlov and Meszaros 1993; Potekhin 1994). Here we illustrate the key issues by considering the hydrogen atom in strong magnetic fields: general quantum mechanical solutions for this two-body problem have been obtained only recently (Vincke *et al.* 1992; Potekhin 1994). Some of the aspects are also important for applications to molecules. A

recent discussion on this subject can be found in Baye and Vincke (1998) (see also Johnson *et al.* 1983 for an earlier review on the general problem of CM motion of atoms and molecules in external fields).

A free electron confined to the ground Landau level, the usual case for  $b \gg 1$ , does not move perpendicular to the magnetic field. Such motion is necessarily accompanied by Landau excitations. When the electron combines with a proton the mobility of the neutral atom across the field depends on the ratio of the atomic excitation energy ( $\sim \ln b$ ) and the Landau excitation energy for the proton,  $\hbar\omega_{cp} = \hbar eB/(m_p c)$ . It is convenient to define a critical field strength  $B_{\text{cm}}$  via (Lai and Salpeter 1995).

$$b_{\text{cm}} \equiv \frac{m_p}{m_e} \ln b_{\text{cm}} = 1.80 \times 10^4; \quad B_{\text{cm}} = b_{\text{cm}} B_0 = 4.23 \times 10^{13} \text{ G}. \quad (3.35)$$

Thus for  $B \gtrsim B_{\text{cm}}$ , the deviation from the free center-of-mass motion of the atom is significant even for small transverse momentum [see Eq. (3.42) below].

Consider now the electron-proton system. It is easy to show that even including the Coulomb interaction, the total pseudomomentum,

$$\mathbf{K} = \mathbf{K}_e + \mathbf{K}_p, \quad (3.36)$$

is a constant of motion. Moreover, all components of  $\mathbf{K}$  commute with each other. Thus it is natural to separate the CM motion from the internal degrees of freedom using  $\mathbf{K}$  as an explicit constant of motion. From Eq. (2.3), we find that the separation between the guiding centers of the electron and the proton is directly related to  $\mathbf{K}_\perp$ :

$$\mathbf{R}_K = \mathbf{R}_{ce} - \mathbf{R}_{cp} = \frac{c\mathbf{B} \times \mathbf{K}}{eB^2}. \quad (3.37)$$

The two-body eigenfunction with a definite value of  $\mathbf{K}$  can be written as

$$\Psi(\mathbf{R}, \mathbf{r}) = \exp \left[ \frac{i}{\hbar} \left( \mathbf{K} + \frac{e}{2c} \mathbf{B} \times \mathbf{r} \right) \cdot \mathbf{R} \right] \phi(\mathbf{r}), \quad (3.38)$$

where  $\mathbf{R} = (m_e \mathbf{r}_e + m_p \mathbf{r}_p)/M$  and  $\mathbf{r} = \mathbf{r}_e - \mathbf{r}_p$  are the center-of-mass and relative coordinates, and  $M = m_e + m_p$  is the total mass. The Schrödinger equation reduces to  $H\phi(\mathbf{r}) = \mathcal{E}\phi(\mathbf{r})$ , with <sup>2</sup>

$$H = \frac{\mathbf{K}^2}{2M} + \frac{1}{2\mu} \left( \mathbf{p} + \frac{e}{2c} \mathbf{B} \times \mathbf{r} \right)^2 - \frac{e}{m_p c} \mathbf{B} \cdot (\mathbf{r} \times \mathbf{p}) - \frac{e^2}{r} + \frac{e}{Mc} (\mathbf{K} \times \mathbf{B}) \cdot \mathbf{r}, \quad (3.39)$$

where  $\mathbf{p} = -i\hbar\partial/\partial\mathbf{r}$  and  $\mu = m_e m_p/M$  (e.g., Lamb 1952; Avron *et al.* 1978; Herold *et al.* 1981). Clearly, the CM motion is coupled to the internal motion through the last term in  $H$ , which has the form of an electrostatic potential produced by an electric field  $(\mathbf{K}/M) \times \mathbf{B}$ . This term represents the so called ‘‘motional Stark effect’’ (although such a description is not exactly accurate, since  $\mathbf{K}_\perp/M$  does not correspond to the CM velocity; see Johnson *et al.* 1983). In the adiabatic approximation ( $b \gg 1$ , with the electron in the ground Landau level), we write the total energy of the atom as

$$\mathcal{E}_{m\nu}(K_z, K_\perp) = \frac{K_z^2}{2M} + m\hbar\omega_{cp} + E_{m\nu}(K_\perp), \quad (3.40)$$

where azimuthal quantum number  $m$  measures the relative electron-proton  $z$ -angular momentum  $J_z = \hat{\mathbf{B}} \cdot (\mathbf{r} \times \mathbf{p}) = -m$  (clearly,  $m$  is a good quantum number only when  $K_\perp = 0$ , but we shall use it as a label of the state even when  $K_\perp \neq 0$ ), and  $\nu$  enumerates the longitudinal excitations. The  $m\hbar\omega_{cp}$  term in Eq. (3.40) represents the Landau energy excitations for the proton; this ‘‘coupling’’ between the electron quantum number  $m$  and the proton Landau excitation results from the conservation of  $\mathbf{K}$ . Clearly, for sufficiently high  $b$ , states with  $m > 0$  become unbound [i.e.,  $\mathcal{E}_{m\nu}(\mathbf{K} = 0) = m\hbar\omega_{cp} + E_{m\nu}(0) > 0$ ].

For small  $K_\perp$ , the motional Stark term in  $H$  can be treated as a perturbation (e.g., Vincke and Baye 1988; Pavlov and Meszaros 1993). For the tightly bound states ( $\nu = 0$ ), we have

---

<sup>2</sup>The spin terms of the electron and the proton are not explicitly included. For the electron in the ground Landau level, the zero-point Landau energy  $\hbar\omega_{ce}/2$  is exactly cancelled by the spin energy. For sake of brevity, we drop the zero-point energy of the proton,  $\hbar\omega_{cp}/2$ , as well as the spin energy  $\pm g_p \hbar\omega_{cp}/2$  (where  $g_p = 2.79$ ).

$$E_{m0}(K_{\perp}) \simeq E_m + \frac{K_{\perp}^2}{2M_{\perp m}}, \quad (\text{for } K_{\perp} \ll K_{\perp p}) \quad (3.41)$$

where  $E_m$  is the energy of a bound electron in the fixed Coulomb potential (the correction due to the reduced mass  $\mu$  can be easily incorporated into  $E_m$ ; this amounts to a small correction). The effective mass  $M_{\perp m}$  for the transverse motion increases with increasing  $b$ . For the  $m = 0$  state,

$$M_{\perp} \equiv M_{\perp 0} = M \left( 1 + \frac{\xi b}{M \ln b} \right) \simeq M \left( 1 + \frac{\xi b}{b_{\text{cm}}} \right), \quad (3.42)$$

where  $\xi$  is a slowly varying function of  $b$  (e.g.,  $\xi \simeq 2 - 3$  for  $b = 10^2 - 10^5$ ). Similar results can be obtained for the  $m > 0$  states:  $M_{\perp m} \simeq M + \xi_m(2m+1)b/l_m$ , where  $\xi_m$  is of the same order of magnitude as  $\xi$ , and  $l_m = \ln[b/(2m+1)]$ . A simple fitting formula for  $M_{\perp m}$  is proposed by Potekhin (1998):

$$M_{\perp m} = M [1 + (b/b_0)^{c_0}], \quad (3.43)$$

with  $b_0 = 6150(1 + 0.0389m^{3/2})/(1 + 7.87m^{3/2})$  and  $c_0 = 0.937 + 0.038m^{1.58}$ . Equation (3.41) is valid only when  $K_{\perp}$  is much less than the ‘‘perturbation limit’’,  $K_{\perp p}$ , given by (for  $m = 0$ )  $K_{\perp p} = b^{1/2}(1 + M \ln b/\xi b)$ , which corresponds to  $K_{\perp p}^2/(2M_{\perp}) \simeq 1.7(1 + b_{\text{cm}}/\xi b)$ . Numerical calculations by Potekhin (1994) indicate that Eq. (3.41) is a good approximation for  $K_{\perp} \lesssim K_{\perp c}$  (see Fig. 2), where

$$K_{\perp c} \simeq \sqrt{2M|E_m|}, \quad (3.44)$$

that is,  $|E_{m0}(K_{\perp c})| \ll |E_m|$ . The states with  $K_{\perp} \lesssim K_{\perp c}$  are sometimes called ‘‘centered states’’.

For  $K_{\perp} \gtrsim K_{\perp c}$ , the motional electric field [see Eq. (3.39)] induces a significant transverse separation (perpendicular to  $\mathbf{K}$ ) between the electron and the proton. It is more convenient to use a new coordinate system to account for this effect. Since  $\mathbf{K}_{\perp}$  measures the separation of the guiding centers of the electron and the proton, we can remove the ‘‘Stark term’’ in Eq. (3.39) by introducing a displaced coordinate  $\mathbf{r}' = \mathbf{r} - \mathbf{R}_K$ . After a gauge transformation with

$$\phi(\mathbf{r}) \rightarrow \exp\left(\frac{i}{\hbar} \frac{m_p - m_e}{2M} \mathbf{K}_{\perp} \cdot \mathbf{r}\right) \phi(\mathbf{r}'), \quad (3.45)$$

we obtain  $H'\phi(\mathbf{r}') = \mathcal{E}\phi(\mathbf{r}')$ , with the Hamiltonian

$$H' = \frac{K_z^2}{2M} + \frac{1}{2\mu} \left( \mathbf{p}' + \frac{e}{2c} \mathbf{B} \times \mathbf{r}' \right)^2 - \frac{e}{m_p c} \mathbf{B} \cdot (\mathbf{r}' \times \mathbf{p}') - \frac{e^2}{|\mathbf{r}' + \mathbf{R}_K|}, \quad (3.46)$$

where  $\mathbf{p}' = -i\hbar\partial/\partial\mathbf{r}'$  (e.g., Avron *et al.* 1978; Herold *et al.* 1981). We can estimate the size  $L_z$  of the atom along the  $z$ -axis and the energy  $E_{m\nu}(K_{\perp})$  for two different regimes of  $R_K$  (see Lai and Salpeter 1995): (i) For  $R_K \lesssim L_z \lesssim 1$  (but not necessarily  $R_K < \rho_m$  or  $K_{\perp} < \sqrt{mb}$ ), we have (for the  $\nu = 0$  states)

$$L_z \sim \left( \ln \frac{1}{\rho_m^2 + R_K^2} \right)^{-1}, \quad E_{m0}(K_{\perp}) \sim -0.16 \left( \ln \frac{1}{\rho_m^2 + R_K^2} \right)^2. \quad (3.47)$$

Mixing between different  $m$ -states is unimportant when  $b \gg b_{\text{cm}}$ . (ii) For  $R_K \gtrsim 1$ , the electron-proton interaction does not contain the Coulomb logarithm, and the energy can be written as  $E_{m0}(K_{\perp}) \sim L_z^{-2} - (L_z^2 + R_K^2)^{-1/2}$ . In the limit of  $R_K \gg 1$ , minimization of  $\mathcal{E}_m$  with respect to  $L_z$  yields

$$L_z \sim R_K^{3/4} \ll R_K, \quad E_{m0}(K_{\perp}) \sim -\frac{1}{R_K} = -\frac{b}{K_{\perp}}, \quad (3.48)$$

independent of  $m$  (e.g., Burkova *et al.* 1976; Potekhin 1994). The states with  $K_{\perp} \gtrsim K_{\perp c}$  (which corresponds to  $R_K \gtrsim \hat{\rho}$  for  $b \gtrsim b_{\text{cm}}$ ) are sometimes referred to as ‘‘decentered states’’ (Vincke *et al.* 1992; Potekhin 1994), but note that for a given  $(m\nu)$  (defined at  $K_{\perp} = 0$ ), there is a continuous energy  $E_{m\nu}(K_{\perp})$  which connects the ‘‘centered state’’ at small  $K_{\perp}$  to the ‘‘decentered state’’ at large  $K_{\perp}$ .

To calculate the energy  $E_{m\nu}(K_{\perp})$  for general  $K_{\perp}$ , we must include mixing between different  $m$ -orbitals. We may use  $\phi(\mathbf{r}) = \sum_{m'} W_{m'}(\mathbf{r}_{\perp}) f_{m'}(z)$  in Eq. (3.39) and obtain a coupled set of equations for  $f_{m'}(z)$ ; alternatively, for  $K_{\perp} \gtrsim K_{\perp c}$ , it is more convenient to use  $\phi(\mathbf{r}') = \sum_{m'} W_{m'}(\mathbf{r}'_{\perp}) f_{m'}(z)$  in Eq. (3.46). Numerical results are presented in Potekhin (1994) (see also Vincke *et al.* 1992); analytical fitting formulae for the energies, atomic sizes and oscillator strengths are given in Potekhin (1998). Figure 2 shows the energy  $E_{m\nu}(K_{\perp})$  (based on Potekhin’s calculation) as a

function of  $K_{\perp}$  for several different states at  $B_{12} = 1$ . Note that the total energies of different states,  $\mathcal{E}_{m\nu}(K_z, K_{\perp})$ , do not cross each other as  $K_{\perp}$  increases.

While for neutral atoms the CM motion can be separated from the internal relative motion, this cannot be done for ions (Avron *et al.* 1981). Ions undergo collective cyclotron motion which depends on the internal state. However, the existence of an approximate constant of motion allows an approximate pseudoseparation up to very high fields (see Bayes and Vincke 1998 and references therein). Numerical results for  $\text{He}^+$  moving in strong magnetic fields are obtained by Bezchastnov *et al.* (1998).

The effects of CM motion on multi-electron systems (heavy atoms and molecules) in strong magnetic fields have not been studied numerically, although many theoretical issues are discussed in Johnson *et al.* (1983) and Schmelcher *et al.* (1988,1994).

## IV. MOLECULES

Most studies of molecules in strong magnetic fields have been restricted to hydrogen. We will therefore focus on H to illustrate the basic magnetic effects and only briefly discuss molecules of heavier elements.

### A. $\text{H}_2$ : Basic Mechanism of Bonding

In a strong magnetic field, the mechanism of forming molecules is quite different from the zero-field case (see Ruderman 1974; Lai *et al.* 1992). The spins of the electrons in the atoms are aligned anti-parallel to the magnetic field, and therefore two atoms in their ground states ( $m = 0$ ) do not bind together according to the exclusion principle. Instead, one H atom has to be excited to the  $m = 1$  state. The two H atoms, one in the ground state ( $m = 0$ ), another in the  $m = 1$  state then form the ground state of the  $\text{H}_2$  molecule by covalent bonding. Since the “activation energy” for exciting an electron in the H atom from the Landau orbital  $m$  to  $(m + 1)$  is small [see Eq. (3.5)], the resulting  $\text{H}_2$  molecule is stable. The size of the  $\text{H}_2$  molecule is comparable to that of the H atom. The interatomic separation  $a_{\text{eq}}$  and the dissociation energy  $D$  of the  $\text{H}_2$  molecule scale approximately as

$$a_{\text{eq}} \sim \frac{1}{\ln b}, \quad D \sim (\ln b)^2, \quad (4.1)$$

although  $D$  is numerically smaller than the ionization energy of the H atom (see Table I).

Another mechanism of forming a  $\text{H}_2$  molecule in a strong magnetic field is to let both electrons occupy the same  $m = 0$  Landau orbital, while one of them occupies the tightly bound  $\nu = 0$  state and the other the  $\nu = 1$  weakly bound state. This costs no “activation energy”. However, the resulting molecule tends to have a small dissociation energy, of order a Rydberg. We shall refer to this electronic state of the molecule as the weakly bound state, and to the states formed by two electrons in the  $\nu = 0$  orbitals as the tightly bound states. As long as  $\ln b \gg 1$ , the weakly bound states constitute excited energy levels of the molecule.

### B. Numerical Calculations and Results

In the Born-Oppenheimer approximation (see Schmelcher *et al.* 1988,1994 for a discussion on the validity of this approximation in strong magnetic fields), the interatomic potential  $U(a, R_{\perp})$  is given by the total electronic energy  $E(a, R_{\perp})$  of the system, where  $a$  is the proton separation along the magnetic field, and  $R_{\perp}$  is the separation perpendicular to the field. Once  $E(a, R_{\perp})$  is obtained, the electronic equilibrium state is determined by locating the minimum of the  $E(a, R_{\perp})$  surface. [For a given  $a$ ,  $E(a, R_{\perp})$  is minimal at  $R_{\perp} = 0$ ].

The simplest system is the molecular ion  $\text{H}_2^+$ . For  $b \gg 1$ , the energy of  $\text{H}_2^+$  can be easily calculated as in the case of H atom (e.g., Wunner *et al.* 1982; Le Guillou and Zinn-Justin 1984; Khersonskii 1984). When the molecular axis is aligned with the magnetic axis ( $R_{\perp} = 0$ ), we only need to solve the Schrödinger equation similar to (3.1), except replacing  $V_m(z)$  by

$$\tilde{V}_m(z) = V_m\left(z - \frac{a}{2}\right) + V_m\left(z + \frac{a}{2}\right). \quad (4.2)$$

The total electronic energy is simply  $E(a, 0) = \varepsilon_{m\nu} + e^2/a$ . The ground state corresponds to  $(m, \nu) = (0, 0)$ .

The Hartree-Fock calculation of  $\text{H}_2$  is similar to the case of multi-electron atoms. For the tightly bound states, the two electrons occupy the  $(m, \nu) = (m_1, 0), (m_2, 0)$  orbitals (the ground state corresponds to  $m_1 = 0, m_2 = 1$ ), with the wavefunction

$$\Psi(\mathbf{r}_1, \mathbf{r}_2) = \frac{1}{\sqrt{2}}[\Phi_{m_1 0}(\mathbf{r}_1)\Phi_{m_2 0}(\mathbf{r}_2) - \Phi_{m_1 0}(\mathbf{r}_2)\Phi_{m_2 0}(\mathbf{r}_1)]. \quad (4.3)$$

We obtain the same Hartree-Fock equation as (3.30) except that  $V_m$  is replaced by  $\tilde{V}_m$  (for aligned configurations,  $R_\perp = 0$ ). The energy is given by

$$\begin{aligned} E(a, 0) &= \frac{e^2}{a} + \varepsilon_{m_1 0} + \varepsilon_{m_2 0} - \frac{e^2}{\hat{\rho}} \int dz_1 dz_2 |f_{m_1 0}(z_1)|^2 |f_{m_2 0}(z_2)|^2 D_{m_1 m_2}(z_1 - z_2) \\ &+ \frac{e^2}{\hat{\rho}} \int dz_1 dz_2 f_{m_1 0}(z_1) f_{m_2 0}(z_2) f_{m_1 0}^*(z_2) f_{m_2 0}^*(z_1) E_{m_1 m_2}(z_1 - z_2). \end{aligned} \quad (4.4)$$

Although the Hartree-Fock method is adequate for small interatomic separations ( $a$  less than the equilibrium value,  $a_{\text{eq}}$ ), the resulting  $E(a, 0)$  becomes less reliable for large  $a$ : as  $a \rightarrow \infty$ ,  $E(a, 0)$  does not approach the sum of the energies of two isolated atoms, one in the  $m_1$ -state, another in the  $m_2$ -state. The reason is that as  $a$  increases, another configuration of electron orbitals,

$$\Psi_2(\mathbf{r}_1, \mathbf{r}_2) = \frac{1}{\sqrt{2}}[\Phi_{m_1 1}(\mathbf{r}_1)\Phi_{m_2 1}(\mathbf{r}_2) - \Phi_{m_1 1}(\mathbf{r}_2)\Phi_{m_2 1}(\mathbf{r}_1)], \quad (4.5)$$

becomes more and more degenerate with the first configuration  $\Psi_1 = \Psi$  in Eq. (4.3), and there must be mixing of these two different configurations. Both  $\Psi_1$  and  $\Psi_2$  have the same symmetry with respect to the Hamiltonian: the total angular momentum along the  $z$ -axis is  $M_{Lz} = 1$ , the total electron spin is  $M_{Sz} = -1$ , and both  $\Psi_1$  and  $\Psi_2$  are even with respect to the operation  $\mathbf{r}_i \rightarrow -\mathbf{r}_i$ . To obtain a reliable  $E(a, 0)$  curve, ‘‘configuration interaction’’ between  $\Psi_1$  and  $\Psi_2$  must be taken into account in the Hartree-Fock scheme (Lai *et al.* 1992; see, e.g., Slater 1963 for a discussion of the zero-field case).

Molecular configurations with  $R_\perp \neq 0$  correspond to excited states of the molecules (see Sec. IV.C). To obtain  $E(a, R_\perp)$ , mixing of different  $m$ -states in single-electron orbital needs to be taken into account. Approximate energy surfaces  $E(a, R_\perp)$  for both small  $R_\perp$  and large  $R_\perp$  have been computed by Lai and Salpeter (1996).

Numerical results of  $E(a, 0)$  (based on the Hartree-Fock method) for both tightly bound states and weakly bound states are given in Lai *et al.* (1992) and Lai and Salpeter (1996). Quantum Monte Carlo calculations have also been performed, confirming the validity of the method (Ortiz *et al.* 1995). Figure 3 depicts some of the energy curves. The dissociation energy of  $\text{H}_2$  in the ground state can be fitted by

$$Q_2^{(\infty)} \equiv 2|E(\text{H})| - |E(\text{H}_2)| = 0.106 [1 + 0.1 l^{0.2} \ln(b/b_{\text{cm}})] l^2, \quad (4.6)$$

(where  $l = \ln b$ ), with an accuracy of  $\lesssim 5\%$  for  $1 \lesssim B_{12} \lesssim 1000$ , where  $b_{\text{cm}} = 1.80 \times 10^4$  is defined in Eq. (3.35) (The superscript ‘‘ $(\infty)$ ’’ implies that the zero-point energy of the molecule is not included in  $Q_2^{(\infty)}$ ; see Sec. IV.C below). Thus  $Q_2^{(\infty)} \simeq 46$  eV for  $B_{12} = 1$  and  $Q_2^{(\infty)} \simeq 150$  eV for  $B_{12} = 10$  (see Table I). By contrast, the zero-field dissociation energy of  $\text{H}_2$  is 4.75 eV.

### C. Molecular Excitations

For the ground state of  $\text{H}_2$ , the molecular axis and the magnetic field axis coincide, and the two electrons occupy the  $m = 0$  and  $m = 1$  orbitals, i.e.,  $(m_1, m_2) = (0, 1)$ . The molecule can have different types of excitation levels (Lai and Salpeter 1996):

(i) *Electronic excitations.* The electrons occupy orbitals other than  $(m_1, m_2) = (0, 1)$ , giving rise to the electronic excitations. The energy difference between the excited state  $(m_1, m_2)$  (with  $\nu_1 = \nu_2 = 0$ ) and the ground state  $(0, 1)$  is of order  $\ln b$ , as in the case for atoms. Typically, only the single-excitation levels (those with  $m_1 = 0$  and  $m_2 > 1$ ) are bound relative to two atoms in the ground states. Another type of electronic excitation is formed by two electrons in the  $(m, \nu) = (0, 0)$  and  $(0, 1)$  orbitals. The dissociation energy of this weakly bound state is of order a Rydberg, and does not depend sensitively on the magnetic field strength (see Fig. 3). Note that since it does not cost any activation energy to form a  $\text{H}_2$  in the weakly bound state, for relatively small magnetic field ( $B_{12} \lesssim 0.25$ ), the weakly bound state actually has lower energy than the tightly bound state.

(ii) *Aligned vibrational excitations.* These result from the vibration of the protons about the equilibrium separation  $a_{\text{eq}}$  along the magnetic field axis. To estimate the excitation energy, we need to consider the excess potential  $\delta U(\delta a) = U(a_{\text{eq}} + \delta a, 0) - U(a_{\text{eq}}, 0)$ . Since  $a_{\text{eq}}$  is the equilibrium position, the sum of the first order terms (proportional to  $\delta a$ ) in  $\delta U$ , coming from proton-proton, electron-electron, proton-electron Coulomb energies and quantum mechanical electron kinetic energy, must cancel, and  $\delta U \propto (\delta a)^2$  for small  $\delta a$ . The dominant contribution to the energy of the molecule comes from the proton-electron Coulomb energy  $\sim l/a$ , where the logarithmic factor  $l \equiv \ln b \gg 1$  results from the Coulomb integral over the elongated electron distribution. The excess potential is of order  $\delta U \sim l(\delta a)^2/a_{\text{eq}}^3 \sim (\xi^{-3}l^4)(\delta a)^2$ , where we have used  $a_{\text{eq}} = \xi/l$  (the dimensionless factor  $\xi$  decreases slowly with increasing  $b$ ; e.g.,  $\xi \simeq 2$  for  $B_{12} = 0.1$  and  $\xi = 0.75$  for  $B_{12} = 100$ ). Thus for small-amplitude oscillations around  $a_{\text{eq}}$ , we obtain a harmonic oscillation spectrum with excitation energy quanta  $\hbar\omega_{\parallel} \sim \xi^{-3/2}l^2\mu^{-1/2}$ , where  $\mu = m_p/2m_e = 918$  is the reduced mass of the two protons in units of the electron mass. Numerical calculations yield a similar scaling relation. For the electronic ground state, the energy quanta can be approximated by

$$\hbar\omega_{\parallel} \simeq 0.13 (\ln b)^{5/2} \mu^{-1/2} (\text{a.u.}) \simeq 0.12 (\ln b)^{5/2} (\text{eV}). \quad (4.7)$$

(This is accurate to within 10% for  $40 \lesssim b \lesssim 10^4$ ). Thus  $\hbar\omega_{\parallel} \simeq 10$  eV at  $B_{12} = 1$  and  $\hbar\omega_{\parallel} \simeq 23$  eV at  $B_{12} = 10$ , in contrast to the vibrational energy quanta  $\hbar\omega_{\text{vib}} \simeq 0.52$  eV for the  $\text{H}_2$  molecule at zero magnetic field.

(iii) *Transverse vibrational excitations.* The molecular axis can deviate from the magnetic field direction, precessing and vibrating around the magnetic axis. Such an oscillation is the high-field analogy of the usual molecular rotation; the difference is that in strong magnetic fields, this “rotation” is constrained around the magnetic field line. To obtain the excitation energy, we need to estimate the excess potential  $\delta U(R_{\perp}) \equiv U(a_{\text{eq}}, R_{\perp}) - U(a_{\text{eq}}, 0)$ . When the protons are displaced by  $\sim R_{\perp}$  from the electron distribution axis, the proton-electron interaction is approximately given by  $a_{\text{eq}}^{-1} \ln [L_z/(\hat{\rho}^2 + R_{\perp}^2)^{1/2}]$ . Thus an order of magnitude expression for  $\delta U$  is  $\delta U(R_{\perp}) \sim (1/2a_{\text{eq}}) \ln(1 + \hat{\rho}^{-2}R_{\perp}^2) \sim \xi^{-1}l \ln(1 + bR_{\perp}^2)$ . This holds for any  $R_{\perp} \ll a_{\text{eq}} = \xi l^{-1}$ . For small-amplitude transverse oscillations, with  $R_{\perp} \lesssim \hat{\rho} = b^{-1/2} \ll a_{\text{eq}}$ , we have  $\delta U \sim \xi^{-1}l b R_{\perp}^2$ . The energy quanta is then  $\hbar\omega_{\perp 0} \sim (\xi^{-1}l b)^{1/2} \mu^{-1/2}$ , where the subscript 0 indicates that we are at the moment neglecting the magnetic forces on the protons which, in the absence of Coulomb forces, lead to proton cyclotron motions (see below). Numerical calculations give a similar scaling relation. For the electronic ground state, the excitation energy quanta  $\hbar\omega_{\perp 0}$  can be approximated by

$$\hbar\omega_{\perp 0} \simeq 0.125 b^{1/2} (\ln b) \mu^{-1/2} (\text{a.u.}) \simeq 0.11 b^{1/2} (\ln b) (\text{eV}). \quad (4.8)$$

(This is accurate to within 10% for  $40 \lesssim b \lesssim 10^4$ ). Thus  $\hbar\omega_{\perp 0} \simeq 14$  eV at  $B_{12} = 1$  and  $\hbar\omega_{\perp 0} = 65$  eV at  $B_{12} = 10$ . (See Lai and Salpeter 1996 for a discussion of large-amplitude oscillations.)

Note that in a strong magnetic field, the electronic and (aligned and transverse) vibrational excitations are all comparable, with  $\hbar\omega_{\perp 0} \gtrsim \hbar\omega_{\parallel}$ . This is in contrast to the zero-field case, where we have  $\Delta\varepsilon_{\text{elec}} \gg \hbar\omega_{\text{vib}} \gg \hbar\omega_{\text{rot}}$ .

Equation (4.8) for the zero-point energy of the transverse oscillation includes only the contribution of the electronic restoring potential  $\mu\omega_{\perp 0}^2 R_{\perp}^2/2$ . Since the magnetic forces on the protons also induce a “magnetic restoring potential”  $\mu\omega_{cp}^2 R_{\perp}^2/2$ , where  $\hbar\omega_{cp} = \hbar eB/(m_p c) \simeq 6.3 B_{12}$  eV is the cyclotron energy of the proton, the zero-point energy of the transverse oscillation is

$$\hbar\omega_{\perp} = \hbar(\omega_{\perp 0}^2 + \omega_{cp}^2)^{1/2} - \hbar\omega_{cp}. \quad (4.9)$$

The dissociation energy of  $\text{H}_2$ , taking into account the zero-point energies of aligned and transverse vibrations, is then

$$Q_2 = Q_2^{(\infty)} - \left( \frac{1}{2} \hbar\omega_{\parallel} + \hbar\omega_{\perp} \right). \quad (4.10)$$

Some numerical values are given in Table I. Variation of  $Q_2$  as a function of  $B$  is depicted in Fig. 1.

#### D. $\text{H}_N$ Molecules: Saturation

At zero magnetic field, two H atoms in their ground states with spins opposite to each other form a  $\text{H}_2$  molecule by covalent bonding; adding more H atoms is not possible by the exclusion principle (unless one excites the third atom to an excited state; but the resulting  $\text{H}_3$  is short-lived). In a strong magnetic field, the spins of the electrons in the atoms are all aligned anti-parallel to the magnetic field, and because of the low excitation energy associated with  $m \rightarrow m + 1$ , more atoms can be added to  $\text{H}_2$  to form larger  $\text{H}_N$  molecules.

For a given magnetic field strength, as the number of H atoms,  $N$ , increases, the electrons occupy more and more Landau orbitals (with  $m = 0, 1, 2, \dots, N - 1$ ), and the transverse size of the molecule increases as  $R \sim (N/b)^{1/2}$ .

Let  $a$  be the atomic spacing, and  $L_z \sim Na$  be the size of the molecule in the  $z$ -direction. The energy per atom in the molecule can be written as  $E \sim L_z^{-2} - la^{-1}$ , where  $l = \ln(2a/R)$ . Variation of  $E$  with respect to  $L_z$  gives

$$E \sim -N^2 l^2, \quad L_z \sim Na \sim (Nl)^{-1}. \quad (4.11)$$

This scaling behavior is valid for  $1 \ll N \ll N_s$ . The ‘‘critical saturation number’’  $N_s$  is reached when  $a \sim R$ , or

$$N_s \sim b^{1/5}, \quad (4.12)$$

(Lai *et al.* 1992). Beyond  $N_s$ , it becomes energetically more favorable for the electrons to settle into the inner Landau orbitals (with smaller  $m$ ) with nodes in their longitudinal wavefunctions (i.e.,  $\nu \neq 0$ ). For  $N \gtrsim N_s$ , the energy per atom of the  $H_N$  molecule,  $E = |E(H_N)|/N$ , asymptotes to a value  $\sim b^{2/5}$ , and size of the atom scales as  $R \sim a \sim b^{-2/5}$ , independent of  $N$  (see Sec. V.A). For a typical magnetic field strength ( $B_{12} = 0.1 - 10^3$ ) of interest here, the energy saturation occurs at  $N_s \sim 2 - 6$  (see Fig. 4).

### E. Intermediate Magnetic Field Regime

For intermediate magnetic field strengths ( $B \sim B_0 \sim 10^9$  G), the only molecule that has been investigated in some detail is the hydrogen molecular ion  $H_2^+$ ; both parallel (e.g., Le Guillou and Zinn-Justin 1984; Vincke and Baye 1985; Brigham and Wadehra 1987; Kappes and Schmelcher 1995; Lopez *et al.* 1997; Kravchenko and Liberman 1997) and nonparallel configurations (Larsen 1982; Wille 1987,1988; Kappes and Schmelcher 1996) have been studied using different variational methods. Other one-electron molecular ions such as  $H_3^{3+}$  and  $H_4^{4+}$  in strong magnetic fields have been studied by Lopez and Turbinder (2000) (and references therein). For the  $H_2$  molecule at intermediate fields, earlier studies (e.g., Turbinder 1983; Basile *et al.* 1987) are of qualitative character; quantitative calculations (for aligned configurations) have been attempted only recently (Detmer *et al.* 1997,1998; Kravchenko and Liberman 1998; Schmelcher *et al.* 2000).

An important issue concerns the nature of the ground electronic state of  $H_2$  as a function of  $B$ . Starting from the strong field regime (see Sec. IV.B and Sec. IV.C) we know that for  $B_{12} \gtrsim 0.2$  ( $b \gtrsim 100$ ), the ground state is the tightly bound state in which the electrons occupy the  $(m, \nu) = (0, 0)$  and  $(1, 0)$  orbitals; this state corresponds to  ${}^3\Pi_u$  in the standard spectroscopic notation. For  $b \lesssim 100$  the lowest energy state becomes the weakly bound state in which the electron orbitals are  $(0, 0)$  and  $(0, 1)$ ; this corresponds to the  ${}^3\Sigma_u$  state. Detmer *et al.* (1998) and Kravchenko and Liberman (1998) found that for  $b \lesssim 0.18$ , the ground state is the usual  ${}^1\Sigma_g$ ; for  $0.2 \lesssim b \lesssim 12 - 14$ , the ground state is  ${}^3\Sigma_u$ ; for  $b \gtrsim 12$ , the ground state is  ${}^3\Pi_u$ . However, their  ${}^3\Sigma_u$  state is predominantly repulsive except for a very shallow van-der-Waals (quadrupole-quadrupole interaction) minimum at large proton separation. The binding of the  ${}^3\Sigma_u$  was not demonstrated in the calculations of Detmer *et al.* (1998) and Kravchenko and Liberman (1998). This is in contradiction to the  $b \gg 1$  behavior of the weakly bound state found in Lai and Salpeter (1996). Obviously, more work is needed to attain a clear picture of how the energies of different  $H_2$  states behave as  $B$  increases from 0 to  $b \gg 1$ .

### F. Molecules of Heavy Elements

Molecules of heavy elements (other than hydrogen) in strong magnetic fields have not been systematically investigated. There is some motivation to study molecules of light elements such as He, since if the hydrogen on a neutron star surface is completely burnt out by nuclear reaction, helium would be the dominant species left in the atmosphere. There are also white dwarfs with pure He atmospheres. (Because of quick gravitational separation of light and heavy elements in the gravitational field of the neutron star or white dwarf, the atmosphere is expected to contain pure elements.) For  $b \gg 1$ , the Hartree-Fock method discussed in Sec. IV.B can be generalized to the case of ion charge  $Z > 1$  (Lai *et al.* 1992). Figure 5 shows the dissociation energy of the  $He_2$  molecule as a function of  $B$ . In general, we expect that, as long as  $a_0/Z \gg (2Z - 1)^{1/2} \hat{\rho}$ , or  $b \gg 2Z^3$ , the electronic properties of the heavy molecule is similar to those of  $H_2$ . When the condition  $b \gg 2Z^3$  is not satisfied, the molecule should be quite different and may be unbound relative to individual atoms (e.g., Fe at  $B = 10^{12}$  G is unlikely to form a bound molecule). Some Hartree-Fock results of diatomic molecules (from  $H_2$  up to  $C_2$ ) at  $b = 1000$  are given in Demeur *et al.* (1994).

## V. LINEAR CHAINS AND CONDENSED MATTER

As discussed in Sec. IV.D, in a strong magnetic field we can add more atoms to a diatomic molecule to form molecular chains. When the number of atoms exceeds the saturation number, the structure of the molecule is the same as that of an infinite chain. By placing a pile of parallel chains together, three-dimensional condensed matter can be formed.

### A. Basic Scaling Relations for Linear Chains

The simplest model for the linear chain is to treat it as a uniform cylinder of electrons, with ions aligned along the magnetic field axis. After saturation, many electrons settle into the  $\nu \neq 0$  states, and the electrons can be treated as a Fermi sea in the  $z$ -direction. In order of magnitude, the electrons occupy states with  $m = 0, 1, 2, \dots, N_s - 1$  and  $\nu = 0, 1, 2, \dots, N/N_s$ . For  $N \gg N_s \gg 1$ , the uniform cylinder approximation becomes increasingly valid because in the transverse direction the area covered by the  $m$  Landau orbitals scales as  $(\sqrt{2m+1})^2 \propto m$ ; hence the volume increases with the number of interior electrons, giving a constant electron density. Let  $R$  be the radius of the cylinder and  $a$  be the atomic spacing  $a$  along the  $z$ -axis. The energy per atom (unit cell) in the chain can be written as (Ruderman 1971,1974; Chen 1973)

$$E_\infty = \frac{2\pi^2 Z^3}{3b^2 R^4 a^2} - \frac{Z^2}{a} \left[ \ln \frac{2a}{R} - \left( \gamma - \frac{5}{8} \right) \right], \quad (5.1)$$

where  $\gamma = 0.5772\dots$  is Euler's constant, and we have restored the dependence on the ion charge  $Z$ . In Eq. (5.1), the first term is the electron kinetic energy [see Eq. (A4)] and the second term is the (direct) Coulomb energy (the Madelung energy for the one-dimensional uniform lattice). Minimizing  $E_\infty$  with respect to  $R$  and  $a$  gives

$$\begin{aligned} R &= 1.65 Z^{1/5} b^{-2/5}, & a/R &= 2.14, \\ E_\infty &= -0.354 Z^{9/5} b^{2/5}. \end{aligned} \quad (5.2)$$

Not surprisingly, these scaling relations are the same as those for heavy atoms [see Eq. (3.20)].

### B. Calculations of Linear Chains

While the uniform cylinder model discussed above gives useful scaling relations for the structure and energy of the linear chain, it is not sufficiently accurate to determine the relative binding energy between the chain and the atom at  $B_{12} \sim 0.1 - 100$ . [The uniform cylinder model becomes accurate only when  $N_s \sim b^{1/5} \gg 1$ .] More refined calculations are needed to obtain accurate energies for field strengths characteristic of neutron star surfaces. Glasser and Kaplan (1975) generalized the uniform cylinder model by considering quantized electron charge distribution in the transverse direction. However, they assumed a uniform electron population in different Landau orbitals. The effect they treated amounts to only a small change in the value of the constant in the Madelung energy expression, and therefore it is still insufficient to account for the binding of linear chains. The next step in a more relaxed variational calculation is to treat the effect of Coulomb potential on the population of electrons in different  $m$  orbitals (Flowers *et al.* 1977; note that the calculation reported in this paper contained numerical errors, and was corrected by Müller 1984). This is clearly an important ingredient for calculating the binding energy of the chain since it allows for more electrons in the inner orbitals (small  $m$ 's), which increases the binding. A further improvement includes the nonuniform electron density distribution in the  $z$ -direction along the magnetic field (Neuhauser, Koonin and Langanke 1987). This effect is important for treating the bound electrons (i.e., the "electron core" in Flowers *et al.* 1977) correctly for chains of heavy atoms like Fe.

The self-consistent Hartree-Fock method for linear chains is similar to that used for calculating multi-electron atoms (see Sec. III.C.2; Neuhauser *et al.* 1987). Consider a chain of length  $Na$  (where  $a$  is the ion spacing). The electron basis functions can be written as

$$\Phi_{m\nu k}(\mathbf{r}) = W_m(\mathbf{r}_\perp) \frac{1}{\sqrt{N}} f_{m\nu}(z) \exp(ikz), \quad (5.3)$$

where  $k$  is the Bloch wavenumber, and  $f_{m\nu}(z) = f_{m\nu}(z+a)$ , normalized via  $\int_{-a/2}^{a/2} |f_{m\nu}(z)|^2 dz = 1$ . In each  $(m\nu)$  band, the electrons occupy the  $k$ -space up to  $k_{m\nu}^F = \sigma_{m\nu}(\pi/a)$ . Here  $\sigma_{m\nu}$  is the number of electrons in the  $(m\nu)$  orbital per unit cell in the chain, and satisfies the constraint

$$\sum_{m\nu} \sigma_{m\nu} = Z. \quad (5.4)$$

For each set of  $\sigma_{m\nu}$ , a coupled set of Hartree-Fock equations for  $f_{m\nu}(z)$  can be derived, and the energy of the system determined. One then varies  $\sigma_{m\nu}$  and repeats the calculation until the energy minimum is attained.

For linear chains consisting of light atoms such as H and He (or in general, for sufficiently strong magnetic fields satisfying  $b \gg 2Z^3$ ), the electron density variation along  $z$ -axis is not significant since all the electrons in the chain are “ionized” and are well approximated by plane waves. Thus a variational calculation which assumes uniform density in the  $z$ -direction is adequate. This calculation is simpler than the full Hartree-Fock calculation since the energy functional can be expressed in semi-analytic form (Lai *et al.* 1992). The basis electron wavefunctions are given by Eq. (5.3) with  $f_{m\nu} = a^{-1/2}$ . Electrons fill the  $m$ -th orbital (band) up to a Fermi wavenumber given by  $k_m^F = \sigma_m(\pi/a)$ , where  $\sigma_m$  is the number of electrons in  $m$ -th orbital per cell, with  $m = 0, 1, 2, \dots, m_0 - 1$ . The energy per cell in a chain can be written as

$$\begin{aligned} E = & \frac{\hbar^2}{2m_e} \sum_m \sigma_m \frac{1}{3} \left( \sigma_m \frac{\pi}{a} \right)^2 \\ & + \frac{Z^2 e^2}{a} \left[ -\ln \left( \frac{2a}{\hat{\rho}} \right) + \gamma + \frac{1}{Z} \sum_m \sigma_m \psi(m+1) - \frac{1}{2Z^2} \sum_{mm'} \sigma_m \sigma_{m'} Y_{mm'} \right] \\ & - \frac{e^2}{2a} \sum_{mm'} \sigma_m \sigma_{m'} \int_{-\infty}^{\infty} dz \frac{\sin(\sigma_m \pi z \hat{\rho}/a)}{\sigma_m \pi z \hat{\rho}/a} \frac{\sin(\sigma_{m'} \pi z \hat{\rho}/a)}{\sigma_{m'} \pi z \hat{\rho}/a} E_{mm'}(z), \end{aligned} \quad (5.5)$$

where the three terms represent the kinetic energy, the direct Coulomb energy and the exchange energy. The digamma function  $\psi$  satisfies  $\psi(m+1) = \psi(m) + (1/m)$ , with  $\psi(1) = -\gamma = -0.5772\dots$ ; the coefficient  $Y_{mm'}$  depends on  $m, m'$ ; the function  $E_{mm'}(z)$  is the same as defined in Eq. (3.29). For a given lattice spacing  $a$ , the occupation numbers  $\sigma_m$  ( $m = 0, 1, 2, \dots, m_0 - 1$ ) are varied to minimize the total energy  $E$  under the constraint (5.4) (with  $\nu$  suppressed). One can increase  $m_0$  until further increase in  $m_0$  results in no change in the distribution, i.e.,  $\sigma_{m_0-1} = 0$ . The constrained variation  $\delta E - \varepsilon_F \delta \sum_{m=0}^{m_0-1} \sigma_m = 0$  yields

$$\begin{aligned} \varepsilon_F = & \frac{\hbar^2}{2m_e} \left( \frac{\pi \sigma_m}{a} \right)^2 + \frac{Z^2 e^2}{a} \left[ \frac{1}{Z} \psi(m+1) - \frac{1}{Z^2} \sum_{m'} \sigma_{m'} Y_{mm'} \right] \\ & - \frac{e^2}{a} \sum_{m'} \int_{-\infty}^{\infty} dz \cos(\sigma_m \pi z \hat{\rho}/a) \frac{\sin(\sigma_{m'} \pi z \hat{\rho}/a)}{\sigma_{m'} \pi z \hat{\rho}/a} E_{mm'}(z). \end{aligned} \quad (5.6)$$

Here  $\varepsilon_F$  is a constant Lagrange multiplier (Fermi energy) which must be determined self-consistently. The system (5.6) consists of  $m_0$  equations for the  $m_0$  unknown parameters  $\sigma_m$  plus the constant  $\varepsilon_F$ . They are solved together with Eq. (5.4) for these unknown quantities.

Density functional theory has also been used to calculate the structure of linear chains in strong magnetic fields (Jones 1985; Relovsky and Ruder 1996). The problem with this approach is that the density functional approximation has not been calibrated in strong magnetic fields, and therefore the accuracy of the approximation is not yet known (for a review of density functional theory as applied to non-magnetic terrestrial solids, see, e.g., Callaway and March 1984). More accurate implementation of the density functional theory in strong magnetic fields requires that the current – magnetic field interaction be taken into account (Vignale and Rasolt 1987,1988) and better exchange-correlation functional be used.

### C. Cohesive Energy of Linear Chains

Selected numerical results of the linear chains for a number of elements (up to  $Z = 26$ ) have been obtained by Neuhauser *et al.* (1987) based on the Hartree-Fock method and by Jones (1985) based on density functional theory, for a limited range of  $B$ 's around  $10^{12}$  G. The numerical results for the energy (per atom) of the hydrogen chain (Lai *et al.* 1992) can be approximated by (to within 2% accuracy for  $1 \lesssim B_{12} \lesssim 10^3$ )

$$E_{\infty}(\text{H}) = -0.76 b^{0.37} \text{ (a.u.)} = -194 B_{12}^{0.37} \text{ (eV)}, \quad (5.7)$$

This expression for  $E_{\infty}$  is a factor of 1.8 times that given in Eq. (5.2). The cohesive energy of the H chain (energy release in  $\text{H} + \text{H}_{\infty} = \text{H}_{\infty+1}$ ) is given (to  $\lesssim 10\%$  accuracy) by

$$Q_{\infty}^{(\infty)}(\text{H}) = |E_{\infty}(\text{H})| - |E(\text{H})| \simeq 0.76 b^{0.37} - 0.16 (\ln b)^2 \quad (5.8)$$

where the superscript “ $(\infty)$ ” indicates that the proton has been treated as having infinite mass (see Sec. V.E). Figure 1 shows the cohesive energy of the H chain as a function of  $B$ , and Table I gives some numerical values. Figure 5 shows the similar result for the He chain. For these light elements, electron density variation along the  $z$ -axis can be safely ignored.

Numerical calculations carried out so far have indicated that for  $B_{12} = 1 - 10$ , linear chains are unbound for large atomic numbers  $Z \gtrsim 6$  (Jones 1986; Neuhauser *et al.* 1987). In particular, the Fe chain is unbound relative to the Fe atom; this is contrary to what some early calculations (e.g., Flowers *et al.* 1977) have indicated. Therefore, the chain-chain interaction must play a crucial role in determining whether the three dimensional zero-pressure Fe condensed matter is bound or not (see Sec. V.E). The main difference between Fe and H is that for the Fe atom at  $B_{12} \sim 1$ , many electrons are populated in the  $\nu \neq 1$  states, whereas for the H atom, as long as  $b \gg 1$ , the electron always settles down in the  $\nu = 0$  tightly bound state. Therefore, the covalent bonding mechanism for forming molecules (see Sec. IV.A) is not effective for Fe at  $B_{12} \sim 1$ . However, for a sufficiently large  $B$ , when  $a_0/Z \gg \sqrt{2Z+1}\hat{\rho}$ , or  $B_{12} \gg 100(Z/26)^3$ , we expect the Fe chain to be bound in a similar fashion as the H chain or He chain.

#### D. 3D Condensed Matter: Uniform Electron Gas Model and its Extension

A linear chain naturally attracts neighboring chains through quadrupole-quadrupole interaction. By placing parallel chains close together (with spacing of order  $b^{-2/5}$ ), we obtain three-dimensional condensed matter (e.g., a body-centered tetragonal lattice; Ruderman 1971).

The binding energy of the magnetized condensed matter at zero pressure can be estimated using the uniform electron gas model (e.g., Kadomtsev 1970). Consider a Wigner-Seitz cell with radius  $r_i = Z^{1/3}r_s$  ( $r_s$  is the mean electron spacing); the mean number density of electrons is  $n_e = Z/(4\pi r_i^3/3)$ . The electron Fermi momentum  $p_F$  is obtained from  $n_e = (eB/hc)(2p_F/h)$ . When the Fermi energy  $p_F^2/(2m_e)$  is less than the cyclotron energy  $\hbar\omega_{ce}$ , or when the electron number density satisfies

$$n_e \leq n_B = \frac{1}{\sqrt{2}\pi^2 \hat{\rho}^3} = 0.0716 b^{3/2}, \quad (5.9)$$

(or  $r_i \geq r_{iB} = 1.49 Z^{1/3}b^{-1/2}$ ), the electrons only occupy the ground Landau level. The energy per cell can be written as

$$E_s(r_i) = \frac{3\pi^2 Z^3}{8b^2 r_i^6} - \frac{0.9Z^2}{r_i}, \quad (5.10)$$

where the first term is the kinetic energy and the second term is the Coulomb energy. For the zero-pressure condensed matter, we require  $dE_s/dr_i = 0$ , and the equilibrium  $r_i$  and energy are then given by

$$r_{i,0} \simeq 1.90 Z^{1/5} b^{-2/5}, \quad (5.11)$$

$$E_{s,0} \simeq -0.395 Z^{9/5} b^{2/5}. \quad (5.12)$$

The corresponding zero-pressure condensation density is

$$\rho_{s,0} \simeq 561 A Z^{-3/5} B_{12}^{6/5} \text{ g cm}^{-3} \quad (5.13)$$

Note that for  $b \gg 1$ , the zero-pressure density is much smaller than the “magnetic” density defined in Eq. (5.9), i.e.,  $\rho_{s,0}/\rho_B = (r_B/r_{i,0})^3 = 0.48 Z^{2/5} b^{-3/10}$ .

We now discuss several corrections to the uniform electron gas model.

(i) *Coulomb exchange interaction.* The exclusion principle for the electrons results in an exchange correction to the Coulomb energy. The Hartree-Fock exchange energy (in atomic units) per Wigner-Seitz cell is given by

$$E_{ex} = -\frac{3Z}{4b r_s^3} F, \quad (5.14)$$

where  $F$  is a function of the ratio  $y \equiv n_e/n_B$  (see Appendix A)

$$F = 3 - \gamma - 2 \ln(2y) - \frac{2}{3} \left[ 2 \ln(2y) + \gamma - \frac{13}{6} \right] y^2 + \dots, \quad (5.15)$$

( $\gamma = 0.5772157 \dots$  is Euler's constant). The effect of this (negative) exchange interaction is to increase  $r_{i,0}$  and  $|E_{s,0}|$ .

(ii) *Relativistic effect.* As noted in Sec. II, the use of non-relativistic quantum mechanics for the bound states is a good approximation even for  $B \gtrsim B_{\text{rel}} \simeq 137^2 B_0$ . We can show that density-induced relativistic effect is also small. The ‘‘magnetic density’’  $n_B$  for onset of Landau excitation is still given by Eq. (5.9). The relativistic parameter for the electron is  $x_e \equiv p_F / (m_e c) = (n_e / n_B) (2B / B_{\text{rel}})^{1/2}$ . At the zero-pressure density as given by Eq. (5.13), we have  $x_e \simeq 5 \times 10^{-3} Z^{2/5} b^{1/5}$ . Thus near the zero-pressure density, relativistic effect is negligible for the range of magnetic field strengths of interest.

(iii) *Nonuniformity of the electron gas.* The Thomas-Fermi screening wavenumber  $k_{\text{TF}}$  is given by (e.g., Ashcroft and Mermin 1976)  $k_{\text{TF}}^2 = 4\pi e^2 D(\varepsilon_F)$ , where  $D(\varepsilon_F) = \partial n_e / \partial \varepsilon_F$  is the density of states per unit volume at the Fermi surface  $\varepsilon = \varepsilon_F = p_F^2 / (2m_e)$ . Since  $n_e = (2eB / h^2 c) p_F$ , we have  $D(\varepsilon_F) = n_e / 2\varepsilon_F = (m_e / n_e) (2eB / h^2 c)^2$ , and

$$k_{\text{TF}} = \left( \frac{4}{3\pi^2} \right)^{1/2} b r_s^{3/2}. \quad (5.16)$$

(More details on the electron screening in strong magnetic fields, including anisotropic effects, can be found in Horing 1969.) The gas is uniform when the screening length  $k_{\text{TF}}^{-1}$  is much longer than the particle spacing  $r_i$ , i.e.,  $k_{\text{TF}} r_i \ll 1$ . For the zero-pressure condensate with density parameter given by Eq. (5.11), we have  $k_{\text{TF}} r_i \simeq 1.83$ , independent of  $B$ . Thus even for  $B \rightarrow \infty$ , the nonuniformity of electron distribution must be considered for the zero-pressure condensed matter. To leading order in  $r_i \ll 1$ , the energy correction (per cell) due to nonuniformity can be calculated using linear response theory, which gives

$$E_{\text{TF}} = -\frac{18}{175} (k_{\text{TF}} r_i)^2 \frac{(Ze)^2}{r_i} \quad (5.17)$$

(e.g., Lattimer *et al.* 1985; Fushiki *et al.* 1989). Using Eq. (5.16), we have

$$E_{\text{TF}} = -0.0139 Z b^2 r_i^4. \quad (5.18)$$

Note that this expression is valid only for  $k_{\text{TF}} r_i \ll 1$ . At lower densities, the nonuniformity effect can be studied only through detailed electronic (band) structure calculations. An approximate treatment relies on the Thomas-Fermi type statistical models, including the exchange-correlation and the Weizsäcker gradient corrections (see Appendix B).

## E. Cohesive Energy of 3D Condensed Matter

Although the simple uniform electron gas model and its Thomas-Fermi type extensions give a reasonable estimate for the binding energy for the condensed state, they are not adequate for determining the cohesive property of the condensed matter. The cohesive energy  $Q_s$  is the difference between the atomic ground-state energy and the energy per atom of the condensed matter ground state. One uncertainty concerns the lattice structure of the condensed state, since the Madelung energy can be very different from the Wigner-Seitz value [the second term in Eq. (5.10)] for a non-cubic lattice. In principle, a three-dimensional electronic band structure calculation is needed to solve this problem, as Jones (1986) has attempted for a few elements using density functional theory. Jones adopted a local approximation in one angular variable in solving the electron eigenfunctions of the lattice Kohn-Sham potential; the validity of this approximation is not easy to justify. Moreover, without calibrations from other methods, the accuracy of density functional approximation in a strong magnetic field is not known (see discussion at the end of Sec. V.B).

The energy difference  $\Delta E_s = |E_{s,0}| - |E_\infty|$  between the 3d condensed matter and the 1d chain must be positive and can be estimated by calculating the interaction (mainly quadrupole-quadrupole) between the chains. Various considerations indicate that the difference is between 0.4% and 1% of  $|E_\infty|$  (Lai and Salpeter 1997). Therefore, for light elements such as hydrogen and helium, the binding of the 3d condensed matter results mainly from the covalent bond along the magnetic field axis, not from the chain-chain interaction. For convenience we shall write the cohesive energy  $Q_s$  of the 3d hydrogen condensate in terms of the cohesive energy ( $Q_\infty$ ) of the linear chain as

$$Q_s(\text{H}) = Q_\infty(\text{H}) + \Delta E_s = (1 + \zeta) Q_\infty(\text{H}), \quad (5.19)$$

with  $\zeta \simeq 0.01 - 0.02$  for  $B_{12} = 1 - 500$ .

For hydrogen, the zero-point energy of the proton is not entirely negligible, and can introduce a correction to the cohesive energy. The zero-point energy has not been rigorously calculated, but a reasonable estimate is as follows. Neglecting the magnetic force, the zero-point energy  $E_{zp}$  of a proton in the the lattice is of order  $\hbar \Omega_p$ ,

where  $\Omega_p = (4\pi e^2 n_e / m_p)^{1/2}$  is the proton plasma frequency. Using the the mean electron density  $n_e \simeq 0.035 b^{6/5}$  as estimated from Eq. (5.2) or Eq. (5.11), we find

$$E_{zp} \sim \hbar \Omega_p \simeq 0.015 b^{3/5}. \quad (5.20)$$

This is much smaller than the total binding energy  $|E_\infty|$  unless  $B_{12} \gtrsim 10^5$ . This means that, for the range of field strengths of interest, the zero-point oscillation amplitude is small compared to the lattice spacing. Thus quantum melting is not effective (e.g., Ceperley and Alder 1980; Jones and Ceperley 1996), and the condensed matter is a solid at zero temperature. Accurate determination of  $E_{zp}$  requires a detailed understanding of the lattice phonon spectra. At zero-field, Monte-Carlo simulations give  $E_{zp} \simeq 3\hbar\Omega_p\eta/2$ , with  $\eta \simeq 0.5$  (Hansen and Pollock 1973). For definiteness, we will adopt the same value for  $E_{zp}$  in a strong magnetic field. Taking into account the magnetic effect on the proton, the corrected cohesive energy of the H chain is expected to be

$$Q_\infty = Q_\infty^{(\infty)} - \frac{1}{2} \left[ \hbar\Omega_p\eta + \hbar (\omega_{cp}^2 + 4\eta^2\Omega_p^2)^{1/2} - \hbar\omega_{cp} \right], \quad (5.21)$$

with  $\eta \simeq 0.5$ , where  $\hbar\omega_{cp} = \hbar eB/(m_p c)$  is the cyclotron energy of the proton.

Figure 1 depicts the cohesive energy of  $H_\infty$  as a function of  $B$ ; the energy releases  $Q_1$  and  $Q_2$  for  $e+p=H$  and  $H+H=H_2$  are also shown. Some numerical values are given in Table I. The zero-point energy corrections for  $Q_2$  and  $Q_\infty$  have been included in the figure (if they are neglected, the curves are qualitatively similar, although the exact values of the energies are somewhat changed.) Although  $b \gg 1$  satisfies the nominal requirement for the “strong field” regime, a more realistic expansion parameter for the stability of the condensed state over atoms and molecules is the ratio  $b^{0.4}/(\ln b)^2$ . This ratio exceeds 0.3, and increases rapidly with increasing field strength only for  $b \gtrsim 10^4$ . We see from Fig. 1 that  $Q_1 > Q_2 > Q_\infty$  for  $B_{12} \lesssim 10$ , and  $Q_1 > Q_\infty > Q_2$  for  $10 \lesssim B_{12} \lesssim 100$  and  $Q_\infty > Q_1 > Q_2$  for  $B_{12} \gtrsim 100$ . These inequalities have important consequences on the composition of the saturated vapor above the condensed phase for different magnetic fields (see Sec. VII.B). Figure 5 shows similar numerical results for He.

The cohesive properties of the condensed state of heavy elements such as Fe are different from hydrogen or helium. As discussed in Sec. V.C, linear Fe chain is not bound relative to Fe atom at  $B_{12} = 1 - 10$  (although we expect the Fe chain to be bound for  $B_{12} \gg 100$ ). Since chain-chain interactions only lower  $E_s$  relative to  $E_\infty$  by about 1% (see above), it is likely that the 3d condensed state is also unbound. Jones (1996) found a very small cohesive energy for the 3d condensed iron, corresponding to about 0.5% of the atomic binding energy. In view of the uncertainties associated with the calculations, Jones’ results should be considered as an upper limit, i.e.,

$$Q_s \lesssim 0.005 |E_{\text{atom}}| \sim Z^{9/5} B_{12}^{2/5} \text{ eV}, \quad (\text{for } Z \gtrsim 10) \quad (5.22)$$

where we have used Eq. (3.34) for  $|E_{\text{atom}}|$ .

## F. Shape and Surface Energy of Condensed Droplets

As we shall discuss in Sec. VII, for sufficiently strong magnetic fields and low temperatures, the condensed phase of hydrogen can be in pressure equilibrium with the vapor phase. The two phases have markedly different densities and one might have an “ocean/atmosphere interface”. The question of droplets might have to be considered, and the shape and energy of a droplet is of interest (Lai and Salpeter 1997).

For the phase equilibrium between the condensed state and the  $H_N$  molecules in the vapor, the most relevant quantity is the “surface energy”  $S_N$ , defined as the energy release in converting the 3d condensate  $H_{s,\infty}$  and a  $H_N$  molecule into  $H_{s,\infty+N}$ . Clearly  $S_1 = Q_s = (1 + \zeta)Q_\infty$  is the cohesive energy defined in Sec. V.E. For a linear  $H_N$  molecule with energy (per atom)  $E_N = E(H_N)$ , we have

$$S_N = N(E_N - E_s) = N\Delta E_s + N(E_N - E_\infty) = N\zeta Q_\infty + \xi Q_\infty, \quad (5.23)$$

where the first term on the right-hand side comes from cohesive binding between chains, and the second term is the “end energy” of the one-dimensional chain. Based on numerical results for  $H_2$ ,  $H_3$ ,  $H_4$  and  $H_5$  (see Fig. 4), we infer that the dimensionless factor  $\xi$  in Eq. (5.23) is of order unity. For  $N \lesssim \xi/\zeta \sim 100$ , the “end energy” dominates, while for  $N \gtrsim 100$  the cohesion between chains becomes important. In the latter case, the configuration which minimizes the surface energy  $S_N$  is not the linear chain, but some highly elongated “cylindrical droplet” with  $N_\perp$  parallel chains each containing  $N_\parallel = N/N_\perp$  atoms. For such a droplet, the “end energy” is of order  $N_\perp \xi Q_\infty$ . On the other hand there are  $\sim N_\perp^{1/2}$  “unpaired” chains in such a droplet, each giving an energy  $N_\parallel \zeta Q_\infty$ . Thus the total surface energy

is of order  $\left[ N_{\perp} \xi + \zeta (N/N_{\perp}) N_{\perp}^{1/2} \right] Q_{\infty}$ . The minimum surface energy  $S_N$  of the droplet, for a fixed  $N \gtrsim 2\xi/\zeta \equiv N_c$ , is then obtained for  $N_{\perp} \simeq (N/N_c)^{2/3}$ ,  $N_{\parallel} \simeq N^{1/3} N_c^{2/3}$ , and is of order

$$S_N \simeq 3\xi \left( \frac{N}{N_c} \right)^{2/3} Q_{\infty}, \quad \text{for } N \gtrsim N_c \equiv \frac{2\xi}{\zeta} \sim 200. \quad (5.24)$$

Thus, although the optimal droplets are highly elongated, the surface energy still grows as  $(N/200)^{2/3}$  for  $N \gtrsim 200$ .

## VI. FREE ELECTRON GAS IN STRONG MAGNETIC FIELDS

In Sections III-V, we have reviewed the electronic structure and binding energies of atoms, molecules and condensed matter in strong magnetic fields. As discussed in Sec. I.A, one of the main motivations to study matter in strong magnetic fields is to understand the neutron star surface layer, which directly mediates the thermal radiation from the star and acts as a boundary for the magnetosphere. Before discussing various properties of neutron star envelope in Sec. VII, it is useful to summarize the basic thermodynamical properties of a free electron gas in strong magnetic fields at finite temperature  $T$ .

The number density  $n_e$  of electrons is related to the chemical potential  $\mu_e$  by

$$n_e = \frac{1}{(2\pi\hat{\rho})^2 \hbar} \sum_{n_L=0}^{\infty} g_{n_L} \int_{-\infty}^{\infty} f dp_z, \quad (6.1)$$

where  $g_{n_L}$  is the spin degeneracy of the Landau level ( $g_0 = 1$  and  $g_{n_L} = 2$  for  $n_L \geq 1$ ), and  $f$  is the Fermi-Dirac distribution

$$f = \left[ 1 + \exp \left( \frac{E - \mu_e}{kT} \right) \right]^{-1}, \quad (6.2)$$

with  $E$  given by Eq. (2.12). The electron pressure is given by

$$P_e = \frac{1}{(2\pi\hat{\rho})^2 \hbar} \sum_{n_L=0}^{\infty} g_{n_L} \int_{-\infty}^{\infty} f \frac{p_z^2 c^2}{E} dp_z. \quad (6.3)$$

Note that the pressure is isotropic, contrary to what is stated in Canuto and Ventura (1977) and some earlier papers<sup>3</sup>. The grand thermodynamic potential is  $\Omega = -P_e V$ , from which all other thermodynamic quantities can be obtained. Note that for nonrelativistic electrons (valid for  $E_F \ll m_e c^2$  and  $kT \ll m_e c^2$ ), we use Eq. (2.10) for  $E$ , and the expressions for the density  $n_e$  and pressure  $P_e$  can be simplified to

$$n_e = \frac{1}{2\pi^{3/2} \hat{\rho}^2 \lambda_{Te}} \sum_{n_L=0}^{\infty} g_{n_L} I_{-1/2} \left( \frac{\mu_e - n_L \hbar \omega_{ce}}{kT} \right), \quad (6.4)$$

$$P_e = \frac{kT}{\pi^{3/2} \hat{\rho}^2 \lambda_{Te}} \sum_{n_L=0}^{\infty} g_{n_L} I_{1/2} \left( \frac{\mu_e - n_L \hbar \omega_{ce}}{kT} \right), \quad (6.5)$$

where  $\lambda_{Te} \equiv (2\pi\hbar^2/m_e kT)^{1/2}$  is the thermal wavelength of the electron, and  $I_{\eta}$  is the Fermi integral:

$$I_{\eta}(y) = \int_0^{\infty} \frac{x^{\eta}}{\exp(x-y) + 1} dx. \quad (6.6)$$

---

<sup>3</sup>The transverse kinetic pressure  $P_{e\perp}$  is given by an expression similar to Eq. (6.3), except that  $p_z^2 c^2$  is replaced by  $\langle p_{\perp}^2 c^2 \rangle = n_L \beta (m_e c^2)^2$ . Thus the kinetic pressure is anisotropic, with  $P_{e\parallel} = P_e = P_{e\perp} + \mathcal{M}B$ , where  $\mathcal{M}$  is the magnetization. When we compress the electron gas perpendicular to  $\mathbf{B}$  we must also do work against the Lorentz force density  $(\nabla \times \mathcal{M}) \times \mathbf{B}$  involving the magnetization current. Thus there is a magnetic contribution to the perpendicular pressure of magnitude  $\mathcal{M}B$ . The composite pressure tensor is therefore isotropic, in agreement with the thermodynamic result  $P_e = -\Omega/V$  (Blandford and Hernquist 1982). For a nonuniform magnetic field, the net force (per unit volume) on the stellar matter is  $-\nabla P_e - \nabla(B^2/8\pi) + (\mathbf{B} \cdot \nabla)\mathbf{B}/(4\pi)$ .

First consider degenerate electron gas at zero temperature. The Fermi energy (excluding the electron rest mass)  $E_F = \mu_e(T=0) - m_e c^2 = (m_e c^2) \epsilon_F$  is determined from

$$n_e = \frac{\beta}{2\pi^2 \lambda_e^3} \sum_{n_L=0}^{n_{\max}} g_{n_L} x_F(n_L), \quad (6.7)$$

with

$$x_F(n_L) = \frac{p_F(n_L)}{m_e c} = [(1 + \epsilon_F)^2 - (1 + 2n_L \beta)]^{1/2}, \quad (6.8)$$

where  $\lambda_e = \hbar/(m_e c)$  is the electron Compton wavelength,  $\beta = B/B_{\text{rel}} = \alpha^2 b$ , and  $n_{\max}$  is set by the condition  $(1 + \epsilon_F)^2 \geq (1 + 2n_{\max} \beta)$ . The electron pressure is given by

$$P_e = \frac{\beta m_e c^2}{2\pi^2 \lambda_e^3} \sum_{n_L=0}^{n_{\max}} g_{n_L} (1 + 2n_L \beta) \Theta \left[ \frac{x_F(n_L)}{(1 + 2n_L \beta)^{1/2}} \right], \quad (6.9)$$

where

$$\Theta(y) = \frac{1}{2} y \sqrt{1 + y^2} - \frac{1}{2} \ln \left( y + \sqrt{1 + y^2} \right) \rightarrow \frac{1}{3} y^3 \quad \text{for } y \ll 1. \quad (6.10)$$

The critical ‘‘magnetic density’’ below which only the ground Landau level is populated ( $n_{\max} = 0$ ) is determined by  $(1 + \epsilon_F)^2 = 1 + 2\beta$ , which gives [see Eq. (5.9)]

$$\rho_B = 0.802 Y_e^{-1} b^{3/2} \text{ g cm}^{-3} = 7.04 \times 10^3 Y_e^{-1} B_{12}^{3/2} \text{ g cm}^{-3}, \quad (6.11)$$

where  $Y_e = Z/A$  is the number of electrons per baryon. Similarly, the critical density below which only the  $n_L = 0, 1$  levels are occupied ( $n_{\max} = 1$ ) is

$$\rho_{B1} = (2 + \sqrt{2}) \rho_B = 3.414 \rho_B. \quad (6.12)$$

For  $\rho < \rho_B$ , equation (6.7) simplifies to

$$\rho = 3.31 \times 10^4 Y_e^{-1} B_{12} [(1 + \epsilon_F)^2 - 1]^{1/2} \text{ g cm}^{-3}. \quad (6.13)$$

For nonrelativistic electrons ( $\epsilon_F \ll 1$ ), the Fermi temperature  $T_F = E_F/k = (m_e c^2/k) \epsilon_F$  is given by

$$T_F = \frac{E_F}{k} = 2.70 B_{12}^{-2} (Y_e \rho)^2 \text{ K} \quad (\text{for } \rho < \rho_B), \quad (6.14)$$

where  $\rho$  is in units of  $1 \text{ g cm}^{-3}$ . For  $\rho \gg \rho_B$ , many Landau levels are filled by the electrons, Eqs. (6.1) and (6.3) reduce to the zero-field expressions. In this limit, the Fermi momentum  $p_F$  is given by

$$x_F = \frac{p_F}{m_e c} = \frac{\hbar}{m_e c} (3\pi^2 n_e)^{1/3} = 1.009 \times 10^{-2} (Y_e \rho)^{1/3}, \quad (B = 0) \quad (6.15)$$

and the Fermi temperature is

$$T_F = \frac{m_e c^2}{k} \left( \sqrt{1 + x_F^2} - 1 \right) \simeq 3.0 \times 10^5 (Y_e \rho)^{2/3} \text{ K}, \quad (B = 0) \quad (6.16)$$

where the second equality applies to nonrelativistic electrons ( $x_F \ll 1$ ). Comparison between Eq. (6.14) and Eq. (6.16) clearly shows that the magnetic field lifts the degeneracy of electrons even at relatively high density (see Fig. 6).

Finite temperature tends to smear out Landau levels. Let the energy difference between the  $n_L = n_{\max}$  level and the  $n_L = n_{\max} + 1$  level be  $\Delta E_B$ . We can define a ‘‘magnetic temperature’’

$$T_B = \frac{\Delta E_B}{k} = \frac{m_e c^2}{k} \left( \sqrt{1 + 2n_{\max} \beta + 2\beta} - \sqrt{1 + 2n_{\max} \beta} \right). \quad (6.17)$$

Clearly,  $T_F = T_B$  at  $\rho = \rho_B$  (see Fig. 6). The effects due to Landau quantization are diminished when  $T \gtrsim T_B$ . For  $\rho \leq \rho_B$ , we have  $T_B = (\sqrt{1+2\beta} - 1)(m_e c^2/k)$ , which reduces to  $T_B \simeq \hbar\omega_{ce}/k$  for  $\beta = \alpha^2 b \ll 1$ . For  $\rho \gg \rho_B$  (or  $n_{\max} \gg 1$ ), equation (6.17) becomes

$$T_B \simeq \frac{\hbar\omega_{ce}}{k} \left( \frac{m_e}{m_e^*} \right) = 1.34 \times 10^8 B_{12} (1 + x_F^2)^{-1/2} \text{ K}, \quad (6.18)$$

where  $m_e^* = \sqrt{m_e^2 + (p_F/c)^2} = m_e \sqrt{1 + x_F^2}$ , with  $x_F$  given by Eq. (6.15).

There are three regimes characterizing the effects of Landau quantization on the thermodynamic properties of the electron gas (Figure 6; see also Yakovlev and Kaminker 1994):

(i)  $\rho \lesssim \rho_B$  and  $T \lesssim T_B$ : In this regime, the electrons populate mostly the ground Landau level, and the magnetic field modifies essentially all the properties of the gas. The field is sometimes termed “strongly quantizing”. For example, for degenerate, nonrelativistic electrons ( $\rho < \rho_B$  and  $T \ll T_F \ll m_e c^2/k$ ), the internal energy density and pressure are

$$u_e = \frac{1}{3} n_e E_F, \quad (6.19)$$

$$P_e = 2u_e = \frac{2}{3} n_e E_F \propto B^{-2} \rho^3. \quad (6.20)$$

These should be compared with the  $B = 0$  expression  $P_e = 2u_e/3 \propto \rho^{5/3}$ . Note that for nondegenerate electrons ( $T \gg T_F$ ), the classical ideal gas equation of state,

$$P_e = n_e kT, \quad (6.21)$$

still holds in this “strongly quantizing” regime, although other thermodynamic quantities are significantly modified by the magnetic field.

(ii)  $\rho \gtrsim \rho_B$  and  $T \lesssim T_B$ : In this regime, the electrons are degenerate (note that  $T_F > T_B$  when  $\rho > \rho_B$ ; see Fig. 6), and populate many Landau levels but the level spacing exceeds  $kT$ . The magnetic field is termed “weakly quantizing”. The bulk properties of the gas (e.g., pressure and chemical potential), which are determined by all the electrons in the Fermi sea, are only slightly affected by such magnetic fields. However, the quantities determined by thermal electrons near the Fermi surface show large oscillatory features as a function of density or magnetic field strength. These de Haas - van Alphen type oscillations arise as successive Landau levels are occupied with increasing density (or decreasing magnetic field). The oscillatory quantities are usually expressed as derivatives of the bulk quantities with respect to thermodynamic variables; examples include heat capacity, magnetization and magnetic susceptibility, adiabatic index ( $\partial \ln P_e / \partial \ln \rho$ ), sound speed, and electron screening length of an electric charge in the plasma (e.g., Ashcroft and Mermin 1976; Blandford and Hernquist 1982; Lai and Shapiro 1991; Yakovlev and Kaminker 1994). With increasing  $T$ , the oscillations become weaker because of the thermal broadening of the Landau levels; when  $T \gtrsim T_B$ , the oscillations are entirely smeared out, and the field-free results are recovered.

(iii) For  $T \gg T_B$  (regardless of density): In this regime, many Landau levels are populated and the thermal widths of the Landau levels ( $\sim kT$ ) are higher than the level spacing. The magnetic field is termed “non-quantizing” and does not affect the thermodynamic properties of the gas.

## VII. SURFACE LAYER OF A MAGNETIZED NEUTRON STAR

In this section we review the properties of the surface layer of a magnetized neutron star (NS). We shall focus on the thermodynamic property and phase diagram. We expect various forms of magnetic bound states discussed in Sections III-V to exist on the stellar envelope depending on the field strength, temperature and density.

The chemical composition of the NS surface is unknown. A NS is formed as a collapsed, hot ( $kT \gtrsim 10$  MeV) core of a massive star in a supernova explosion. The NS matter may be assumed to be fully catalyzed and in the lowest energy state (e.g., Salpeter 1961; Baym, Pethick and Sutherland 1971). We therefore expect the NS surface to consist of iron ( $^{56}\text{Fe}$ ) formed at the star’s birth. This may be the case for young radio pulsars that have not accreted any gas. However, once the NS accretes material, or has gone through a phase of accretion, either from the interstellar medium or from a binary companion, the surface (crust) composition can be quite different due to surface nuclear reactions and weak interactions during the accretion (e.g., Haensel and Zdunik 1990; Blaes *et al.* 1990; Schatz *et al.* 1999). Moreover, a hydrogen-helium envelope will form on the top of the surface unless it has completely burnt out. While a strong magnetic field and/or rapid stellar spin may prevent large-scale accretion, it should be noted that even with a

low accretion rate of  $10^{10} \text{ g s}^{-1}$  (typical of accretion from the interstellar medium) for one year, the accreted material will be more than enough to completely shield the original iron surface of the NS. The lightest elements, H and He, are likely to be the most important chemical species in the envelope due to their predominance in the accreting gas and also due to quick separation of light and heavy elements in the gravitational field of the NS (see Alcock and Illarionov 1980 for a discussion of gravitational separation in white dwarfs; applied to NSs, we find that the settling time of C in a  $10^6 \text{ K}$  hydrogen photosphere is of order a second). If the present accretion rate is low, gravitational settling produces a pure H envelope. Alternatively, a pure He layer may result if the hydrogen has completely burnt out.

In this section, we shall mostly focus on the hydrogen envelope (Sec. VII.A and Sec. VII.B) both because of its predominance in the outer layer of the NS and because the properties of different phases of H are better understood. A pure He envelope would presumably have similar properties as the H envelope. The Iron surface layer and deeper crust will be discussed in Sec. VII.C and Sec. VII.E. We are only interested in the temperature regime  $T \gtrsim 10^5 \text{ K}$ , since NSs with  $T \lesssim 10^5 \text{ K}$  are nearly impossible to observe.

### A. Warm Hydrogen Atmosphere

We now consider the physical conditions and chemical equilibrium in a hydrogen atmosphere with photospheric temperature in the range  $T_{\text{ph}} \sim 10^5 - 10^{6.5} \text{ K}$  and magnetic field strength in the range  $B_{12} \sim 0.1 - 20$ . These conditions are likely to be satisfied by most observable NSs. For such relatively low field strengths, the atmosphere is largely nondegenerate, and consists mainly of ionized hydrogen, H atoms and small  $\text{H}_N$  molecules, and we can neglect the condensed phase in the photosphere. (In Sec. VII.B we shall consider the more extreme situation of  $B_{12} \gg 10$  in which the nondegenerate atmosphere has negligible optical depth and the condensed phase becomes important.) Although the density scale height of the atmosphere is only  $h \simeq kT_{\text{ph}}/m_p g \simeq 0.08 T_{\text{ph},5} g_{14}^{-1} \text{ cm}$ , where  $T_{\text{ph},5} = T_{\text{ph}}/(10^5 \text{ K})$ , and  $g = 10^{14} g_{14} \text{ cm s}^{-2}$  is the gravitational acceleration, the atmosphere has significant optical depth and therefore the atmospheric properties determine the thermal radiation spectrum from the NS (see Pavlov *et al.* 1995 and references therein).

The photosphere of the NS is located at the characteristic photon optical depth  $\tau = \int_{r_{\text{ph}}}^{\infty} \rho \kappa_R dr = 2/3$ , where  $\kappa_R$  (in units of  $\text{cm}^2/\text{g}$ ) is the Rosseland mean opacity; the photosphere pressure is  $P_{\text{ph}} \simeq 2g/(3\kappa_R)$ . An accurate determination of the photosphere conditions requires a self-consistent solution of the atmosphere structure and radiative transport, but an order-of-magnitude estimate is as follows. In a strong magnetic field, the radiative opacity becomes anisotropic and depends on polarization (e.g., Canuto *et al.* 1971; Lodenquai *et al.* 1974; Pavlov and Panov 1976; Ventura 1979; Nagel and Ventura 1980; see Meszaros 1992 and references therein). For photons with polarization vector perpendicular to the magnetic field (the “extraordinary mode”) the free-free absorption and electron scattering opacities are reduced below their zero-field values by a factor  $(\omega/\omega_{ce})^2$ , while for photons polarized along the magnetic field (the “ordinary mode”), the opacities are not affected. Pavlov and Yakovlev (1977) and Silant’ev and Yakovlev (1980) have calculated the appropriate averaged Rosseland mean free-free and scattering opacity; in the magnetic field and temperature regime of interest, an approximate fitting formula is

$$\kappa_R(B) \simeq 400 \eta \left( \frac{kT}{\hbar\omega_{ce}} \right)^2 \kappa_R(0), \quad (7.1)$$

where  $\eta \simeq 1$  and  $\kappa_R(0)$  is the zero-field opacity. Using the ideal gas equation of state,  $P_{\text{ph}} \simeq \rho_{\text{ph}} kT_{\text{ph}}/m_p$ , we obtain the photosphere density

$$\rho_{\text{ph}} \simeq 0.5 \eta^{-1/2} g_{14}^{1/2} T_{\text{ph},5}^{1/4} B_{12} \text{ g cm}^{-3}. \quad (7.2)$$

Note that for  $\eta \sim 1/400$ , this equation also approximately characterizes the density of the deeper layer where the extraordinary photons are emitted. Other sources of opacity such as bound-free and bound-bound absorptions will increase the opacity and reduce the photosphere density, but the above estimate defines the general range of densities in the atmosphere if the  $T_{\text{ph}}$  is large enough for the neutral H abundance to be small. Clearly, a typical atmosphere satisfies  $\rho \ll \rho_B$  and  $T \ll T_B$ , but  $T \gg T_F$  (see Sec. VI and Fig. 6), i.e., the magnetic field is strongly quantizing in the atmosphere, but the electrons are nondegenerate.

An important issue for NS atmosphere modeling concerns the ionization equilibrium (or Saha equilibrium) of atoms in strong magnetic fields. Earlier treatments of this problem (e.g., Gnedin *et al.* 1974; Khersonskii 1987) assumed that the atom can move freely across the magnetic field; this is generally not valid for the strong field regime of interest here (see Sec. III.E). Lai and Salpeter (1995) gave an approximate analytic solution for a limited temperature-density regime (see below). To date the most complete treatment of the problem is that of Potekhin *et al.* (1999), who used

the numerical energy levels of a moving H atom as obtained by Potekhin (1994,1998) and an approximate description of the nonideal gas effect to derive the thermodynamic properties of a partially ionized hydrogen plasma in strong magnetic fields. Here we discuss the basic issues of ionization equilibrium in strong magnetic fields, and refer to Potekhin *et al.* (1999) for a more detailed treatment.

For nondegenerate electrons in a magnetic field, the partition function (in volume  $V$ ) is

$$\begin{aligned} Z_e &= \frac{V}{2\pi\hat{\rho}^2} \sum_{n_L=0}^{\infty} g_{n_L} \exp\left(\frac{-n_L\hbar\omega_{ce}}{kT}\right) \int_{-\infty}^{\infty} \frac{dp_z}{h} \exp\left(\frac{-p_z^2}{2m_e kT}\right) \\ &= \frac{V}{2\pi\hat{\rho}^2 \lambda_{Te}} \tanh^{-1}\left(\frac{\hbar\omega_{ce}}{2kT}\right) \\ &\simeq \frac{V}{2\pi\hat{\rho}^2 \lambda_{Te}}, \end{aligned} \quad (7.3)$$

where  $\lambda_{Te} = (2\pi\hbar^2/m_e kT)^{1/2}$  is the electron thermal wavelength, and the last equality applies for  $T \ll T_B$ . For protons, we shall drop the zero-point energy and the spin energy in both free states and bound states [i.e.,  $E = n_L\hbar\omega_{cp} + p_z^2/(2m_p)$  for a free proton]. Treating the proton as a spinless particle ( $g_{n_L} = 1$ ), we find that the partition function of free protons is

$$Z_p = \frac{V}{2\pi\hat{\rho}^2 \lambda_{Tp}} \left[1 - \exp\left(-\frac{\hbar\omega_{cp}}{kT}\right)\right]^{-1}, \quad (7.4)$$

where  $\lambda_{Tp} = (2\pi\hbar^2/m_p kT)^{1/2}$  is the proton thermal wavelength.

Using Eq. (3.40) for the energy of the H atom, we write the partition function for the bound states as

$$Z_H = \frac{V}{h^3} \sum_{m\nu} \int d^3K w_{m\nu}(K_{\perp}) \exp\left(-\frac{\mathcal{E}_{m\nu}}{kT}\right) = \frac{V}{\lambda_{TH}^3} Z_w, \quad (7.5)$$

where  $\lambda_{TH} = (2\pi\hbar^2/MkT)^{1/2}$ , and

$$Z_{m\nu} = \frac{\lambda_{TH}^2}{2\pi\hbar^2} \int dK_{\perp} K_{\perp} w_{m\nu}(K_{\perp}) \exp\left(-\frac{m\hbar\omega_{cp} + E_{m\nu}(K_{\perp})}{kT}\right), \quad (7.6)$$

$$Z_w = \sum_{m\nu} Z_{m\nu}. \quad (7.7)$$

The Saha equation for the ionization equilibrium in strong magnetic fields then reads

$$\frac{n_H}{n_p n_e} = \frac{V Z_H}{Z_e Z_p} = \frac{\lambda_{Te} \lambda_{Tp} (2\pi\hat{\rho}^2)^2}{\lambda_{TH}^3} \left[1 - \exp\left(-\frac{\hbar\omega_{cp}}{kT}\right)\right] Z_w. \quad (7.8)$$

In Eqs. (7.5)-(7.6),  $w_{m\nu}(K_{\perp})$  is the occupation probability of the hydrogen bound state characterized by  $m, \nu, K_{\perp}$ , and it measures deviation from Maxwell-Boltzmann distribution due to the medium effect. Physically, it arises from the fact that an atom tends to be “destroyed” when another particle in the medium comes close to it. The atom–proton interaction introduces a correction to the chemical potential of the atomic gas

$$\Delta\mu_H \simeq 2n_p kT \int d^3r [1 - \exp(-U_{12}/kT)], \quad (7.9)$$

(see, e.g., Landau and Lifshitz 1980), where  $U_{12}$  is the interaction potential. Similar expressions can be written down for atom–electron and atom–atom interactions. For  $r$  much larger than the size of the elongated atom, the atom–proton potential  $U_{12}$  has the form  $U_{12} \sim eQ(3\cos^2\theta - 1)/r^3$ , where  $\theta$  is the angle between the vector  $\mathbf{r}$  and the  $z$ -axis, and  $Q \sim eL_z^2$  is the quadrupole moment of the atom; the atom–atom interaction potential has the form  $U_{12} \sim Q^2(3 - 30\cos^2\theta + 35\cos^4\theta)/r^5$ . Since the integration over the solid angle  $\int d\Omega U_{12} = 0$  at large  $r$ , the contribution to  $\Delta\mu(\text{H})$  from large  $r$  is negligible. (An atom with  $K_{\perp} \neq 0$  also acquires a dipole moment in the direction of  $\mathbf{B} \times \mathbf{K}_{\perp}$ , the resulting dipole interaction also satisfies  $\int d^3r U_{12} = 0$ .) Thus the main effect of particle interactions is the “excluded volume effect”: Let  $L_{m\nu}(K_{\perp})$  be the characteristic size of the atom such that we can set  $U_{12} \rightarrow \infty$  when  $r \lesssim L_{m\nu}$ . We then have  $\Delta\mu_H \sim n_b kT (4\pi L_{m\nu}^3/3)$ , where  $n_b = n_H + n_p$  is the baryon number density. Therefore, the occupation probability is of order

$$w_{m\nu}(K_{\perp}) \sim \exp \left[ -\frac{4\pi}{3} n_b L_{m\nu}^3(K_{\perp}) \right]. \quad (7.10)$$

The size of the atom can be estimated as follows (see Sec. III.A and Sec. III.E): when  $K_{\perp} = 0$ , the tightly bound state ( $\nu = 0$ ) has  $L_z \sim l_m^{-1}$ ,  $L_{\perp} \sim \rho_m$ , while the  $\nu > 0$  state has  $L_z \sim \nu^2$ ,  $L_{\perp} \sim \rho_m$ ; when  $K_{\perp} \neq 0$ , the electron and proton are displaced in the transverse direction by a distance  $d \lesssim K_{\perp}/b$ ; thus we have  $L_{m\nu}(K_{\perp}) \sim \max(L_z, L_{\perp}, K/b)$ . More accurate fitting formula for  $L_{m\nu}(K_{\perp})$  is given in Potekhin (1998).

More precise calculation of the occupation probability requires detailed treatment of interactions between various particles in the plasma. Even at zero magnetic field, the problem is challenging and uncertainties remain (e.g., Hummer and Mihalas 1988; Mihalas et al. 1988; Saumon and Chabrier 1991,1992; Potekhin 1996). In strong magnetic fields, additional complications arise from the nonspherical shape of the atom. Nevertheless, using the hard-sphere approximation similar to the field-free situation, Potekhin *et al.* (1999) have constructed a free energy model for partially ionized hydrogen, from which  $w_{m\nu}(K_{\perp})$  can be calculated along with other thermodynamic quantities. Figure 7 shows some numerical results based on the calculations of Potekhin *et al.* (1999). The general trend that the neutral fraction  $n_H/n_b$  increases with increasing  $B$  is the result of larger binding energy  $|E_{m\nu}(K_{\perp})|$  for larger  $B$ , although this trend is offset partially by the fact that the electron phase space also increases with  $B$  [see Eq. (7.3)]. For a given  $T$  and  $B$ , the neutral fraction increases with density until  $\rho$  reaches  $\rho_c \sim 10\text{-}100 \text{ g cm}^{-3}$  [for  $B = 10^{12}\text{-}10^{13} \text{ G}$  (see Potekhin *et al.* 1999);  $\rho_c$  scales with  $b$  roughly as  $(\ln b)^3$ ], above which the neutral fraction declines because of pressure ionization.

It is instructive to consider the relative importance of the ‘‘centered states’’ and the ‘‘decentered states’’ to the neutral hydrogen fraction. As discussed in Sec. III.E, the H energy can be approximated by  $E_0(K_{\perp}) \simeq E_0 + K_{\perp}^2/(2M_{\perp})$  for  $K_{\perp} \lesssim K_{\perp c} \sim \sqrt{2M|E_0|}$  (we consider only the  $m = \nu = 0$  state for simplicity). Setting  $w_{00}(K_{\perp}) = 1$  for low densities, the contribution of the  $K_{\perp} \lesssim K_{\perp c}$  states to  $Z_w$  is given by (in a.u.)

$$Z_w^{(c)} \simeq \exp \left( -\frac{E_0}{T} \right) \left( \frac{M_{\perp}}{M} \right), \quad (7.11)$$

for  $K_{\perp c}^2/(2M_{\perp}) \sim (M/M_{\perp})|E_0| \gg T$ . On the other hand, the contribution from the decentered states to  $Z_w$  can be estimated as

$$Z_w^{(d)} \simeq \frac{1}{MT} \int_{K_{\perp c}}^{K_{\max}} K_{\perp} \exp \left[ -\frac{E_0(K_{\perp})}{T} \right] dK_{\perp}, \quad (7.12)$$

where  $K_{\max}$  is given by  $(4\pi/3)(K_{\max}/b)^3 n_b \simeq 1$ . Since  $|E_0(K_{\perp})|$  for  $K \gtrsim K_{\perp c}$  is much less than  $|E_0|$ , we find

$$\frac{Z_w^{(c)}}{Z_w^{(d)}} \sim \frac{2M_{\perp}T}{K_{\max}^2} \exp \left( \frac{|E_0|}{T} \right) \sim \frac{5M_{\perp}T}{b^2} n_b^{2/3} \exp \left( \frac{|E_0|}{T} \right). \quad (7.13)$$

Thus for the centered states to dominate the atomic population, we require  $|E_0|/T \gtrsim \ln \left( b^2/5M_{\perp}T n_b^{2/3} \right)$ ; for example, at  $T = 10^{5.5} \text{ K}$ , this corresponds to  $B \gtrsim 10^{13.5} \text{ G}$ , or  $|E_0|/T \gtrsim 15$  (see the dotted lines in Fig. 7).

For sufficiently high  $B$  or sufficiently low  $T$ , we expect the atmosphere to have appreciable abundance of  $\text{H}_2$  molecules. Since detailed study of the effect of motion on  $\text{H}_2$  is not available, only an approximate estimate is possible (Lai and Salpeter 1997; Potekhin *et al.* 1999). For example, at  $B = 10^{13} \text{ G}$  there exists a large amount of  $\text{H}_2$  in the photosphere ( $\rho \sim 10 - 100 \text{ g cm}^{-3}$ ) when  $T \lesssim 10^{5.5} \text{ K}$ . As we go deeper into the atmosphere, we expect larger molecules to appear; when the density approaches the internal density of the atom/molecule, the bound states lose their identities and we obtain a uniform, ionized plasma. With increasing density, the plasma becomes degenerate, and gradually transforms into a condensed phase (Lai and Salpeter 1997).

## B. Surface Hydrogen at Ultrahigh Fields: The Condensed Phase

We have seen in Sec. VII.A that for  $T \gtrsim 10^5 \text{ K}$  and  $B \lesssim 10^{13.5} \text{ G}$ , the outermost layer of the neutron star is nondegenerate, and the surface material gradually transforms into a degenerate Coulomb plasma as density increases. As discussed in Sections III-V, the binding energy of the condensed hydrogen increases as a power-law function of  $B$ , while the binding energies of atoms and small molecules increase only logarithmically. We therefore expect that for sufficiently strong magnetic fields, there exists a critical temperature  $T_{\text{crit}}$ , below which a first-order phase transition occurs between the condensed hydrogen and the gaseous vapor; as the vapor density decreases with increasing  $B$  or decreasing  $T$ , the outermost stellar surface would be in the form of condensed hydrogen (Lai and Salpeter 1997).

While a precise calculation of  $T_{\text{crit}}$  for the phase transition is not available at present, we can get an estimate by considering the equilibrium between the condensed hydrogen (labeled “s”) and the gaseous phase (labeled “g”) in the ultrahigh field regime (where phase separation exists). The gaseous phase consists of a mixture of free electrons, protons, bound atoms and molecules. Phase equilibrium requires the temperature, pressure and the chemical potentials of different species to satisfy the conditions

$$P_s = P_g = [2n_p + n(\text{H}) + n(\text{H}_2) + n(\text{H}_3) + \dots]kT = P, \quad (7.14)$$

$$\mu_s = \mu_e + \mu_p = \mu(\text{H}) = \frac{1}{2}\mu(\text{H}_2) = \frac{1}{3}\mu(\text{H}_3) = \dots \quad (7.15)$$

For the condensed phase near zero-pressure, the density is approximately

$$\rho_s \simeq 561 B_{12}^{6/5} \text{ g cm}^{-3}, \quad (7.16)$$

and the electron Fermi temperature is  $T_F \simeq 0.236 b^{2/5} = 8.4 \times 10^5 B_{12}^{2/5}$  K; thus at a given temperature, the condensed hydrogen becomes more degenerate as  $B$  increases. Let the energy per Wigner-Seitz cell in the condensate be  $E_s(r_s)$  [see Eq. (5.10) for an approximate expression;  $r_s = r_i$  for hydrogen]. The pressure and chemical potential of the condensed phase are given by

$$P_s = -\frac{1}{4\pi r_s^2} \frac{dE_s}{dr_s}, \quad (7.17)$$

$$\mu_s = E_s(r_s) + P_s V_s \simeq E_{s,0} + P_s V_{s,0}, \quad (7.18)$$

where the subscript “0” indicates the zero-pressure values. We have assumed that the vapor pressure is sufficiently small so that the deviation from the zero-pressure state of the condensate is small, i.e.,  $\delta \equiv |(r_s - r_{s,0})/r_{s,0}| \ll 1$ ; this is justified when the saturation vapor pressure  $P_{\text{sat}}$  is much less than the critical pressure  $P_{\text{crit}}$  for phase separation, or when  $T \ll T_{\text{crit}}$ . The finite temperature correction  $\Delta\mu_s$  to the chemical potential of the condensed phase, as given by  $\Delta\mu_s(T) \simeq \pi^2 T^2 / (12T_F)$ , is much smaller than the cohesive energy and can be neglected. Using the partition functions of free electrons, protons and atoms as given in Sec. VII.A, we find that in the saturated vapor,

$$n_p = n_e \simeq \frac{bM^{1/4}T^{1/2}}{(2\pi)^{3/2}} \left[ 1 - \exp\left(-\frac{b}{MT}\right) \right]^{-1/2} \exp\left(-\frac{Q_1 + Q_s}{2T}\right), \quad (7.19)$$

$$n(\text{H}) \simeq \left(\frac{MT}{2\pi}\right)^{3/2} \left(\frac{M'_1}{M}\right) \exp\left(-\frac{Q_s}{T}\right). \quad (7.20)$$

where  $Q_s = |E_{s,0}| - |E(\text{H})|$  is the cohesive energy of the condensed hydrogen (we have neglected  $P_s V_{s,0}$  in comparison to  $Q_s$ ), and  $Q_1 = |E(\text{H})|$  is the ionization energy of the hydrogen atom. In Eq. (7.20) we have included only the ground state ( $m = \nu = 0$ ) of the H atom and have neglected the “decentered states”; this is valid for  $T \lesssim Q_1/20$  (see Sec. VII.A). The equilibrium condition  $N\mu_s = \mu_N$  for the process  $\text{H}_{s,\infty} + \text{H}_N = \text{H}_{s,\infty+N}$  (where  $\text{H}_N$  represents a small molecular chain or a 3d droplet) yields

$$n(\text{H}_N) \simeq N^{3/2} \left(\frac{MT}{2\pi}\right)^{3/2} \exp\left(-\frac{S_N}{T}\right), \quad (7.21)$$

where  $S_N = NE_N - NE_s$  is the surface energy discussed in Sec. V.F. In Eq. (7.21), we have assumed that the  $\text{H}_N$  molecule (or 3d droplet) moves across the field freely; this should be an increasingly good approximation as  $N$  increases.

The critical temperature  $T_{\text{crit}}$ , below which phase separation between the condensed hydrogen and the gaseous vapor occurs, is determined by the condition  $n_s = n_g = n_p + n(\text{H}) + 2n(\text{H}_2) + 3n(\text{H}_3) + \dots$ . Although Eqs. (7.19)-(7.21) are derived for  $n_g \ll n_s$ , we may still use them to obtain an estimate of  $T_{\text{crit}}$ . Using the approximate surface energy  $S_N$  as discussed in Sec. V.F, we find

$$T_{\text{crit}} \sim 0.1 Q_s \simeq 0.1 Q_\infty. \quad (7.22)$$

Thus  $T_{\text{crit}} \simeq 8 \times 10^4$ ,  $5 \times 10^5$  and  $10^6$  K for  $B_{12} = 10$ , 100 and 500. Figure 8 shows some examples of the saturation vapor density as a function of temperature for several values of  $B$ . It should be emphasized that the calculation is very uncertain around  $T \sim T_{\text{crit}}$ . But when the temperature is below  $T_{\text{crit}}/2$  (for example), the vapor density becomes much less than the condensation density  $n_s$  and phase transition is unavoidable. When the temperature

drops below a fraction of  $T_{\text{crit}}$ , the vapor density becomes so low that the optical depth of the vapor is negligible and the outermost layer of the NS then consists of condensed hydrogen. The condensate will be in the liquid state when  $\Gamma = e^2/(r_i kT) \lesssim 175$  (see Sec. VII.E), or when  $T \gtrsim 1.3 \times 10^3 (\rho/1 \text{ g cm}^{-3})^{1/3} \text{ K} \simeq 7 \times 10^4 B_{14}^{2/5} \text{ K}$ . The radiative properties of such condensed phase are of interest to study (see Sec. VII.D).

The protons in the condensed hydrogen phase can undergo significant pycnonuclear reactions. Unlike the usual situation of pycnonuclear reactions (see Salpeter and Van Horn 1969; Ichimaru 1993), where the high densities needed for the reactions at low temperatures are achieved through very high pressures, here the large densities (even at zero pressure) result from the strong magnetic field — this is truly a “zero-pressure cold fusion” (Lai and Salpeter 1997). For slowly accreting neutron stars (so that the surface temperature is low enough for condensation to occur), the inflowing hydrogen can burn, almost as soon as it has condensed into the liquid phase. It is not clear whether this burning proceeds smoothly or whether there is some kind of oscillatory relaxation (e.g., cooling leads to condensation, leading to hydrogen burning and heat release, followed by evaporation which stops the burning and leads to further cooling; see Salpeter 1998).

### C. Iron Surface Layer

For neutron stars that have not accreted much gas, one might expect the surfaces to consist of iron formed at the neutron star’s birth. As discussed in Sec. V.E the cohesive energy of Fe is uncertain. If the condensed Fe is unbound with respect to the Fe atom ( $Q_s = |E_s| - |E_{\text{atom}}| < 0$ ), then the outermost Fe layer of the NS is characterized by gradual transformation from nondegenerate gas at low densities, which includes Fe atoms and ions, to degenerate plasma as the pressure (or column density) increases. The radiative spectrum will be largely determined by the property of the nondegenerate layer. However, even a weak cohesion of the Fe condensate ( $Q_s > 0$ ) can give rise to a phase transition at sufficiently low temperatures.<sup>4</sup> The number density of atomic Fe in the saturated vapor is of order

$$n_A \simeq \left( \frac{AMT}{2\pi} \right)^{3/2} \exp\left( -\frac{Q_s}{T} \right). \quad (7.23)$$

The gas density in the vapor is  $\rho_g \gtrsim AMn_A$ . The critical temperature for phase transition can be estimated from  $\rho_g = \rho_s$ . Using Eq. (5.13) as an estimate for the condensation density  $\rho_s$ , and using Eq. (5.22) as the upper limit of  $Q_s$ , we find

$$T_{\text{crit}} \lesssim 0.1 Q_s \lesssim 10^{5.5} B_{12}^{2/5} \text{ K}. \quad (7.24)$$

As in the case of hydrogen (see Sec. VII.B), we expect the vapor above the condensed iron surface to have negligible optical depth when  $T \lesssim T_{\text{crit}}/3$ .

The iron surface layers of magnetic NSs have also been studied using Thomas-Fermi type models (e.g., Fushiki, Gudmundsson and Pethick 1989; Abrahams and Shapiro 1991; Rönvaldsson *et al.* 1993; Thorolfsson *et al.* 1998; see Appendix B). While these models are too crude to determine the cohesive energy of the condensed matter, they provide a useful approximation to the gross properties of the NS surface layer. Figure 9 depicts the equation of state of iron at  $B = 10^{12} \text{ G}$  and  $B = 10^{13} \text{ G}$  based on Thomas-Fermi type statistical models. At zero temperature, the pressure is zero at a finite density which increases with increasing  $B$ . This feature is qualitatively the same as in the uniform electron gas model (Sec. V.D). Neglecting the exchange-correlation energy and the nonuniformity correction, we can write the pressure of a zero-temperature uniform electron gas as

$$P = P_e - \frac{3}{10} \left( \frac{4\pi}{3} \right)^{1/3} (Ze)^2 \left( \frac{\rho}{Am_p} \right)^{4/3}, \quad (7.25)$$

where the first term is given by Eq. (6.9) [or by Eq. (6.20) in the strong field, degenerate limit], and the second term results from the Coulomb interactions among the electrons and ions. Setting  $P = 0$  gives the condensation density  $\rho_{s,0}$  as in Eq. (5.13). Note that near zero-pressure, all these models are approximate (e.g., the calculated  $\rho_{s,0}$  can differ from the true value by a factor of a few), and more detailed electronic structure calculations are needed to

---

<sup>4</sup>The condensation of Fe was first discussed by Ruderman and collaborators (see Ruderman 1974; Flowers *et al.* 1977), although these earlier calculations greatly overestimated the cohesive energy  $Q_s$  of Fe (see Sec. V.B and Sec. V.E).

obtain reliable pressure – density relation. Figure 9 also shows the results of the finite-temperature Thomas-Fermi model (Thorolfsson *et al.* 1998). Obviously, at finite temperatures, the pressure does not go to zero until  $\rho \rightarrow 0$ , i.e., an atmosphere is present. Note that the finite-temperature Thomas-Fermi model only gives a qualitative description of the dense atmosphere; important features such as atomic states and ionizations are not captured in this model.

#### D. Radiative Transfer and Opacities

As discussed in Sec. I.A, the surface thermal radiation detected from isolated NSs provides valuable information on the structure and evolution of NSs. To calculate the radiation spectrum from the NS surface, one needs to understand the radiative opacities and study radiative transport in the atmosphere. A thorough review of these subjects is beyond the scope of this paper. Here we briefly discuss what has been done and provide a pointer to recent papers.

Nonmagnetic ( $B = 0$ ) NS atmosphere models were first constructed by Romani (1987). Further works (Rajagopal and Romani 1996; Zavlin *et al.* 1996) used improved opacity and equation of state data from the OPAL project (Iglesias and Rogers 1996) for pure hydrogen, helium and iron compositions. These works showed that the radiation spectra from light-element (hydrogen or helium) atmospheres deviate significantly from the blackbody spectrum. The zero-field models may be relevant for the low-field ( $B \sim 10^8 - 10^9$  G) recycled pulsars (e.g., PSR J0437-4715, from which thermal X-rays have apparently been detected; see Zavlin and Pavlov 1998), but it is possible that these intermediate magnetic fields can have non-negligible effects, at least for atmospheres of light elements (e.g., even at  $B \sim 10^9$  G, the binding energies of light elements can differ significantly from the zero-field values, and at low temperatures the OPAL equation of state underestimates the abundance of the neutral species in the atmosphere).

The basic properties of radiation emerging from a completely ionized magnetic NS atmosphere (under the assumption of constant temperature gradient in the radiating layer) were considered by Pavlov & Shibano (1978). Magnetic NS atmosphere modeling (which requires determining the temperature profile in the atmosphere as well as the radiation field self-consistently) was first attempted by Miller (1992), who adopted the polarization-averaged bound-free (photoionization) opacities (calculated by Miller and Neuhauser 1991) while neglecting other radiative processes. However, separate transport of polarization modes (which have very different opacities) dramatically affects the emergent spectral flux. So far the most comprehensive models of magnetic hydrogen atmospheres have been constructed by Pavlov and collaborators (e.g., Shibano *et al.* 1992; Pavlov *et al.* 1994; Zavlin *et al.* 1995; see Pavlov *et al.* 1995 for a review). These models correctly take account of the transport of different photon modes through a mostly ionized medium in strong magnetic fields. The opacities adopted in the models include free-free transitions (bremsstrahlung absorption) and electron scattering, while bound-free (photoionization) opacities are treated in a highly approximate manner and bound-bound transitions are completely ignored. The models of Pavlov *et al.* are expected to be valid for relatively high temperatures ( $T \gtrsim$  a few  $\times 10^6$  K) where hydrogen is almost completely ionized. As the magnetic field increases, we expect these models to break down at even higher temperatures as bound atoms, molecules and condensate become increasingly important. The atmosphere models of Pavlov *et al.* have been used to compare with the observed spectra of several radio pulsars and radio-quiet isolated NSs (e.g., Meyer *et al.* 1994; Pavlov *et al.* 1996; Zavlin, Pavlov and Trümper 1998) and some useful constraints on the NS properties have been obtained. Magnetic iron atmospheres were considered by Rajagopal *et al.* (1997), who adopted an approximate treatment of radiative opacities and transport.

As discussed in Sec. VII.A, the strong magnetic field increases the abundance of neutral atoms in a hydrogen atmosphere as compared to the zero-field case (see Fig. 7). Therefore one could in principle expect some atomic or molecular line features in the soft X-ray or UV spectra. For example, the Lyman ionization edge is shifted to 160 eV at  $10^{12}$  G and 310 eV at  $10^{13}$  G. The free-free and bound-free (for a ground-state hydrogen atom at rest) cross-sections for a photon in the extraordinary mode (with the photon electric field perpendicular to the magnetic field) are approximately given by (e.g., Gnedin, Pavlov and Tsygan 1974; Ventura *et al.* 1992) <sup>5</sup>

$$\sigma_{\text{ff}\perp} \simeq 1.7 \times 10^3 \rho T_5^{-1/2} \alpha^2 a_0^2 \omega^{-1} b^{-2}, \quad (7.26)$$

$$\sigma_{\text{bf}\perp} \simeq 4\pi\alpha a_0^2 \left(\frac{Q_1}{\omega}\right)^{3/2} b^{-1}, \quad (7.27)$$

---

<sup>5</sup>Note that equations (7.27) and (7.30) are based on the Born approximation, which breaks down near the photoionization threshold. A more accurate fitting to  $\sigma_{\text{bf}}$ , valid for any tightly bound state and photon polarization, is given by eqs. (39)-(43) of Potekhin & Pavlov (1993).

where  $\alpha = 1/137$  is the fine structure constant,  $a_0$  is the Bohr radius,  $\rho$  is the density in  $\text{g cm}^{-3}$ ,  $\omega$  is the photon energy in the atomic units,  $Q_1$  is the ionization potential, and  $b$  is the dimensionless field strength defined in Eq. (1.3). Near the absorption edge, the ratio of the free-free and bound-free opacities is

$$\frac{\kappa_{\text{ff}\perp}}{\kappa_{\text{bf}\perp}} \sim 10^{-4} \frac{\rho}{T_5^{1/2} B_{12} f_H}. \quad (7.28)$$

Thus even for relatively small neutral H fraction  $f_H$ , the discontinuity of the total opacity at the Lyman edge is pronounced and we expect the absorption feature to be prominent. Note that since the extraordinary mode has smaller opacity, most of the X-ray flux will come out in this mode. For photons in the ordinary mode, we have

$$\sigma_{\text{ff}\parallel} \simeq 1.65 \times 10^3 \rho T_5^{-1/2} \alpha^2 a_0^2 \omega^{-3}, \quad (7.29)$$

$$\sigma_{\text{bf}\parallel} \simeq 10^2 \pi \alpha a_0^2 (Q_1/\omega)^{5/2} (\ln b)^{-2}, \quad (7.30)$$

( $\sigma_{\text{ff}\parallel}$  is the same as in zero field), which give  $\kappa_{\text{ff}\parallel}/\kappa_{\text{bf}\parallel} \sim 10^{-2} \rho T_5^{-1/2} f_H^{-1}$  for  $B_{12} \sim 1$ . Thus the absorption edge for the ordinary mode is less pronounced. Clearly, the position and the strength of the absorption edge can provide useful diagnostic of the NS surface magnetic field.

A detailed review on electron scattering and free-free absorption opacities in a magnetized plasma can be found in Mészáros (1992). Bound-bound transitions in strong magnetic fields have been thoroughly investigated for hydrogen and helium atoms at rest (see Ruder *et al.* 1994 for review and tabulations of numerical results). Bound-free absorptions for hydrogen atoms at rest have also been extensively studied (e.g., Gnedin *et al.* 1974; Ventura *et al.* 1992; Potekhin and Pavlov 1993). Since the motion of the atom in strong magnetic fields modifies the atomic structure significantly (see Sec. III.E), the motional effects on opacities need to be included (see Pavlov and Potekhin 1995 for bound-bound opacities and Potekhin and Pavlov 1997 for bound-free opacities; see also Potekhin *et al.* 1998 for total opacities). Some approximate results for radiative transitions in heavy atoms were presented by Miller and Neuhauser (1991).

In the regime where the outermost layer of the NS is in the formed of condensed matter, radiation directly emerges from the hot (but degenerate) condensed phase. The usual radiative transfer does not apply to this situation. Because of the high condensation density, the electron plasma frequency is larger than the frequency of a typical thermal photon. Thus the photons cannot be easily excited thermally inside the condensate. This implies that the NS surface has a high reflectivity. The spectral emissivity is determined by the bulk dielectric properties of the condensed phase (see Itoh 1975; Brinkmann 1980).

## E. Magnetized Neutron Star Crust

As discussed in Sec. VI, the effect of Landau quantization is important only for  $\rho \lesssim \rho_B$  [see Eq. (6.11)]. Deeper in the NS envelope (and the interior), we expect the magnetic field effect on the bulk equation of state to become negligible as more and more Landau levels are filled. In general, we can use the condition  $\rho_B \gtrsim \rho$ , or  $B_{12} \gtrsim 27 (Y_e \rho_6)^{2/3}$ , to estimate the critical value of  $B$  above which Landau quantization will affect physics at density  $\rho$ . For example, at  $B \gtrsim 10^{14}$  G, the neutronization transition from  $^{56}\text{Fe}$  to  $^{62}\text{Ni}$  (at  $\rho = 8.1 \times 10^6 \text{ g cm}^{-3}$  for  $B = 0$ ; Baym, Pethick and Pines 1971) in the crust can be significantly affected by the magnetic field (Lai and Shapiro 1991).

The ions in the NS envelope form a one-component plasma and are characterized by the Coulomb coupling parameter

$$\Gamma = \frac{(Ze)^2}{r_i kT} = 22.75 \frac{Z^2}{T_6} \left( \frac{\rho_6}{A} \right)^{1/3}, \quad (7.31)$$

where  $r_i = (3/4\pi n_i)^{1/3}$  is the Wigner-Seitz cell radius,  $n_i = \rho/m_i = \rho/(Am_p)$  is the ion number density,  $\rho_6 = \rho/(10^6 \text{ g cm}^{-3})$  and  $T_6 = T/(10^6 \text{ K})$ . For  $\Gamma \ll 1$ , the ions form a classical Boltzmann gas whose thermodynamic property is unaffected by the magnetic field. For  $\Gamma \gtrsim 1$ , the ions constitute a strongly coupled Coulomb liquid. The liquid freezes into a Coulomb crystal at  $\Gamma = \Gamma_m \simeq 175$ , corresponding to the classical melting temperature  $T_m$  (e.g., Slattery *et al.* 1980; Nagara *et al.* 1987; Potekhin & Chabrier 2000). The quantum effects of ion motions (zero-point vibrations) tends to increase  $\Gamma_m$  (e.g., Chabrier, Ashcroft and DeWitt 1992; Chabrier 1993) or even suppress freezing (e.g., Ceperley and Alder 1980; Jones and Ceperley 1996). At zero-field, the ion zero-point vibrations have characteristic frequency of order the ion plasma frequency  $\Omega_p$ , with

$$\hbar\Omega_p = \hbar \left( \frac{4\pi Z^2 e^2 n_i}{m_i} \right)^{1/2} = 675 \left( \frac{Z}{A} \right) \rho_6^{1/2} \text{ eV}. \quad (7.32)$$

For  $T \ll T_{\text{Debye}} \sim \hbar \Omega_p / k$ , the ion vibrations are quantized. The effects of magnetic field on strongly coupled Coulomb liquids and crystals have not been systematically studied (but see Usov *et al.* 1980). The cyclotron frequency of the ion is given by

$$\hbar \omega_{ci} = \hbar \frac{ZeB}{Am_p c} = 6.3 \left( \frac{Z}{A} \right) B_{12} \text{ eV}. \quad (7.33)$$

The ion vibration frequency in a magnetic field may be estimated as  $(\Omega_p^2 + \omega_{ci}^2)^{1/2}$ . Using Lindeman's rule, we obtain a modified melting criterion:

$$\Gamma \left( 1 + \frac{\omega_{ci}^2}{\Omega_p^2} \right) \simeq 175. \quad (7.34)$$

For  $\omega_{ci} \ll \Omega_p$ , or  $B_{12} \ll 100 \rho_6^{1/2}$ , the magnetic field does not affect the melting criterion and other properties of ion vibrations.

Even in the regime where the magnetic quantization effects are small ( $\rho \gg \rho_B$ ), the magnetic field can still strongly affect the transport properties (e.g., electric conductivity and heat conductivity) of the NS crust. This occurs when the effective gyro-frequency of the electron,  $\omega_{ce}^* = eB/(m_e^* c)$ , where  $m_e^* = \sqrt{m_e^2 + (p_F/c)^2}$ , is much larger than the electron collision frequency, i.e.,

$$\omega_{ce}^* \tau_0 \simeq 1.76 \times 10^3 \frac{m_e}{m_e^*} B_{12} \left( \frac{\tau_0}{10^{-16} \text{ s}} \right), \quad (7.35)$$

where  $\tau_0$  is the effective electron relaxation time ( $10^{-16}$  s is a typical value in the outer crust). For example, when  $\omega_{ce}^* \tau_0 \gg 1$ , the electron heat conductivity perpendicular to the magnetic field is suppressed by a factor  $(\omega_{ce}^* \tau_0)^{-2}$ . A detailed review on the transport properties of the magnetized NS crust is given in Hernquist (1984) and Yakovlev and Kaminker (1994) where many earlier references can be found (see Potekhin 1999 for a recent calculation). The thermal structure of a magnetized neutron star crust has been studied by, e.g., Hernquist (1995), Van Riper (1988), Schaaf (1990), Heyl and Hernquist (1998).

## VIII. CONCLUDING REMARKS

The properties of matter in strong magnetic fields has always been an interesting subject for physicists. While early studies (e.g., Elliot and Loudon 1960; Hasegawa and Howard 1961) were mainly motivated by the fact that the strong magnetic field conditions can be mimicked in some semiconductors where a small effective electron mass and a large dielectric constant reduce the electric force relative to the magnetic force, recent work on this subject has been motivated by the huge magnetic field  $\sim 10^{12}$  G known to exist in many neutron stars and the tentative evidence for fields as strong as  $10^{15}$  G (see Sec. I.A). The study of matter in strong magnetic fields is obviously an important component of neutron star astrophysics research. In particular, interpretation of the ever improving spectral data of neutron stars requires a detailed theoretical understanding of the physical properties of highly-magnetized atoms, molecules, and condensed matter.

In this review, we have focused on the electronic structure and the bulk properties of matter in strong magnetic fields. We have only briefly discussed the issues of radiative opacities and conductivities in a magnetized medium (see Sec. VII.D-E). There are other related problems that are not covered in this paper. For example, neutrino emissions in the neutron star crust and interior, which determine the cooling rate of the star, can be affected by strong magnetic fields (e.g., Yakovlev and Kaminker 1994; Baiko and Yakovlev 1999; van Dalen *et al.* 2000 and references therein). In proto-neutron stars, sufficiently strong magnetic fields ( $B \gtrsim 10^{15}$  G) can induce asymmetric neutrino emission and impart a kick velocity to the star (e.g., Dorofeev *et al.* 1985; Vilenkin 1995; Horowitz and Li 1998; Lai and Qian 1998a,b; Arras and Lai 1999a,b and references therein). We have not discussed the magnetic field effects on the nuclear matter equation of state (e.g., Chakrabarty *et al.* 1997; Yuan and Zhang 1999; Broderick *et al.* 2000; Suh & Mathews 2000), which are relevant for  $B \gtrsim 10^{17} - 10^{18}$  G. Many other aspects of physics in strong magnetic fields are reviewed in Meszaros (1992).

The study of matter in strong magnetic fields spans a number of different subareas of physics, including astrophysics, atomic and molecular physics, condensed matter physics and plasma physics. As should be apparent from the preceding sections, although there has been steady progress over the years, many open problems remain to be studied in the future. Some of the problems should be easily solvable by specialists in their respective subareas. Since there is no recent review that covers this broad subject area, our emphasis has been on producing a self-contained account on the

basic physical pictures, while relegating the details to the original literature (although we have also discussed aspects of calculational techniques). We hope that this review will make the original literature on matter in strong magnetic fields more easily accessible and stimulate more physicists to work on this problem.

## ACKNOWLEDGMENTS

I am grateful to Edwin Salpeter for providing many insights on the subject of this paper and for his advice on writing this article. I thank George Pavlov and Alexander Potekhin for detailed comments and suggestions. I also thank Wynn Ho, Edwin Salpeter and Ira Wasserman for commenting on an early draft of this paper, as well as Elliot Lieb, Peter Schmelcher and Jokob Yngvason for useful comments/communications. This work has been supported in part by NASA grants NAG 5-8484 and NAG 5-8356, by NSF grant AST 9986740, and by a research fellowship from the Alfred P. Sloan foundation.

## APPENDIX A: JELLIUM MODEL OF ELECTRON GAS IN STRONG MAGNETIC FIELDS

Consider an electron gas in a uniform background of positive charges (the ‘‘Jellium model’’). The interelectronic spacing  $r_s$  is related to the electron number density  $n_e$  by  $n_e^{-1} = 4\pi r_s^3/3$ . At zero magnetic field, the energy per electron can be written as (e.g., Ashcroft and Mermin 1976)

$$E = \frac{3}{5} \frac{\hbar^2 k_F^2}{2m_e} - \frac{3}{4} \frac{e^2 k_F}{\pi} + E_{\text{corr}} = \frac{2.21}{r_s^2} - \frac{0.916}{r_s} + 0.0622 \ln(r_s) - 0.094 \text{ (Ryd)}. \quad (\text{A1})$$

The first term on the right-hand side is the kinetic energy, the second term the (Hartree-Fock) exchange energy, and the remaining terms are the correlation energy (the expression for the correlation energy given here applies to the  $r_s \ll 1$  limit; see Ceperley and Alder 1980 for the full result).

Now consider the magnetic case. When the density is low (or the magnetic field high) so that only the ground Landau level is occupied, the Fermi wavenumber  $k_F$  can be calculated from

$$n_e = \frac{eB}{hc} \frac{1}{2\pi} \int_{-k_F}^{k_F} dk_z = \frac{2k_F}{(2\pi\hat{\rho})^2} \implies k_F = 2\pi^2 \hat{\rho}^2 n_e. \quad (\text{A2})$$

It is convenient to introduce the new parameters, the inverse Fermi wavenumber  $r_F$  and the filling factor for the lowest Landau level  $t$ ,

$$r_F = \frac{1}{\pi k_F} = \frac{2}{3\pi^2} \frac{r_s^3}{\hat{\rho}^2}, \quad t = \frac{\varepsilon_F}{\hbar\omega_{ce}} = \left(\frac{n_e}{n_B}\right)^2 = \frac{9\pi^2}{8} \left(\frac{\hat{\rho}}{r_s}\right)^6, \quad (\text{A3})$$

where  $\varepsilon_F = (\hbar k_F)^2/(2m_e)$  is the Fermi energy. For the electrons to occupy only the ground Landau level we require  $t \leq 1$ , or  $n_e \leq n_B$  [see Eq. (5.9)]. The kinetic energy per electron is

$$\varepsilon_k = \frac{1}{n_e} \frac{1}{(2\pi\hat{\rho})^2} \int_{-k_F}^{k_F} \frac{\hbar^2 k_z^2}{2m_e} dk_z = \frac{\hbar^2}{6\pi^2 m_e r_F^2}. \quad (\text{A4})$$

The (Hartree-Fock) exchange energy can be written as (Danz and Glasser 1971)

$$\varepsilon_{ex} = -\frac{F(t)e^2}{2\pi^2 r_F}, \quad (\text{A5})$$

where the dimensionless function  $F(t)$  is

$$F(t) = 4 \int_0^\infty dx \left[ \tan^{-1} \left( \frac{1}{x} \right) - \frac{x}{2} \ln \left( 1 + \frac{1}{x^2} \right) \right] e^{-4tx^2}. \quad (\text{A6})$$

The function  $F(t)$  can be expressed in terms of generalized hypergeometric functions; for small  $t$ , it can be expanded as (Fushiki *et al.* 1989)

$$F(t) = 3 - \gamma - \ln(4t) + \frac{2t}{3} \left( \frac{13}{6} - \gamma - \ln 4t \right) + \frac{8t^2}{15} \left( \frac{67}{30} - \gamma - \ln 4t \right) + \mathcal{O}(t^3 \ln t), \quad (\text{A7})$$

where  $\gamma = 0.5772\dots$  is Euler's constant. The expressions of exchange energy for higher Landau levels are given in Fushiki *et al.* (1992).

Correlation energy in strong magnetic fields has been calculated by Steinberg and Ortner (1998) in the limit of  $r_F \ll 1$  and  $t \ll 1$  in the random phase approximation (see also Skudlarski and Vignale 1993). The leading order terms have the form

$$\varepsilon_{\text{corr}} = D(t) \ln r_F + C(t), \quad (\text{A8})$$

with  $D(t) = (16\pi^2 t)^{-1}$  (Horing *et al.* 1972); asymptotic ( $t \ll 1$ ) expression for  $C(t)$  is given in Steinberg and Ortner (1998). There are also some studies (e.g., Kleppmann and Elliot 1975; Usov *et al.* 1980; MacDonald and Bryant 1987) for the very low density regime ( $r_F \gg 1$ , but  $t < 1$ ), where the electron gas is expected to form a Wigner crystal; a strong magnetic field tends to increase the density at which crystalization occurs. The low-density and high-density limits may be used to establish an interpolation formula for the correlation energy.

## APPENDIX B: THOMAS-FERMI MODELS IN STRONG MAGNETIC FIELDS

Thomas-Fermi (TF) and related theories (e.g., Thomas-Fermi-Dirac theory, which includes the exchange energy of electrons) have been thoroughly studied as models of atoms and bulk matter in the case of zero magnetic field (e.g., Lieb 1981; Spruch 1991). Since the early studies of Kadomtsev (1970) and Mueller, Rau and Spruch (1971), there has been a long succession of papers on TF type models in strong magnetic fields. An excellent review on the subject is given in Fushiki *et al.* (1992); rigorous theorems concerning the validity of TF theory in magnetic fields as an approximation of quantum mechanics are discussed in Yngvason (1991), Lieb *et al.* (1992,1994a,b) and references therein. Here we briefly summarize the basics of the theory.

The TF type theory is the simplest case of a density functional theory. For a spherical atom (or a Wigner-Seitz cell of bulk matter), we write the energy as a functional of the local electron density  $n(r)$ :

$$\mathcal{E}[n(r)] = \int w_e[n(r)] d^3r - Ze^2 \int \frac{n(r)}{r} d^3r + \frac{e^2}{2} \int \frac{n(r)n(r')}{|\mathbf{r} - \mathbf{r}'|} d^3r d^3r', \quad (\text{B1})$$

where  $w_e[n(r)]$  is the energy density of electrons at density  $n(r)$ , which includes kinetic, exchange, and correlation energy (see Appendix A). Minimizing  $\mathcal{E}$  with respect to  $n(r)$  yields the TF equation:

$$\frac{dw_e}{dn} - e\Phi(r) = \mu_{\text{TF}}, \quad (\text{B2})$$

where  $\Phi(r)$  is the total electrostatic potential, and  $\mu_{\text{TF}}$  is a constant to be determined by the constraint  $\int n(r) d^3r = Z$  (for neutral system). Equation (B2) can be solved together with the Poisson equation

$$\nabla^2 \Phi = -4\pi Ze\delta(\mathbf{r}) + 4\pi en(r), \quad (\text{B3})$$

to obtain  $n(r)$  and  $\Phi(r)$ , and the energy  $\mathcal{E}$  can then be evaluated. The pressure of the bulk matter is then given by  $P = -d\mathcal{E}/(4\pi r_i^2 dr_i)$  and is equal to the pressure of a uniform electron gas at density  $n(r_i)$  (where  $r_i$  is the Wigner-Seitz radius).

Consider the TF model, in which we include in  $w_e[n(r)]$  only the kinetic energy of the electrons. We then have  $dw_e/dn = \mu_e(r) = e\Phi(r) + \mu_{\text{TF}}$ . Using Eq. (6.4) (for nonrelativistic electrons) we can express the local electron density  $n(r)$  in terms of  $\Phi(r)$ . At zero temperature, we have

$$n(r) = \frac{1}{\sqrt{2}\pi^2 \hat{\rho}^3} \sum_{n_L}^{n_{\text{max}}} g_{n_L} \left[ \frac{\mu_{\text{TF}} + e\Phi(r)}{\hbar\omega_{ce}} - n_L \right]^{1/2}. \quad (\text{B4})$$

This can be substituted into Eq. (B3) to solve for  $\Phi(r)$ .

Many TF type studies (e.g., Kadomtsev 1970; Mueller, Rau and Spruch 1971; Banerjee *et al.* 1974; Constantinescu and Reháč 1976; Skjervold and Östgaard 1984; Fushiki *et al.* 1989; Abrahams and Shapiro 1991) adopted the adiabatic approximation (only the ground Landau level is occupied, i.e.,  $n_{\text{max}} = 0$ ). Abrahams and Shapiro (1991) also considered the Weizsäcker gradient correction where a term of the form  $(\hbar^2/m_e)(\nabla n)^2/n$  is included in  $w_e[n]$ , although

the actual form of the Weizsäcker term in magnetic fields is uncertain (see Fushiki *et al.* 1992 for a critical review). Tomishima & Yonei (1978), Tomishima *et al.* (1982), Gadiyak *et al.* (1981), and Rönqvaldsson *et al.* (1993) studied TF models allowing for  $n_{\max} > 0$ . Constantinescu and Moruzzi (1978), Abrahams and Shapiro (1991) (who restricted to  $n_{\max} = 0$ ) and Thorolfsson *et al.* (1998) (allowing for  $n_{\max} > 0$ ) studied the finite temperature TF models for condensed matter. Examples of TF type equations of state for iron are shown in Fig. 9.

As mentioned, the TF model is too crude to determine the relative binding between atoms, molecules and condensed matter. But the model becomes increasingly accurate in certain asymptotic limits (see Fushiki *et al.* 1992; Lieb *et al.* 1992,1994a,b). In general, the validity of the TF theory requires the local Fermi wavelength  $\lambda_F$  to be much less than the size of the atom (or Wigner-Seitz cell)  $r_i$ . For zero or weak magnetic fields ( $n_{\max} \gg 1$ ),  $\lambda_F \sim n_e^{-1/3} \sim r_i/Z^{1/3}$ , the validity of TF theory requires  $Z^{1/3} \gg 1$ . The size of the atom in weak fields is estimated from  $\hbar^2/(m_e \lambda_F^2) \sim Ze^2/r_i$ , which gives  $r_i \sim Z^{-1/3} a_0$ .

For atoms in strong magnetic fields ( $n_{\max} = 0$ ), we have  $\lambda_F \sim r_i^2/(Z\hat{\rho}^2)$ , and the size is  $r_i \sim Z^{1/5} b^{-2/5} a_0$ . The condition  $\lambda \ll r_i$  becomes  $b \ll Z^3$ . The TF theory of the atom is exact when  $Z, b \rightarrow \infty$ , as long as  $Z^3/b \rightarrow \infty$ . To be in the strong field regime requires the mean electron spacing in a nonmagnetic atom,  $a_0/Z^{2/3}$ , to be greater than  $\hat{\rho}$ , i.e.,  $b > Z^{4/3}$ . For bulk matter in strong magnetic fields ( $n_{\max} = 0$ ), the TF model is valid when  $\lambda_F \sim r_i^3/(Z\hat{\rho}^2) \ll r_i$ , i.e.,  $b \ll Zr_i^{-2}$  (at zero-pressure,  $r_i \sim Z^{1/5} b^{-2/5}$ , this condition reduces to  $b \ll Z^3$ ). The strong field condition is  $Z^{-1/3} r_i > \hat{\rho}$ , i.e.,  $b > Z^{2/3} r_i^{-2}$  (this reduces to  $b > Z^{4/3}$  at zero-pressure density).

- Abrahams, A.M., and S.L. Shapiro, 1991, *Astrophys. J.* **374**, 652.  
Al-Hujaj, O.-A., and P. Schmelcher, 2000, *Phys. Rev. A* **61**, 063413.  
Angelie, C., and C. Deutch, 1978, *Phys. Lett.* **67A**, 353.  
Arras, P., and D. Lai, 1999a, *Astrophys. J.* **519**, 745.  
Arras, P., and D. Lai, 1999b, *Phys. Rev. D* **60**, 043001.  
Ashcroft, N.W., and N.D. Mermin, 1976, *Solid State Physics* (Saunders College: Philadelphia).  
Avron, J.E., I.B. Herbst, and B. Simon, 1978, *Ann. Phys. (NY)* **114**, 431.  
Bahcall, J.N., and R.A. Wolf, 1965, *Phys. Rev. B* **140**, 1425.  
Baiko, D.A., and D.G. Yakovlev, 1999, *Astron. Astrophys.* **342**, 192.  
Banerjee, B., D.H. Constantinescu, and P. Reháč, 1974, *Phys. Rev. D* **10**, 2384.  
Basile, S., F. Trombetta, and G. Ferrante, 1987, *Nuovo Cimento D* **9**, 457.  
Baye, D., and M. Vincke, 1990, *J. Phys. B* **23**, 2467.  
Baye, D., and M. Vincke, 1998, in *Atoms and Molecules in Strong Magnetic Fields*, edited by P. Schmelcher and W. Schweizer (Plenum Press, New York), p. 141.  
Baym, G., C. Pethick, and P. Sutherland, 1971, *Astrophys. J.* **170**, 299.  
Becken, W, P. Schmelcher, and F.K. Diakonov, 1999, *J. Phys. B* **32**, 1557.  
Becken, W, and P. Schmelcher, 2000, *J. Phys. B* **33**, 545.  
Becker, W., 2000, in *Highly Energetic Physical Processes and Mechanisms for Emission from Astrophysical Plasmas*, Proceedings of IAU Symposium No. 195 (ASP, San Francisco), p. 49.  
Becker, W., and G.G. Pavlov 2001, in *The Century of Space Science*, eds. J. Bleeker, J. Geiss and M. Huber (Kluwer Acad. Pub.).  
Becker, W., and J. Trümper, 1997, *Astron. Astrophys.* **326**, 682.  
Bezchastnov, V.G., G.G. Pavlov, and J. Ventura, 1998, *Phys. Rev. A* **58**, 180.  
Blaes, O., R. Blandford, P. Madau, and S. Koonin, 1990, *Astrophys. J.* **363**, 612.  
Blaes, O, and Madau, P. 1993, *Astrophys. J.* **403**, 690.  
Blandford, R.D., and Hernquist, L. 1982, *J. Phys. C* **15**, 6233.  
Brigham, D.R., and J.M. Wadehra, 1987, *Astrophys. J.* **317**, 865.  
Brinkmann, W. 1980, *Astron. Astrophys.* **82**, 352.  
Broderick, A., M. Prakash, and J.M. Lattimer, 2000, *Astrophys. J.* **537**, 351.  
Callaway, J., and N.H. March, 1984, *Solid State Phys.* **38**, 135.  
Canuto, V., and D.C. Kelley, 1972, *Astrophys. Space Sci.* **17**, 277.  
Canuto, V., J. Lodenquai, and M. Ruderman, 1971, *Phys. Rev. D* **3**, 2303.  
Canuto, V., and J. Ventura, 1977, *Fund. Cosmic Phys.*, **2**, 203.  
Caraveo, P.A., G.F. Bignami, and J. Trümper, 1996, *Astron. Astrophys. Rev.* **7**, 209.  
Caraveo, P.A., R.P. Mignani, G.G. Pavlov, and G.F. Bignami, 2000, in *Proc. a Decade of HST Science* (Baltimore, USA); e-print astro-ph/0008523.

Ceperley, D., and B. Alder, 1980, Phys. Rev. Lett. **45**, 566.

Chabrier, G., 1993, Astrophys. J. , **414**, 695.

Chabrier, G., N.W. Ashcroft, H.E. DeWitt, 1992, Nature **360**, 6399.

Chakrabarty, S., D. Bandyopadhyay, and S. Pal, 1997, Phys. Rev. Lett. **78**, 2898.

Chandrasekhar, S., and E. Fermi, 1953, Astrophys. J. **118**, 116.

Chen, H.-H., 1973, Ph.D. Thesis (Columbia University).

Chen, Z., and S.P. Goldman, 1992, Phys. Rev. A **45**, 1722.

Chiu, H.Y., and E.E. Salpeter, 1964, Phys. Rev. Lett. **12**, 413.

Constantinescu, D.H., and P. Reháč, 1976, Il Nuovo Cimento **32**, 177.

Constantinescu, D.H., and G. Moruzzi, 1978, Phys. Rev. D **18**, 1820.

Crow, J.E., J.R. Sabin, and N.S. Sullivan, 1998, in *Atoms and Molecules in Strong Magnetic Fields*, edited by P. Schmelcher and W. Schweizer(Plenum Press, New York), p. 77 (see also <http://www.magnet.fsu.edu/>).

Danz, R.W., and M.L. Glasser, 1971, Phys. Rev. B **4**, 94.

Demeur, M., P.-H. Heenen, and M. Godefroid, 1994, Phys. Rev. A **49**, 176.

Detmer, T., P. Schmelcher, F.K. Diakonov, and L.S. Cederbaum, 1997, Phys. Rev. A **56**, 1825.

Detmer, T., P. Schmelcher, and L.S. Cederbaum, 1998, Phys. Rev. A **57**, 1767.

Dorofeev, O.F., *et al.*, 1985, Pis'ma Astron. Zh. **11**, 302 [Sov. Astron. Lett. **11**, 123 (1985)].

Duncan, R.C., and C. Thompson, 1992, Astrophys. J. **392**, L9.

Edelstein, J., R.S. Foster, and S. Bowyer, 1995, Astrophys. J. **454**, 442.

Elliot, R.J., and R. Loudon, 1960, J. Phys. Chem. Solids **15**, 196.

Fassbinder, P., and W. Schweizer, 1996, Phys. Rev. A **53**, 2135.

Fassbinder, P., and W. Schweizer, 1996, Astron. Astrophys. **314**, 700.

Flowers, E.G., J.F. Lee, M.A. Ruderman, P.G. Sutherland, W. Hillebrandt, and E. Müller, 1977, Astrophys. J. **215**, 291.

Fushiki, I., E.H. Gudmundsson, and C.J. Pethick, 1989, Astrophys. J. **342**, 958.

Fushiki, I., E.H. Gudmundsson, C.J. Pethick, and J. Yngvason, 1992, Ann. Phys. (NY) **216**, 29.

Gadiyak, G.V., M.S. Obrecht, and N.N. Yanenko, 1981, Astrofizica **17**, 765 [Astrophysics **17**, 416 (1982)].

Garstang, R.H., 1977, Rep. Prog. Phys. **40**, 105.

Glasser, M.L., and J.I. Kaplan, 1975, Astrophys. J. **199**, 208.

Gnedin, Yu. N., G.G. Pavlov, and A.I. Tsygan, 1974, Sov. Phys. JETP **39**, 201.

Goldman, S.P., and Z. Chen, 1991, Phys. Rev. Lett., **67**, 1403.

Gor'kov, L.P., and I.E. Dzyaloshinskii, 1968, Sov. Phys. JETP **26**, 449.

Haensel, P., and J.L. Zdunik, 1990, Astron. Astrophys. **222**, 353.

Haines, L.K., and D.H. Roberts, 1969, Am. J. Phys. **37**, 1145.

Hansen, J.P., and E.L. Pollock, 1973, Phys. Rev. A **8**, 3110.

Hasegawa, H., and R.E. Howard, 1961, J. Phys. Chem. Solids **21**, 179.

Hernquist, L. 1984, Astrophys. J. Suppl. Ser. **56**, 325.

Hernquist, L. 1985, Mon. Not. R. Astron. Soc. **213**, 313.

Herold, H., H. Ruder, and J. Wunner, 1981, J. Phys. B **14**, 751.

Heyl, J.S., and L. Herquist, 1998, Mon. Not. R. Astron. Soc. **300**, 599.

Horing, N.J. 1969, Ann. Phys. (NY), **54**, 405.

Horing, N.J., R.W. Danz, and M.L. Glasser, 1972, Phys. Rev. A **6**, 2391.

Horowitz, C.J., and G. Li, 1998, Phys. Rev. Lett. **80**, 3694.

Hummer, D.G., and D. Mihalas 1988, Astrophys. J. **331**, 794.

Hurley, K., *et al.*, 1999, Nature **397**, 41.

Ichimaru, S. 1993, Rev. Mod. Phys. **65**, 255.

Itoh, N., 1975, Mon. Not. R. Astron. Soc. **173**, 1P.

Ivanov, M.V., and P. Schmelcher, 1998, Phys. Rev. A **57**, 3793.

Ivanov, M.V., and P. Schmelcher, 1999, Phys. Rev. A **60**, 3558.

Ivanov, M.V., and P. Schmelcher, 2000, Phys. Rev. A **61**, 2505.

Johnsen, K., and J. Yngvason, 1996, Phys. Rev. A **54**, 1936.

Johnson, B.R., J.O. Hirschfelder, and K.-H. Yang, 1983, Rev. Mod. Phys. **55**, 109.

Johnson, M.H., and B.A. Lippmann, 1949, Phys. Rev. **76**, 828.

Jones, M.D., and D.M. Ceperley, 1996, Phys. Rev. Lett. **76**, 4572.

Jones, M.D., G. Ortiz, and D.M. Ceperley, 1996, Phys. Rev. A. **54**, 219.

Jones, M.D., G. Ortiz, and D.M. Ceperley, 1997, Phys. Rev. E **55**, 6202.

Jones, M.D., G. Ortiz, and D.M. Ceperley, 1999a, Phys. Rev. A. **59**, 2875.

Jones, M.D., G. Ortiz, and D.M. Ceperley, 1999b, Astron. Astrophys. **343**, L91.

Jones, P.B., 1985, Mon. Not. R. Astron. Soc. **216**, 503.

Jones, P.B., 1986, Mon. Not. R. Astron. Soc. **218**, 477.

Jordan, S. 1998, in *Atoms and Molecules in Strong Magnetic Fields*, edited by P. Schmelcher and W. Schweizer(Plenum Press,

- New York), p. 9.
- Jordan, S., P. Schmelcher, W. Becken, and W. Schweizer, 1998, *Astron. Astrophys.* **336**, L33.
- Kadomtsev, B.B., 1970, *Zh. Eksp. Teor. Fiz.* **58**, 1765 [*Sov. Phys. JETP* **31**, 945 (1970)].
- Kadomtsev, B.B., and V.S. Kudryavtsev, 1971, *Pis'ma Zh. Eksp. Teor. Fiz.* **13**, 61 [*Sov. Phys. JETP Lett.* **13**, 42 (1971)].
- Kappes, U., and P. Schmelcher, 1995, *Phys. Rev. A* **51**, 4542.
- Kappes, U., and P. Schmelcher, 1996, *Phys. Rev. A* **53**, 3869.
- Kaspi, V.M., D. Chakrabarty, and J. Steinberger, 1999, *Astrophys. J.* **525**, L33
- Kastner, M.A. 1992, *Rev. Mod. Phys.* **64**, 849.
- Khersonskii, V.K., 1984, *Astrophys. Space Sci.* **98**, 255; 1985, *ibid.* **117**, 47.
- Khersonskii, V.K., 1987, *Sov. Astron.* **31**, 225.
- Klaassen, T.O., J.L. Dunn, and C.A. Bates, 1998, in *Atoms and Molecules in Strong Magnetic Fields*, edited by P. Schmelcher and W. Schweizer (Plenum Press, New York), p. 291.
- Kleppmann, W.G., and R.J. Elliot, 1975, *J. Phys. C* **8**, 2729.
- Koester, D., and G. Chanmugan, 1990, *Rep. Prog. Phys.* **53**, 837.
- Korpela, E.J., and Bowyer, S. 1998, *Astron. J.* **115**, 2551.
- Kössl, D., R. G. Wolff, E. Müller, and W. Hillebrandt, 1988, *Astron. Astrophys.* **205**, 347.
- Kouveliotou, C., *et al.* 1998, *Nature*, **393**, 235.
- Kouveliotou, C., *et al.* 1999, *Astrophys. J.* , **510**, L115.
- Kravchenko, Yu. P., and M. A. Liberman, 1997, *Phys. Rev. A* **55**, 2701.
- Kravchenko, Yu. P., and M. A. Liberman, 1998, *Phys. Rev. A* **57**, 3403.
- Kravchenko, Yu. P., M. A. Liberman, and B. Johansson 1996, *Phys. Rev. A* **54**, 287.
- Lai, D., and Y.-Z. Qian, 1998a, *Astrophys. J.* **495**, L103 (Erratum: **501**, L155).
- Lai, D., and Y.-Z. Qian, 1998b, *Astrophys. J.* **505**, 844.
- Lai, D., E.E. Salpeter, and S.L. Shapiro, 1992, *Phys. Rev. A* **45**, 4832.
- Lai, D., and E.E. Salpeter, 1995, *Phys. Rev. A* **52**, 2611.
- Lai, D., and E.E. Salpeter, 1996, *Phys. Rev. A* **53**, 152.
- Lai, D., and E.E. Salpeter, 1997, *Astrophys. J.* **491**, 270.
- Lai, D., and S.L. Shapiro, 1991, *Astrophys. J.* **383**, 745.
- Lamb, W. E., Jr., 1952, *Phys. Rev.* **85**, 259.
- Landau, L. D., and E. M. Lifshitz, 1977, *Quantum Mechanics*, 3rd Ed. (Pergamon Press: Oxford).
- Landau, L. D., and E. M. Lifshitz, 1980, *Statistical Physics*, Part 1, 3rd Ed. (Pergamon: Oxford).
- Le Guillou, J.C., and J. Zinn-Justin 1984, *Ann. Phys. (N.Y.)*, 154, 440.
- Lewin, W.H.G., J. van Paradijs, and E.P.J. van den Heuvel, 1995, *X-Ray Binaries* (Cambridge Univ. Press: Cambridge).
- Lieb, E.H. 1981, *Rev. Mod. Phys.* **53**, 603 (Erratum: 1982, *ibid.* **54**, 311).
- Lieb, E.H., J.P. Solovej, and J. Yngvason, 1992, *Phys. Rev. Lett.* **69**, 749.
- Lieb, E.H., J.P. Solovej, and J. Yngvason, 1994a, *Commun. Pure and Applied Math.* **47**, 513
- Lieb, E.H., J.P. Solovej, and J. Yngvason, 1994b, *Commun. Math. Phys.*, **161**, 77.
- Lieb, E.H., J.P. Solovej, and J. Yngvason, 1995, *Phys. Rev. B* **51**, 10646.
- Lodenquai, J., V. Canuto, M. Ruderman, and S. Tsuruta, 1974, *Astrophys. J.* **190**, 141.
- Lopez, J.C., P. Hess, and A. Turbiner, 1997, *Phys. Rev. A* **56**, 4496.
- Lopez, J.C., and A. Turbiner, 2000, *Phys. Rev. A* **62**, 022510.
- Lyne, A.G., and Graham-Smith, F. 1998, *Pulsar Astronomy* (Cambridge Univ. Press: Cambridge).
- MacDonald, A.H., and G.W. Bryant, 1986, *Phys. Rev. Lett.* **58**, 515
- Melezhik, V.S. 1993, *Phys. Rev. A* **48**, 4528.
- Mereghetti, S. 2000, in "The Neutron Star – Black Hole Connection" (NATO Advanced Study Institute); e-print astro-ph/9911252.
- Mészáros, P. 1992, *High Energy Radiation from Magnetized Neutron Stars* (The Univ. of Chicago Press: Chicago).
- Michel, F.C. 1991, *Theory of Neutron Star Magnetospheres* (Univ. of Chicago Press, Chicago).
- Mihalas, D., W. Däppen, and D.G. Hummer 1988, *Astrophys. J.* **331**, 815.
- Miller, M.C. 1992, *Mon. Not. R. Astron. Soc.* **255**, 129.
- Miller, M.C., and D. Neuhauser 1991, *Mon. Not. R. Astron. Soc.* **253**, 107.
- Mueller, R.O., A.R.P. Rau, and L. Spruch, 1971, *Phys. Rev. Lett.*, **26**, 1136.
- Müller, E., 1984, *Astron. Astrophys.*, **130**, 415.
- Nagara, H., Nagata, Y., and Nakamura, T. 1987, *Phys. Rev. A* **36**, 1859.
- Negel, W., and Ventura, J. 1980, *Astron. Astrophys.* **118**, 66.
- Nelson, R. W., Salpeter, E. E., and Wasserman, I. 1993, *Astrophys. J.* **418**, 874.
- Neuhauser, D., S.E. Koonin, and K. Langanke, 1987, *Phys. Rev. A* **36**, 4163.
- Ortiz, G., M. D. Jones, and D. M. Ceperley, 1995, *Phys. Rev. A.* **52**, R3405.
- Paczyński, B. 1992, *Acta Astron.* **42**, 145.
- Page, D., 1998, in *Many Faces of Neutron Stars*, edited by R. Buccheri, J. van Paradijs and M.A. Alpar (Kluwer Academic

- Publishers: Dordrecht)
- Pavlov, G.G., and P. Mészáros, 1993, *Astrophys. J.* **416**, 75.
- Pavlov, G.G., and Panov, A.N. 1976, *Sov. Phys. JETP* **44**,300.
- Pavlov, G.G., and Potekhin, A.Y. 1995, *Astrophys. J.* **450**, 883.
- Pavlov, G.G., and Y.A. Shibano, 1978, *Astron. Zh. (Sov. Astronomy)*, **55**, 373.
- Pavlov, G.G., Y.A. Shibano, J. Ventura, and V.E. Zavlin, 1994, *Astron. and Astrophys.* **289**, 837.
- Pavlov, G.G., Y.A. Shibano, V.E. Zavlin, and R.D. Meyer, 1995, in “The Lives of the Neutron Stars”, edited by A. Alpar, U. Kiziloglu and J. van Paradijs (Kluwer: Dordrecht).
- Pavlov, G.G., and D.G. Yakovlev, 1977, *Astrofizika (Sov. Astrophysics)* **13**, 173
- Pavlov, G.G., V.E. Zavlin, J. Trümper, and R. Neuhäuser, 1996, *Astrophys. J.* **472**, L33.
- Pavlov, G.G., A.D. Welty, and F.A. Cordova, 1997, *Astrophys. J.* **489**, L75.
- Pethick, C.J. 1992, *Rev. Mod. Phys.* **64**, 1133.
- Potekhin, A.Y., 1994, *J. Phys. B* **27**, 1073.
- Potekhin, A.Y. 1996, *Phys. Plasmas*, **3**, 4156.
- Potekhin, A.Y. 1998, *J. Phys. B* **31**, 49.
- Potekhin, A.Y. 1999, *Astron. Astrophys.* **351**, 787.
- Potekhin, A.Y., G. Chabrier 2000, *Phys. Rev. E* **62**, 8554 (astro-ph/0009261).
- Potekhin, A.Y., G. Chabrier, and Y.A. Shibano 1999, *Phys. Rev. E* **60**, 2193 (Erratum: *Phys. Rev. E* **63**, 019901).
- Potekhin, A.Y., and G.G. Pavlov, 1993, *Astrophys. J.* **407**, 330.
- Potekhin, A.Y., and G.G. Pavlov, 1997, *Astrophys. J.* **483**, 414.
- Potekhin, A.Y., Yu.A. Shibano, and J. Ventura, 1998, in “Neutron Stars and Pulsars”, eds. N. Shibasaki *et al.*(Univ. Academy Press, Tokyo), p.161.
- Prakash, M., J.M. Lattimer, J.A. Pons, A.W. Steiner, and S. Reddy, in “Physics of Neutron Star Interiors”, eds. D. Blaschke, N.K. Glendenning and A. Sedrakian (Springer) (astro-ph/0012136).
- Pröschel, P., W. Rösner, G. Wunner, H. Ruder, and H. Herold, 1982, *J. Phys. B* **15**, 1959.
- Rajagopal, M., and R.W. Romani, 1996, *Astrophys. J.* **461**, 327.
- Rajagopal, M., R.W. Romani, and M.C. Miller, 1997, *Astrophys. J.* **479**, 347.
- Rögnvaldsson, Ö.E., *et al.*1993, *Astrophys. J.* **416**, 276.
- Romani, R.W. 1987, *Astrophys. J.* **313**, 718.
- Rösner, W., G. Wunner, H. Herold, and H. Ruder, 1984, *J. Phys. B* **17**, 29.
- Ruder, H. *et al.*1994, *Atoms in Strong Magnetic Fields* (Springer-Verlag).
- Ruderman, M. 1971, *Phys. Rev. Lett.* **27**, 1306.
- Ruderman, M. 1974, in *Physics of Dense Matter* (I.A.U. Symp. No. 53), edited by C.J. Hansen (Dordrecht-Holland: Boston), p.117.
- Ruderman, M., and P.G. Sutherland, 1975, *Astrophys. J.* **196**, 51.
- Salpeter, E.E. 1961, *Astrophys. J.* **134**, 669.
- Salpeter, E.E. 1998, *J. Phys.: Condens. Matter*, **10**, 11285.
- Salpeter, E.E., and H.M. van Horn, 1969, *Astrophys. J.* **155**, 183.
- Saumon, D., and G. Chabrier 1991, *Phys. Rev. A* **44**, 5122.
- Saumon, D., and G. Chabrier 1992, *Phys. Rev. A* **46**, 2084.
- Schaaf, M.E. 1990, *Astron. Astrophys.* **227**, 61.
- Schatz, H., L. Bildsten, A. Cumming, and M. Wiescher, 1999, *Astrophys. J.* **524**, 1014.
- Schmelcher, P., L.S. Cederbaum and H.-D. Meyer, *Phys. Rev. A.* **38**, 6066 (1988).
- Schmelcher, P., L. S. Cederbaum, and U. Kappers 1994, in *Conceptual Trends in Quantum Chemistry*, edited by E.S. Kryachko (Kluwe Academic Publishers).
- Schmelcher, P., M.V. Ivanov, and W. Becken, 1999, *Phys. Rev. A* **59**, 3424.
- Schmelcher, P., T. Detmer, L.S. Cederbaum, 2000, *Phys. Rev. A* **6104**, 3411.
- Schwinger, J., 1988, *Particles, Sources and Fields* (Addison-Wesley, Redwood City).
- Shapiro, S.L., and S.A. Teukolsky, 1983, *Black Holes, White Dwarfs and Neutron Stars* (John Wiley and Sons, New York).
- Shibano, Y.A., G.G. Pavlov, and V.E. Zavlin, and J. Ventura, 1992, *Astron. Astrophys.* **266**, 313.
- Silant’ev, N.A., and D.G. Yakovlev, 1980, *Astrophys. Space Sci.* **71**, 45.
- Simola, J., and J. Virtamo, 1978, *J. Phys. B* **11**, 3309.
- Skjervold, J.E., and E. Östgaard, 1984, *Physica Scripta* **29**, 543.
- Skudlarski, P., and G. Vignale, 1993, *Phys. Rev. B* **48**, 8547.
- Slater, J.C., 1963, *Quantum Theory of Molecules and Solids*, Vol. 1 (McGraw-Hill Book Company, Inc.).
- Slattery, W.L., G.D. Doolen, and H.E. DeWitt, 1980, *Phys. Rev. A* **21**, 2087.
- Sokolov, A.A., and I.M. Ternov, 1968, *Synchrotron Radiation* (Oxford: Pergamon Press).
- Spruch, L., 1991, *Rev. Mod. Phys.* **63**, 151.
- Steinberg, M., and J. Ortner 1998, *Phys. Rev. B* **58**, 15460; Erratum: *Phys. Rev. B* **59**, 12693 (1999).
- Suh, I.-S., and Mathews, G.J. 2000, *Astrophys. J.* in press; e-print astro-ph/9912301.

Thompson, C., and R.C. Duncan 1993, *Astrophys. J.* **408**, 194.

Thompson, C., and R.C. Duncan 1995, *Mon. Not. R. Astron. Soc.* , **275**, 255.

Thompson, C., and R.C. Duncan 1996, *Astrophys. J.* , **473**, 322.

Thorolfsson, A., Ö.E. Rögnvaldsson, J. Yngvason, and E.H. Gudmundsson, 1998, *Astrophys. J.* **502**, 847.

Timofeev, V.B., and A.V. Chernenko, 1995, *Pis'ma Zh. Eksp. Teor.* **61**, 603 [*Sov. Phys. JETP Lett.* **61**, 617 (1995)].

Tomishima, Y., and K. Yonei, 1978, *Prog. Theor. Phys.* **59**, 683.

Tomishima, Y., K. Matsuno, and K. Yonei, 1982, *J. Phys. B* **15**, 2837.

Treves, A., and Colpi, M. 1991, *Astron. Astrophys.* **241**, 107.

Treves, A., R. Turolla, S. Zane, and M. Colpi, 2000, *Pub. Astron. Soc. Pac.* **112**, 297; e-print astro-ph/9911430.

Tsuruta, S., 1964, Ph.D. thesis, Columbia University.

Tsuruta, S., 1998, *Phys. Rep.* **292**, 1.

Turbiner, A.V., 1983, *Pis'ma Zh. Eksp. Teor. Fiz.* **38**, 510. [*Sov. Phys. JETP Lett.* **38**, 618 (1983)].

Usov, N.A., Grebenshchikov, Yu.B., and F.R. Ulinich, 1980, *Sov. Phys. JETP* **51**, 148.

Usov, V.V., and D.B. Melrose, 1996, *Astrophys. J.* **464**, 306.

van Dalen, E.N.E., A.E.L. Dieperink, A. Sedrakian, and R.G.E. Timmermans 2000, *Astron. Astrophys.* **360**, 549.

Van Riper, K.A., 1988, *Astrophys. J.* **329**, 339.

Vasisht, G., and E.V. Gotthelf 1997, *Astrophys. J.* , L129.

Ventura, J., 1979, *Phys. Rev. D* **19**, 1684.

Ventura, J., H. Herold, H. Ruder, and F. Geyer, 1992, *Astron. Astrophys.* **261**, 235.

Ventura, J., H. Herold, and Kopidakis, 1994, in *Lives of Neutron Stars*, edited by A. Alpar, U. Kiziloglu and J. van Paradijs (Kluwer, Dordrecht).

Vignale, G., and M. Rasolt, 1987, *Phys. Rev. Lett.* **59**, 2360.

Vignale, G., and M. Rasolt, 1988, *Phys. Rev. B* **37**, 10685.

Vilenkin, A. 1995, *Astrophys. J.* **451**, 700.

Vincke, M., and D. Baye, 1985, *J. Phys. B* **18**, 167.

Vincke, M., and D. Baye, 1988, *J. Phys. B* **21**, 2407.

Vincke, M., M. Le Dourneuf and D. Baye, 1992, *J. Phys. B* **25**, 2787.

Virtamo, J., 1976, *J. Phys. B* **9**, 751.

Virtamo, J., and P. Jauho, 1975, *Nuovo Cimento* **26B**, 537.

Walter, F.M., S.J. Wolk, and R. Neuhäuser, 1996, *Nature* **379**, 233.

Walter, F.M., and L.D. Matthews, 1997, *Nature* **389**, 358.

Weissbluth, M., 1978, *Atoms and Molecules* (Academic, New York), p. 400.

Wickramasinghe, D.T., and L. Ferrario, 2000, *Pub. Astron. Soc. Pacific* **112**, 873.

Wille, U., 1987, *J. Phys. B* **20**, L417.

Wille, U., 1988, *Phys. Rev. A* **38**, 3210.

Wunner, G., H. Herold, and H. Ruder, 1982, *Phys. Lett.* **88A**, 344.

Yakovlev, D.G., and A.D. Kaminker 1994, in *The Equation of State in Astrophysics*, edited by G. Chabrier and E. Schatzman (Cambridge University Press, Cambridge), p.214.

Yakovlev, D.G., A.D. Kaminker, O.Y. Gnedin, and P. Haensel 2001, *Phys. Rep.*, in press (astro-ph/0012122).

Yngvason, J., 1991, *Lett. Math. Phys.*, **22**, 107.

Yuan, Y.F., and J.L. Zhang, 1999, *Astrophys. J.* **525**, 950.

Zavlin, V.E., G.G. Pavlov, Y.A. Shibano, and J. Ventura, 1995, *Astron. Astrophys.* **297**, 441.

Zavlin, V.E., G.G. Pavlov, and Y.A. Shibano, 1996, *Astron. Astrophys.* **315**, 141.

Zavlin, V.E., and G.G. Pavlov, 1998, *Astron. Astrophys.* **329**, 583.

Zhang, B., and A.K. Harding, 2000, *Astrophys. J.* , in press; e-print astro-ph/0004067.

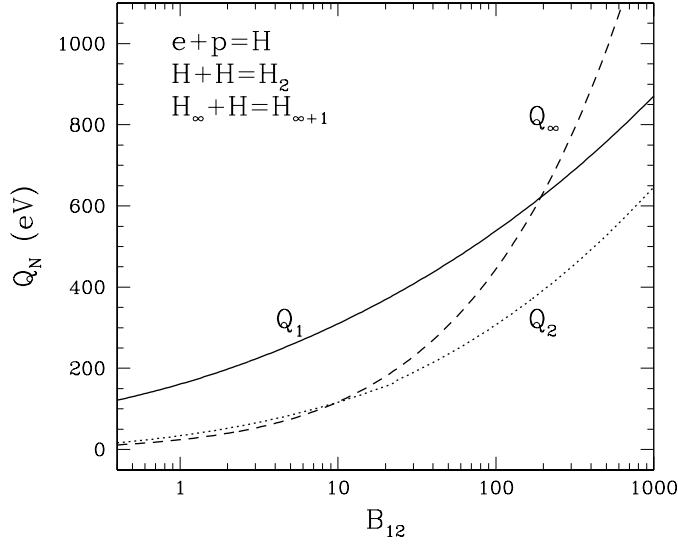


FIG. 1. Energy releases from several atomic and molecular processes as a function of the magnetic field strength. The solid line shows the ionization energy  $Q_1$  of H atom, the dotted line shows the dissociation energy  $Q_2$  of  $H_2$ , and the dashed line shows the cohesive energy  $Q_\infty$  of linear chain  $H_\infty$ . The zero-point energy corrections have been included in  $Q_2$  and  $Q_\infty$ .

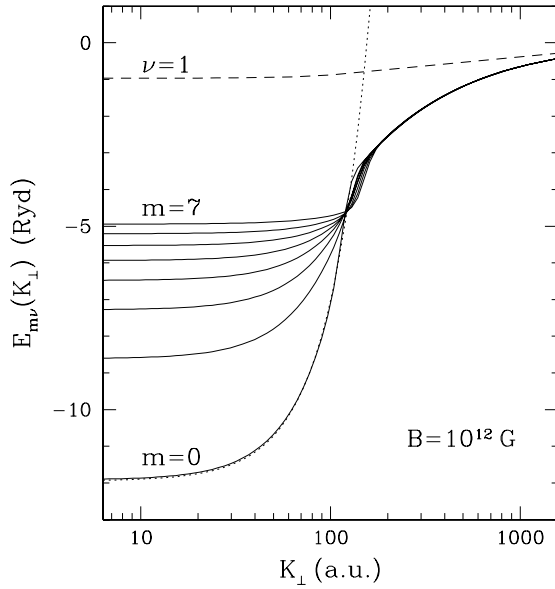


FIG. 2. Energy spectrum of a hydrogen atom moving across a magnetic field with  $B = 10^{12}$  G. The solid lines are for the tightly bound states ( $\nu = 0$ ) with  $m = 0, 1, 2, \dots, 7$ , and the dashed line is for weakly bound state with  $\nu = 1, m = 0$ . The dotted line corresponds to  $E_{00}(K_\perp) = E_{00}(0) + K_\perp^2 / (2M_\perp)$ . The total energy of the atom is  $\mathcal{E}_{m\nu} = K_z^2 / (2M) + m\hbar\omega_{cp} + E_{m\nu}(K_\perp)$ .

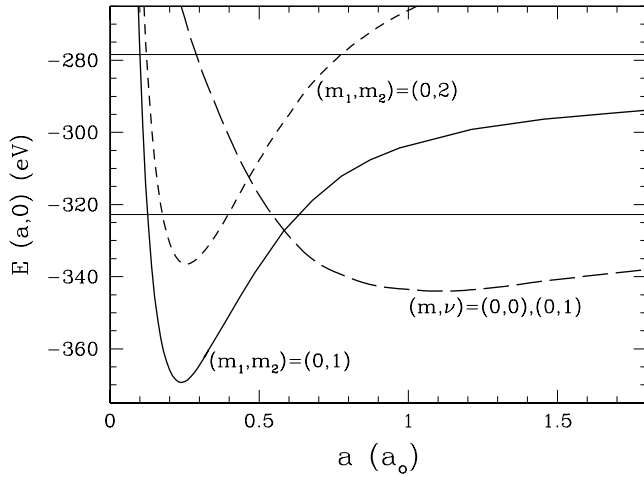


FIG. 3. The electronic energy curves  $E(a, 0)$  of  $H_2$  molecule at  $B = 10^{12}$  G when the molecular axis is aligned with the magnetic field axis ( $a$  is the proton separation). For the solid curve the electrons occupy the  $m_1 = 0$  and  $m_2 = 1$  orbitals (both with  $\nu = 0$ ), for the short-dashed curve  $(m_1, m_2) = (0, 2)$ . The long-dashed curve corresponds to the weakly bound state with  $(m, \nu) = (0, 0), (0, 1)$ . The solid horizontal lines correspond to  $E = -323$  eV (the total energy of two isolated atoms in the ground state) and  $E = -278$  eV [the total energy of two isolated atoms, one in the ground state ( $-161$  eV), another in the first excited state ( $-117$  eV)].

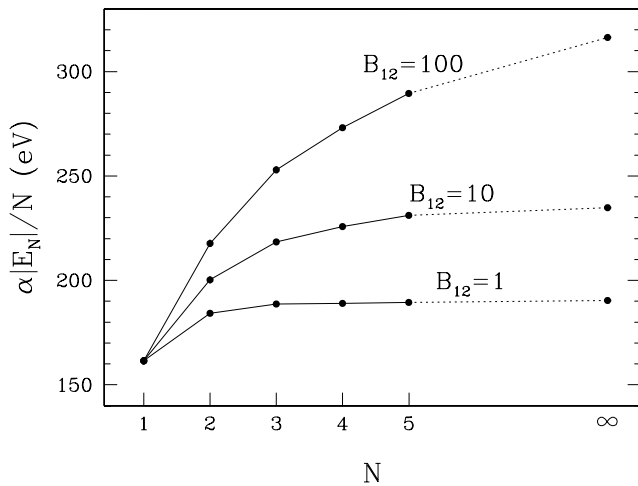


FIG. 4. Binding energy per atom,  $|E_N|/N$ , for  $H_N$  molecules in strong magnetic fields as a function of  $N$ . To facilitate plotting, the values of  $|E_1|$  at different  $B_{12}$  are normalized to its value (161.5 eV) at  $B_{12} = 1$ ; This means  $\alpha = 1$  for  $B_{12} = 1$ ,  $\alpha = 161.5/309.6$  for  $B_{12} = 10$  and  $\alpha = 161.5/541$  for  $B_{12} = 100$ .

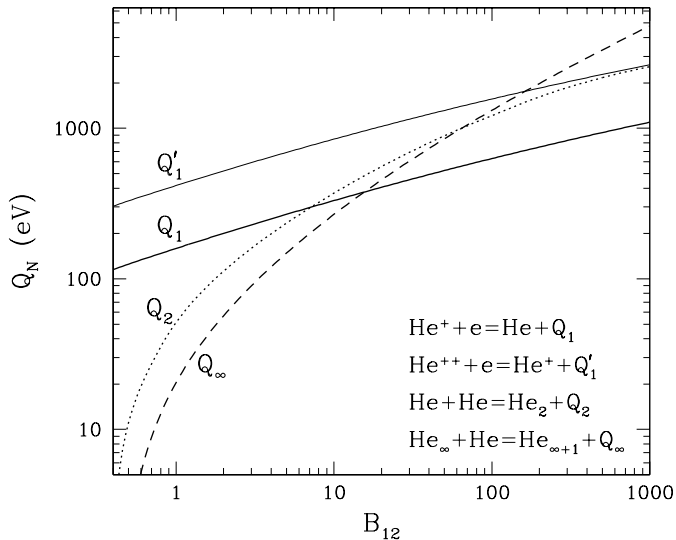


FIG. 5. Energy releases from several atomic and molecular processes as a function of the magnetic field strength. The solid line shows the ionization energy  $Q_1$  of He atom, the dotted line shows the dissociation energy  $Q_2$  of  $\text{He}_2$ , and the dashed line shows the cohesive energy  $Q_\infty$  of linear chain  $\text{He}_\infty$ . The zero-point energy corrections are not included.

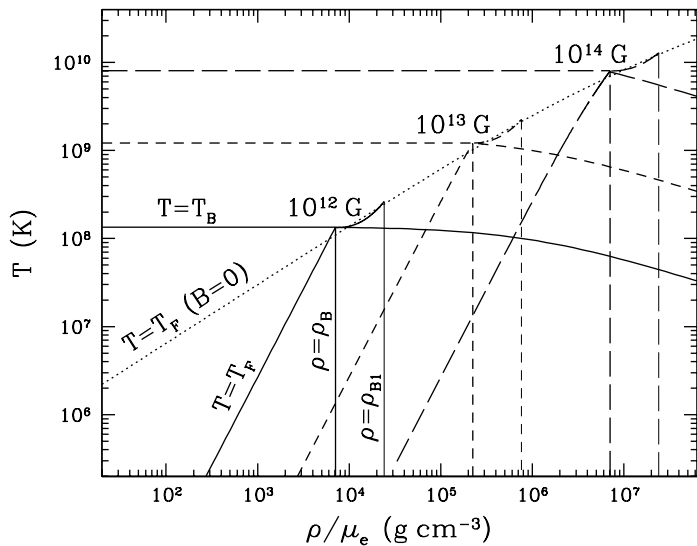


FIG. 6. Temperature-density diagram illustrating the different regimes of magnetic field effects on the thermodynamic properties of a free electron gas. The solid lines are for  $B = 10^{12}$  G, short-dashed lines for  $B = 10^{13}$  G, and long-dashed lines for  $B = 10^{14}$  G. For each value of  $B$ , the vertical lines correspond to  $\rho = \rho_B$  (the density below which only the ground Landau level is occupied by the degenerate electrons) and  $\rho = \rho_{B1}$  (the density below which only the  $n_L = 0, 1$  levels are occupied); the Fermi temperature is shown for  $\rho \leq \rho_B$  and for  $\rho_B < \rho \leq \rho_{B1}$ ; the line marked by “ $T = T_B$ ” [see Eq. (6.17)] corresponds to the temperature above which the Landau level effects are smeared out. The dotted line gives the Fermi temperature at  $B = 0$ . The magnetic field is strongly quantizing when  $\rho \lesssim \rho_B$  and  $T \lesssim T_B$ , weakly quantizing when  $\rho \gtrsim \rho_B$  and  $T \lesssim T_B$ , and non-quantizing when  $T \gg T_B$ . See Sec. VI for detail.

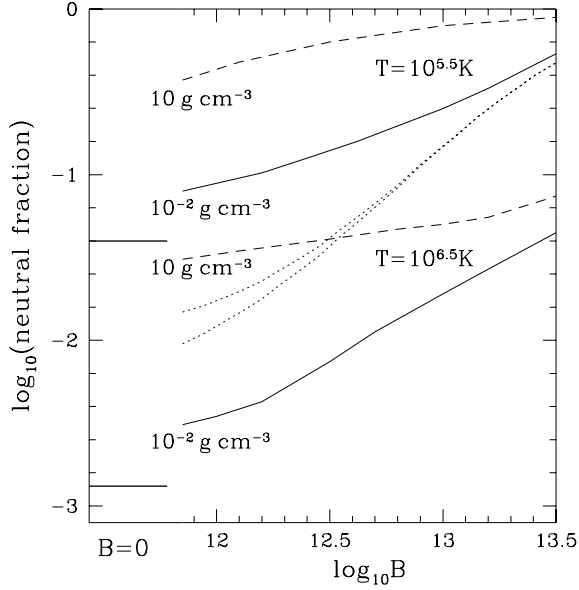


FIG. 7. Atomic hydrogen fraction  $n_H/n_b$  as a function of magnetic field strength. The solid lines (for  $T = 10^{5.5}$  K and  $T = 10^{6.5}$  K) are for density  $\rho = 0.01$  g cm $^{-3}$ , and the dashed lines for  $\rho = 10$  g cm $^{-3}$ . These results are based on the calculations of Potekhin *et al.* (1999). The two dotted lines (for  $T = 10^{5.5}$  K,  $\rho = 0.01$  g cm $^{-3}$ ) correspond to the hydrogen fraction  $n_H/n_b$  calculated ignoring the “decentered states” (the lower line includes only the  $m = 0$  state, while the upper line includes all  $m$ -states). The two horizontal lines on the left correspond to zero-field results (for  $\rho = 0.01$  g cm $^{-3}$  and  $T = 10^{5.5}, 10^{6.5}$  K; for  $\rho = 10$  g cm $^{-3}$ , all atoms are pressure-ionized at zero field).

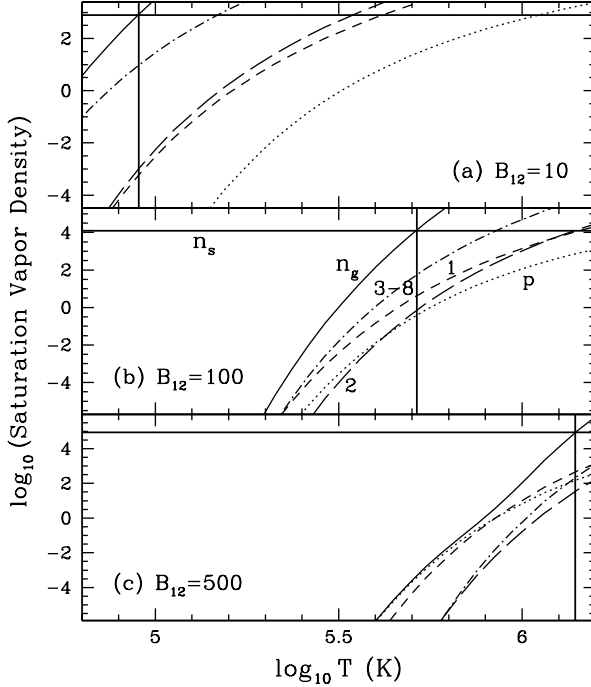


FIG. 8. The saturation vapor densities of various species (in the atomic units,  $a_0^{-3}$ ) of condensed metallic hydrogen as a function of temperature for different magnetic field strengths: (a)  $B_{12} = 10$ ; (b)  $B_{12} = 100$ ; (c)  $B_{12} = 500$ . The dotted curves give  $n_p$ , the short-dashed curves give  $n(\text{H})$ , the long-dashed curves give  $n(\text{H}_2)$ , the dot-dashed curves give  $[3n(\text{H}_3) + 4n(\text{H}_4) + \dots + 8n(\text{H}_8)]$ , and the solid curves give the total baryon number density in the vapor  $n_g = n_p + n(\text{H}) + 2n(\text{H}_2) + \dots$ . The horizontal solid lines denote the condensation density  $n_s \simeq 50 B_{12}^{6/5}$  (a.u.), while the vertical solid lines correspond to the critical condensation temperature at which  $n_g = n_s$  (From Lai and Salpeter 1997).

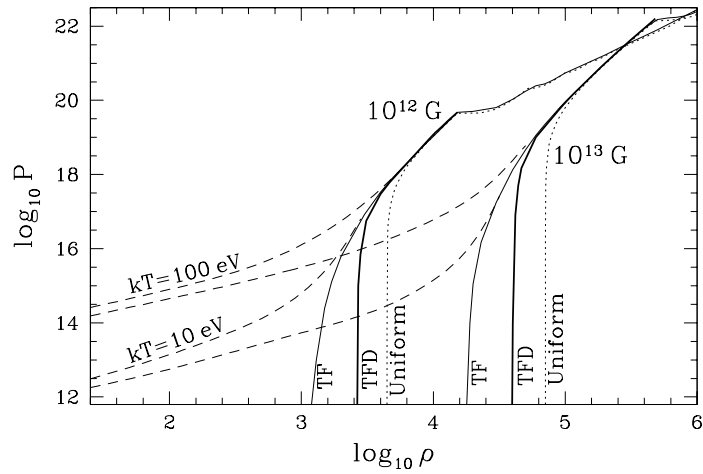


FIG. 9. Equation of state of Fe in strong magnetic fields ( $B = 10^{12}, 10^{13}$  G) based on Thomas-Fermi type models. The light solid lines are results of Thomas-Fermi (TF) model allowing for many Landau levels (Rögnvaldsson *et al.* 1993), the thick solid lines are results of Thomas-Fermi-Dirac model allowing only for the ground Landau level (Fushiki *et al.* 1989), and the dotted lines are results of the uniform gas model as described by Eq. (7.25), all for zero temperature. The dashed lines are results of Thomas-Fermi models with  $kT = 10, 100$  eV (Thorolfsson *et al.* 1998).